REVIEW ON EXISTING DATA ON UNDERWATER SOUNDS FROM PILE DRIVING ACTIVITIES

A report prepared by Seiche Ltd
for the Joint Industry Programme (JIP)
on E&P Sound and Marine Life

JIP Topic - Sound source characterisation and propagation

E&P **SOUND**
& MARINE LIFE
PROGRAMME

September 2020

About the E&P Sound & Marine Life Programme

The ocean is filled with a wide variety of natural and anthropogenic sounds. Since the early 1990s, there has been increasing environmental and regulatory focus on anthropogenic sounds in the sea and on the effects these sounds may have on marine life. There are now many national and international regimes that regulate how we introduce sound to the marine environment. We believe that effective policies and regulations should be firmly rooted in sound independent science. This allows regulators to make consistent and reasonable regulations while also allowing industries that use or introduce sound to develop effective mitigation strategies.

In 2005, a broad group of international oil and gas companies and the International Association of Geophysical Contractors (IAGC) committed to form a Joint Industry Programme under the auspices of the International Association of Oil and Gas Producers (IOGP) to identify and conduct a research programme that improves understanding of the potential impact of exploration and production sound on marine life. The Objectives of the programme were (and remain):

1. To support planning of exploration and production (E&P) operations and risk assessments
2. To provide the basis for appropriate operational measures that are protective of marine life
3. To inform policy and regulation.

The members of the JIP are committed to ensuring that wherever possible the results of the studies it commissions are submitted for scrutiny through publication in peer-reviewed journals. The research papers are drawn from data and information in the contract research report series. Both contract reports and research paper abstracts (and in many cases full papers) are available from the Programme's web site at www.soundandmarinelife.org.

Seiche Ltd
Bradworthy Industrial Estate
Langdon Road, Bradworthy
Holsworthy, Devon EX22 7SF
United Kingdom
Tel: +44 (0) 1409 404050
Email: info@seiche.com
Web: www.seiche.com

Seiche Measurements LLC
10355 Centre park Dr
Suite 240
Houston TX77043
United States of America
Tel: +1 713 201 5726
Email: info@seiche.com
Web: www.seiche.com

Review on Existing Data on Underwater Sounds from Pile Driving Activities

Guillermo Jiménez-Arranz, Nikhil Banda, Stephen Cook and Roy Wyatt

June 2020

Prepared by:
Seiche Ltd.

Submitted to:
E&P Sound & Marine Life (JIP)

Document Control

Project Reference	P784		
Client	E & P Sound & Marine Life, Joint Industry Programme	Client Reference	
		Revision	Date
Prime Author(s)	Guillermo Jiménez-Arranz	5.1	15 June 2020
Reviewed by	Nikhil Banda, Stephen Cook		
Authorised for release	Mark Burnett		

Disclaimer

Copyright Notice

Executive Summary

Along with seismic surveys, pile driving is one of the most intense sources of anthropogenic noise in the sea (Bailey et al., 2010). The extended use of pile driving in construction of coastal and offshore structures has raised concerns about its potential impact on marine animals. The increasing evidence of the negative effects of anthropogenic noise on marine life has motivated environmental organisations, regulatory agencies and governments to look for solutions, and various international agreements related to underwater noise have been reached in recent years (Erbe, 2013).

The purpose of the current review is to compile and analyse published acoustic data from pile driving operations, in order to improve the understanding of their impact on the marine environment and the effectiveness of the available mitigation methods. A description of the main elements contributing to the received sound levels is given in the main body of this document (Chapters 1-6). Tables with relevant published information on pile driving sounds are presented in Appendix I. The tabulated data includes measured sound levels for different types of pile and hammer, their evolution with distance, and additional, contextual information. For a correct interpretation and comparison of results, as much information as possible is provided about the environment, pile and pile driver, characteristics of the measured acoustic signal, and characteristics and efficacy of the attenuation method, if used.

The information in this report has been extracted from journal articles, technical reports, product specifications, and books. Only literature with a detailed description of measuring procedures, data processing and metrics has been considered; secondary sources and grey literature have not been included, except when information is scarce.

The majority of measurements in this report have been conducted during pile driving activities from wind farm construction. Very few pile driving operations conducted by the oil and gas industry have been made widely available. These two activities may not be directly comparable as wind farms are usually built in coastal waters whereas the pile driving activity for oil and gas (e.g. installation of jacket structures) may not take place in shallow waters. More research needs to be conducted on the sound levels produced from pile driving by the oil and gas industry.

Symbols and Acronyms

$\emptyset$	Pile diameter [m]
$\emptyset_{in}$	Internal pile diameter [m]
$\emptyset_{out}$	External pile diameter [m]
$@$	"At", used to indicate measured distance of a source level (e.g. 180 dB re 1µPa@50m)
A	Bubble area in air bubble curtain [m^2]
A_{hole}	Free-bubble area in air bubble curtain [m^2]
AF	Attenuation Factor
c_w	Speed of sound in water (≈1500 m/s) [m/s]
c_p	Speed of sound in the pile [m/s]
c_b	Speed of sound in the sea bottom [m/s]
$CIDH$	Cast-In-Drilled Hole
$CISS$	Cast-In-Steel Shell
$cSEL$	Cumulative sound exposure level
E	Sound exposure magnitude subscript, blow energy
$Eq.$	Equation
$Fig.$	Figure
f	Frequency, operating frequency [Hz]
f_b	Resonant frequency of air bubble in water [Hz]
f_w	Cut-off frequency from water depth [Hz]
h_w	Depth of water column [m]
HSD	Hydro Sound Damper
L_E	Sound exposure level [dB re 1 $\mu Pa^2 \cdot s$ or dB_E]
$L_{p(,rms)}$	Root-mean-square sound pressure level [dB re 1 $\mu Pa_{(rms)}$ or $dB_{(rms)}$]
$L_{p,pk}$	Peak sound pressure level [dB re 1 μPa_{pk} or dB_{pk}]
$L_{p,pk-pk}$	Peak-to-peak sound pressure level [dB re 1 $\mu Pa_{pk\text{-}pk}$ or $dB_{pk\text{-}pk}$]
$L_{E,f}$	Sound exposure spectral density level [dB re 1 $\mu Pa^2 \cdot s/Hz$]
$L_{p,f}$	Mean-square sound pressure spectral density level [dB re 1 $\mu Pa^2/Hz$]
oct	Octave
φ_w	Angle of aperture of pile's Mach cone, in water
$p_{(rms)}$	Root-mean-square sound pressure [$Pa_{(rms)}$]
p_{pk}	Peak sound pressure [Pa_{pk}]
p_{pk-pk}	Peak-to-peak sound pressure [Pa_{pk}]

pk	Peak magnitude subscript
$pk-pk$	Peak to peak magnitude subscript
RMS	Root-mean-square
R	Range [m]
R_b	Bubble radius [m]
RL	Received Level [$dB_{(rms)}$, dB_{pk}, dB_E]
rms	Root-mean square magnitude subscript
SEL	Sound exposure level
SLF	Spreading Loss Factor
SPL	Sound Pressure Level
SL	Source Level [$dB_{(rms)}$, dB_{pk}, dB_E]
$Tab.$	Table
T	Repetition period (impact hammer) [s]
TL	Transmission Loss [dB]
TTS	Temporal Threshold Shift [dB]
τ	Pulse duration [s]
τ_{pk}	Rise time [s]
typ	Typical
w	Water subscript
z	Depth below water surface [m]
z_r	Receiver depth below water surface [m]

Units

atm	Atmosphere (= 101 kPa)
bpm	Blows per minute
dB	Decibel
Hz	Hertz
J	Joule [$\mathrm{kg\ m^2\ s^{-2}}$]
k	Kilo (10^3)
kn	Knot (= 0.514 m/s)
M	Mega (10^6)
m	Metre, Milli (10^{-3})
N	Newton [$\mathrm{kg\ m\ s^{-2}}$]
µ	Micro (10^{-6})
Pa	Pascal [$\mathrm{kg\ m^{-1}\ s^{-2}}$]
ppt	Parts per thousand
s	Second
t	Tonne or metric ton (= 10^3 kg)

Terminology

Attenuation Factor: level of attenuation with range. The attenuation factor depends on the reflection coefficient of the seabed, scattering of the sea surface and absorption of sea water. This factor dominates in shallow waters and at long distances from the source.

Bandwidth: difference between the upper and lower frequency of a frequency band.

Continuous Sound: acoustic signal of long or undetermined duration.

Cumulative Energy Curve: representation of the accumulated energy of a sound event with time. This curve is typically used for the calculation of the *RMS sound pressure* or the *sound exposure* of a transitory signal.

Decibel: unit equal to ten times the logarithm of a power ratio. The decibel is used to quantify variables characterised by a large dynamic range, such as the acoustic pressure. The decibel can be used to express an absolute quantity by using a reference value. Quantities express in decibels are referred to as *levels*. The factor that accompanies the logarithm is 10 for acoustic power and intensity, and 10 for acoustic pressure. The decibel is denoted by the letters dB.

Density: mass per unit volume. Its unit is kilograms per cubic metre (kg/m^3). The density of sea water is a function of temperature, salinity and hydrostatic pressure, and has a value of 1022 kg/m^3 for 25 °C, 33 ppt and 1 atm.

Directivity: directional signature of a sound source. A source is more *directive* when its directivity pattern diverts from a perfect sphere or *omnidirectional pattern*. At wavelengths that are comparable to or lower than the dimensions of a source, the directional behaviour is more pronounced.

Far Field: region of the sound field in which the sound waves originated in different parts of the source arrive practically in phase. In this region, the irregular wavefront at the source becomes virtually spherical, resulting in a sound pressure attenuation proportional to range. The far field occurs at an approximate range of L^2/λ, with L the largest dimension of the source.

Frequency: number of cycles of a periodic or harmonic wave per unit time. Reciprocal of the *period*. Denoted by letter *f*. Its unit is the Hertz (Hz).

Frequency Band: region of the frequency spectrum delimited by a lower and upper frequency. The frequency spectrum is divided into frequency bands, which can be *constant*, as is the case in a narrowband spectrum calculated with the DFT (see PSD), or with a *bandwidth* proportional to the band's central frequency. Octave and third-octave band spectra a examples of the latter. In an octave band spectrum, consecutive central frequencies are spaced by a factor of 2, and in a third-octave band spectrum, by a factor of $2^{1/3}$.

Frequency Spectrum: distribution of amplitudes and phases of a time signal in the frequency domain. The conversion between the time and frequency domains is achieved with the Fourier Transform. The complex frequency spectrum of a discrete time signal is calculated with the Discrete Fourier Transform (DFT).

Harmonics: integer multiples of a fundamental frequency.

Impulsive Sound: transitory sound characterised by high pressure and short rise time.

Near Field: region of the sound field in which different vibrating parts of the source behave as individual emitters. In this region, the difference in the travelled distance of the sound waves generated by each of these emitters is comparable to or higher than the wavelength, which results in a pressure pattern of constructive and destructive interferences. In the near field, the wavefront is irregular (non-spherical).

Pulse Length: effective duration of a transitory signal or pulsed sound event. The pulse length is generally calculated as the time between the 5 % and 95 % energy on the cumulative energy curve of the event.

Peak Pressure: also referred to as zero-to-peak pressure, is the maximum absolute value of the pressure waveform. This metric is preferred for impulsive sounds. The unit of the peak acoustic pressure is the pascal (Pa) peak. The metric descriptor (i.e. peak) should always accompany the units for this metric. The peak acoustic pressure is calculated as follows:

$$p_{0-p} = \max\{|p(t)|\}$$

Peak-to-Peak Pressure: difference between the maximum and minimum values of the pressure waveform. Along with the peak pressure, this metric is preferred for impulsive sounds. The unit of the peak-to-peak acoustic pressure is the pascal (Pa) peak-to-peak. The metric descriptor (i.e. peak-to-peak) should always accompany the units for this metric. The peak-to-peak acoustic pressure is calculated as follows:

$$p_{p-p} = \max\{p(t)\} - \min\{p(t)\}$$

Peak Sound Pressure Level: decibel representation of the peak acoustic pressure. The peak sound pressure level uses a logarithmic factor of 20 and a reference value of 1 µPa.

$$SPL_{0-p} = 20\log\left(\frac{p_{0-p}}{1\ \mu\text{Pa}}\right)$$

Peak-to-Peak Sound Pressure Level: decibel representation of the peak-to-peak acoustic pressure. The peak sound pressure level uses a logarithmic factor of 20 and a reference value of 1 µPa.

$$SPL_{p-p} = 20\log\left(\frac{p_{p-p}}{1\ \mu\text{Pa}}\right)$$

Percentile: value below which a given percentage of observations falls.

Period: duration of one cycle of a periodic or harmonic wave. Reciprocal of the *frequency*. Denoted by letter *T*. Its unit is the second (s).

Pressure: force per unit area. There are three types of pressure that are interesting in underwater acoustics: the atmospheric, which results from the weight of the column of air at the sea surface; the hydrostatic, which is the combination of the weight of the water column per unit area at a given depth and the atmospheric pressure; and acoustic, which represents pressure fluctuations with respect to the hydrostatic pressure. Atmospheric and hydrostatic pressures are time-invariant, at least for the time scales considered in acoustic measurements, whereas the acoustic pressure is time-dependent. Their unit is the Pascal (Pa).

Power Spectral Density: frequency spectrum of the power of a signal, computed in constant-width bands of 1 Hz. For a sound pressure waveform, the amplitude of the spectrum is given in Pa^2/Hz. To calculate the power spectral density of a N-sample discrete (digital) time signal, the magnitude of the Discrete Fourier transform (DFT) is divided by the number of samples, squared and then multiplied by the signal duration ($T = N/f_s$). The PSD of a discrete signal $x[n]$, with frequency spectrum $X[k]$, is given by:

$$s_{xx}[k] = \left(\frac{|X[k]|}{N}\right)^2 \cdot T \quad [\text{Pa}^2/\text{Hz}]$$

Power Spectral Density Level: logarithmic representation of the power spectral density. The unit is dB re. 1 $\mu Pa^2/Hz$.

$$S_{xx}[k] = 10\log(s_{xx}[k]) \quad [\text{dB re. } 1\ \mu\text{Pa}^2/\text{Hz}]$$

Range: distance from the sound source to the receiver.

Received Level: sound level at a given range. The received level is related to the source and transmission levels by the following equation:

$$RL = SL - TL$$

Regression Equation: equation that establishes a relationship between two variables by minimising the error between its solution and a set of observations. A simple regression equation of the form $RL = SL - SLF \cdot \log(r) - AF \cdot r$ is used in underwater acoustics to estimate the source level SL from measurements. In the previous equation RL is the received level, r the range or distance from the source, SLF the spreading loss factor and AF the attenuation factor. Compared to a sound propagation model, this approach is simpler but has the disadvantage of being only applicable at ranges that are long enough for late reflections to dominate.

RMS Pressure: root-mean square acoustic pressure, that is the square root of the squared pressure averaged over time. This is the most common acoustic metric and is particularly useful in the characterisation of the amplitude of *continuous sounds*. However, the RMS pressure has been widely used in underwater acoustics to characterise *impulsive sounds*, for which this metric is not best suited as pulses of different energy and duration could result in similar RMS values. The *cumulative energy curve* with a 90% energy interval is typically used for the estimation of the pulse length, necessary for the calculation of the RMS pressure. The unit of the RMS acoustic pressure is the pascal (Pa) RMS. If a pressure value is given in Pa, without a metric descriptor, it will be assumed to be of RMS type. The RMS acoustic pressure is calculated as follows:

$$p_{rms} = \sqrt{\frac{1}{\tau}\int_{\tau} p^2(t)\,dt}$$

Specific Acoustic Impedance: ratio of *acoustic pressure* to *particle velocity*. The specific acoustic impedance is a property of the medium and indicates the opposition of that medium to the motion of a longitudinal wave. Denoted by letter Z_0. Its unit is the pascal second per metre (Pa·s/m) or rayl. The specific acoustic impedance of an homogeneous medium is related to its density and sound speed by:

$$Z_0 = \rho c$$

Speed of Sound: distance per unit time. Its units are metres per second (m/s). The speed of sound in water is a function of temperature, salinity, hydrostatic pressure and acidity, and has a value of 1532 m/s for 25 °C, 33 ppt and 1 atm. It is related to the wavelength and frequency of a propagating sound wave by:

$$c = \lambda f$$

Sound Exposure: integral of the square pressure. The sound exposure is related to the energy contained in the acoustic signal. As such, the sound exposure is suitable for both continuous and transitory signals, in particular for dose or noise impact assessment. Its unit is the pascal square second (Pa^2·s). The sound exposure is related to the RMS pressure and is calculated as follows:

$$p_{0-p} = \int_{\tau} p^2(t)\,dt = p_{rms}^2 \cdot \tau$$

Sound Exposure Level: decibel representation of the *sound exposure*. The sound exposure level uses a logarithmic factor of 10 and a reference value of 1 μPa^2·s.

$$SEL = 10\log\left(\frac{p_{rms}^2 \cdot \tau}{1\ \mu\text{Pa}^2\text{s}}\right) = SPL_{rms} + 10\log\tau$$

Sound Level: any acoustic metric expressed in decibels. This includes sound pressure level (rms, peak, peak-to-peak) and sound exposure level.

Sound Pressure Level: decibel representation of the *RMS acoustic pressure*. The sound pressure level uses a logarithmic factor of 20 and a reference RMS pressure of 1 µPa.

$$SPL_{rms} = 20\log\left(\frac{p_{rms}}{1\ \mu\text{Pa}}\right)$$

Sound Propagation Model: mathematical algorithm that uses a numerical approximation to predict the transmission loss experienced by the sound emitted by an acoustic source as it propagates in a given underwater environment. Some of the most widely used propagation modelling theories and examples of algorithms are raytracing (Bellhop), parabolic equation (RAMGeo), normal modes (Kraken) and wavenumber integration (OASES).

Source Level: sound level produced at one metre from a point source. The source level of a real source is an hypothetical value, obtained from back-propagating measurements taken in the far-field of the source using a sound propagation model or an empirical regression equation. The source level must not be interpreted as a true representation of the sound level at one metre from the source, but as an intermediate metric necessary for the estimation of sound levels in the source's far field.

Spreading Loss Factor: level of attenuation per ten-times distance increase. A factor of 20 indicates spherical propagation of sound, associated with free-field (i.e. unbounded) conditions, and a factor of 10 indicates cylindrical propagation, associated with long-range propagation in-between two parallel, perfectly rigid, semi-infinite planes i.e. waveguide). The spreading loss factor can be lower than 10 or higher than 20, specially at ranges where the direct sound or early reflections dominate.

Transitory Sound: acoustic signal of limited or determined duration.

Transmission Loss: sound attenuation level at a given range, referenced to one metre. The transmission loss can be calculated with a sound propagation model or estimated with a regression equation fitted to sound level measurements.

Wavelength: distance of a cycle in a propagating periodic or harmonic wave. Denoted by Greek letter λ. Its unit is the metre (m).

Content

Executive Summary i
Symbols and Acronyms iii
Units v
Terminology vii
1 Introduction 1
1.1 General Notes on Underwater Acoustics 2
1.2 Outline of Review 3
1.3 Notes on Tables 3
1.4 Report Structure 5
2 The Pile 7
2.1 Pile Type based on Load Transfer and Installation 9
2.2 Pile Type based on Shape and Material 10
3 The Hammer 13
3.1 The Impact Hammer 14
3.1.1 Types of Impact Hammer 15
3.1.2 Mechanisms of Sound Radiation 16
3.2 The Vibratory Hammer 17
3.2.1 Parts of a Vibratory Hammer 17
3.2.2 Operation of a Vibratory Hammer 18
3.2.3 Types of Vibratory Hammer 18
3.2.4 Mechanisms of Sound Radiation 18
4 The Pile Driving Operation 21
4.1 Pile Installation 21
4.2 Pile-Hammer Contact 21
4.3 Soft Start 21
4.4 Pile Direction 22
4.5 Pile Penetration 22
5 The Environment 25
5.1 Bathymetry and Water Depth 25
5.2 Seabed Composition 26
5.3 Water Surface 26
5.4 Receiver Distance 26
5.5 Receiver Depth 27

6 Sound Mitigation and Attenuation Methods 29
6.1 Air Bubble Curtains 29
6.2 Air-Filled Resonators 33
6.3 Cofferdams 33
6.4 Pile Sleeves 34
6.5 Hammer Type 35
6.6 Pile Type 36
6.7 Prolonging Impact Duration 36
6.8 Pile Cap 37
6.9 Jetting in Piles 38
6.10 Pile Driver Silencer 38
6.11 Pre-Drilled Pile 38
6.12 Decoupling Sound Sources 39
6.13 Hammer Impact Energy 39
References 41
A.I Tabulated Data 45
A.II Noise & Absorption in Sea Water 61

1 Introduction

The growing interest in marine renewable energies over the last decade has resulted in a rapid development of offshore wind power. The extended use of pile driving for wind farm construction and other types of coastal and offshore structures, such as bridges, wharfs and jack-up rigs, has raised concerns about the impact of pile driving noise on marine animals.

Along with marine seismic surveys, pile-driving is one of the most intense sources of anthropogenic noise (Bailey et al., 2010). Impact pile driving generates a high energy acoustic pulse with each strike of a hammer, which operates at a rate of 15-60 blows per minute and requires 500-5000 strokes to drive the pile into the seabed. Marine vertebrates, to a greater or lesser extent, rely on their auditory system for communication, mating and social interaction, navigation, foraging, prey detection and predator avoidance. Background noise can mask these vital sounds and cause stress reactions, behavioural changes or even physical damage on individuals, which may result in population impacts in the long term. The high intensity and long duration of pile driving operations are potentially detrimental to marine species.

Pile driving sounds have been shown to disrupt the behaviour of bottlenose dolphins and minke whales at ranges of up to 50 km (Bailey et al., 2010) and to produce a strong avoidance response in harbour porpoises at ranges of 1.5 km or less (Jong & Ainslie, 2012). Changes in prey species and habitat as a consequence of long-term disturbance can also be expected (Evans, 2008; Gordon et al., 2007). At close range, piling sounds could cause hearing impairment in marine mammals (Thomson et al., 2010); permanent and temporary threshold shifts are likely to occur within a range of a few hundred metres (Bailey et al., 2010; Jong & Ainslie, 2012).

Fish are classified into *hearing specialists* and *hearing generalists*, with the latter being the least sensitive to sound. The hearing capabilities of fish vary greatly among species, but the inner ear and swim bladder are in general key elements for their perception of sound. The swim bladder is particularly at risk as it can resonate when acoustically excited, and if damaged the chances of survival are seriously reduced (Abbot & Reyff, 2004). Fish are sensitive to pressure and particle motion, and can be particularly affected by large peak amplitudes, sharp impulses and long term exposure (Popper et al., 2006). Barotrauma, a pathology associated with drastic changes in pressure, can lead to immediate or delayed fish mortality; Abbot & Reyff (2004) detected no near-term mortality on fish at ranges higher than 70 m from the pile or levels less than 204 dB. Popper et al. (2006) propose a conservative threshold level for temporal hearing loss (TTS) of 187 dB_E and 208 dB_{pk} Fish behaviour could be affected at ranges of several kilometres (Evans, 2008).

The increasing concern in recent years about the impact of pile driving noise on marine animals has motivated the measurement and study of these sounds. The purpose of the current review is to compile and analyse published acoustic data from pile driving operations, in order to improve the understanding of their impact on the marine environment and the effectiveness of the available mitigation methods.

1.1 General Notes on Underwater Acoustics

The propagation of sound in water is very complex and sound may travel through several different paths before reaching the receiver. Acoustic waves can either travel directly through the water, be reflected and scattered off the sea surface and seabed, or even propagate within the seabed and emerge in the water column at some distance from the source. It then becomes evident that the environment will have a strong effect on the sound field. The characteristics of the received sound depend on the acoustic properties of the source, the nature of the propagation environment and the relative position between source, receiver and boundary surfaces. The received level of the source signal at a specific point in the water column is dependent on many variables, including source and receiver depths, salinity and temperature gradients in the water column, sea bed properties, sea state and bathymetry. Many of the environmental variables exhibit important differences depending on the geographical location and time scale (with day-night, seasonal and long-term changes).

The propagation in the water is mainly governed by its sound speed, which varies with depth and range, and gives rise to focusing, channelling and shadowing effects (Coats, 2006; Lurton, 2010; Urick, 1983). Complex vertical variations in temperature and salinity in the water column allow for occurrence of acoustic channels at certain depths, where sound might get trapped by the effect of vertical sound speed gradients of opposite sign. Except for long ranges, shallow waters and regions with oceanic fronts, the sound speed can be considered *horizontally stratified* (i.e. strong depth dependence, weak range dependence).

The ocean is a dynamic medium, with tides, internal and surface waves, eddies, turbulences, mixtures of water bodies of different temperature and densities, and temperature and salinity varying throughout the water column. These phenomena introduce a degree of variability into the sound speed profiles of the ocean, resulting in space and time variations on the sound propagation conditions and sound levels. These variations dominate near the sea surface, and despite being relatively small, have a significant effect on long range propagation.

The *transmission loss* or sound level attenuation between source and receiver depends on four main factors: geometric spreading, acoustic impedance of the seabed, absorption in water, and scattering from sea surface and seabed. The spherical wave front of an acoustic wave results in a 6 dB sound pressure attenuation per doubled distance in free field or deep waters; in shallow waters this wave front can be shaped into a cylindrical form, reducing the attenuation to 3 dB per doubled distance. The sea surface returns a phase-inverted version of the incident sound wave, producing a dipole effect which brings about a maximum attenuation at constant depth of 12 dB per doubled distance. In shallow waters or at long distances the acoustic impedance of the seabed has an important effect on the transmission loss. The absorption in sea water depends on its temperature, salinity, acidity and hydrostatic pressure, and is particularly high for high frequency sounds (Fisher & Simmons, 1977; Francois & Garrison,1982a; Francois & Garrison,1982b); a 100 Hz sound signal may be detectable after travelling hundreds, or even thousands, of kilometres from the source, whereas a 100 kHz sound signal may be completely attenuated in only a few kilometres from the source (Marine Mammal Commission, 2007). The typical attenuation characteristics of different acoustic frequencies in seawater with distance from the source are given in Appendix II.

The *received level* equals the source level minus the transmission losses (RL = SL – TL). The *source level* is the sound pressure level that a point source version of the original acoustic source would generate at one metre. The source level is a theoretical value used in sound propagation models, and with time has become a standard for the characterisation of the acoustic power of a sound source. Real sources, due to their dimensions and radiation pattern, exhibit a complex sound pressure distribution in their proximity, in the so called near field region. The size of the source and operational constraints make it either impractical to measure the sound pressure level at 1 m from the source, and the measurements are taken in the far

field. Measuring in the far field is simpler and ensures comparison of results from different sources, since in that region the source behaves as a monopole, which is more predictable and easier to model. However, in order to make a good estimate of the sound level, the acoustic parameters of the environment must be accurate and the prediction should support this highly detailed environment definition. In general, information about properties of the environment is limited, especially seabed composition, which in many cases leads to the use of oversimplified models or simple regression equations fitted to a few range dependent measurements. Hence, source levels should be taken carefully, but transmission loss curves with range are a good aid in comparing and interpreting these source levels.

1.2 Outline of Review

This report aims to be a quick reference guide to the characteristics and acoustic properties of pile driving activities carried out by the oil and gas industry. The current review is an update to an overall review conducted by Wyatt (2008) on underwater sounds produced by the oil and gas industry. Due to the lack of published information at that time on pile driving, a separate report is now deemed necessary to fill the gaps.

The following chapters are dedicated to those elements of the piling operation that have a critical impact on the sound field, such as the pile, the hammer, operational factors, the environment, and mitigation and attenuation methods. A brief approach to the relative contribution of these elements to the sound level, frequency response, duration and spatial and temporal distribution of the acoustic event is addressed in the document. A series of tables with published sound level data on pile driving and additional contextual information are included in Appendix I. Broadband or single band levels are included in the tables. The in-band frequency responses are not tabulated; instead, these spectra are shown as graphs to make interpretation and comparisons easier. A detailed explanation of what is included in the tables and the approach followed to build them is given in Section 1.3, "Notes on Tables".

Gathering meaningful and representative measurements is especially challenging due to the complexity of the underwater environment. It is then essential for the comparison and interpretation of data included in this report to consider only literature that provides a detailed description of measuring procedures, data processing and metrics. Secondary sources and grey literature, i.e. literature with insufficient or irrelevant information, have not been included, except when there is a scarcity of information. For this review, journal papers, technical reports, product specifications and books have been the main sources of information.

1.3 Notes on Tables

The tables presented in this report include the following fields: pile type, pile dimensions, hammer type, hammer dimensions, water depth, seabed type, measurement (peak, RMS and exposure sound levels), source level, regression equation, signal characteristics, description and references.

The *type of pile* (shape and material) is indicated in bold letters in the first column. The main types of pile included in the tables are: steel pipes and monopiles, steel H piles, steel sheets, timber piles, and concrete piles – standard reinforcement, Cast-In-Steel-Shell (CISS), and Cast-In-Drilled-Holes (CIDH). The *dimensions of the pile*, in the second column, inform about the length, width/diameter and thickness of the pile.

The *type of hammer*, and its model in brackets, are shown in the third column. Information is included for the main types of impact hammer, i.e. diesel, hydraulic, drop and air/steam, and for vibratory hammers. The current limited use of air/steam impact hammers explains the scarcity of acoustic measurements; only one publication with acoustic data for this type of pile driver has been found. The length and width of the

hammer, along with the ram weight (impact) or driving force, are included, when available, in the fourth column to give an idea of the energy transmitted to the pile.

The *depth of the water column* is a critical parameter that can have large effect on the underwater propagation of low frequency sounds (see Chapter 5, "The Environment"); similarly, the *geological composition of the seabed* will contribute to the amount of acoustic energy in the water column and the general multipath reflection pattern. The water depth and seabed type are included in the fifth and sixth columns.

In the *measurement* column, the broadband sound level measured at a certain range from the source is quoted. In some cases, a single band or single frequency value is given. Multiple sound levels at different ranges might be provided if the data is clear and considered relevant, but generally the closest to the source is quoted in the tables, as the direct sound from the source is predominant in these conditions and this is likely to provide a better representation of its acoustic behaviour. The distances quoted by the authors are generally far enough from the source to be unaffected by the complexity of the near field interactions. The tabulated sound levels can be peak, RMS or SEL. Cumulative sound exposure levels (cSEL) calculated from measurements are infrequent and sensitive to the species of concern, which makes comparisons difficult; for these reasons, cSEL values are not included in the tables.

In the *source level* column the sound level at 1 m is quoted. It is common practice in the literature to provide a source level for each measured level at range. If just the measurement is quoted by the author, the source level is estimated from the provided spreading loss factor. If the transmission loss curve or spreading factor are not provided, a transmission loss of $15 \cdot \log_{10} R$ is assumed, where R represents the *range* or distance from the source in metres. The coefficient 15 in the previous equation is considered to be a typical value to be used for spreading loss in shallow water (Urick, 1983). In the reviewed literature, rarely a source level is estimated using an analytical or numerical sound propagation model: instead, a simple regression equation in the form $RL = SL - SLF \cdot \log R - AF \cdot R$ is used, where SLF is the spreading loss factor, AF the absorption factor, and R the range. These regression equations are simple fitting curves and do not account for the propagation characteristics of the environment to determine the source level, so their accuracy beyond the measured ranges is limited. Source levels estimated in this way, and not through a calibrated propagation model, must be considered carefully.

The *regression equation* column contains, whenever given by the author, the curve fitted to the experimental data, the percentile used (95%, 90%, or 50% or *median*) and the range of validity, which corresponds to the range covered by the measurements. The source level quoted in the tables is obtained from the regression equation.

The *signal characteristics* column includes information such as pulse duration, rise time, frequency range, maximum energy bands, bandwidth, tonal frequencies or temporal characteristics of the signal.

The *attenuation method* column shows the degree of attenuation achieved with tested attenuation devices, such as bubble curtains, pile caps or cofferdams.

The *description* column contains any additional information that may be useful for interpreting the measurements and does not fit in any of the other columns. In general, things like the context of the measurements, the location, receiver depth, impact rate, driving energy and notes on the values presented in the other columns are shown in the description column.

The *reference* column simply cites the document or documents used for the data presented.

1.4 Report Structure

This report is structured in six chapters, references and appendices. An introductory chapter and five chapters describing the main factors that contribute to the sound field during pile driving operations comprise the main body of this document. The tabulated data on pile driving sounds is included in Appendix I.

Chapter 1, i.e. the current chapter, contains background information on pile driving noise and its potential impact on marine life. Highlights on underwater acoustics and sound propagation are also given to help with interpreting the results and understanding some of the concepts referred to in the main body. A brief outline of this review, and detailed comments about the content of the tables and the approach taken to build them are also included.

Chapter 2 introduces the different types of piles according to load transfer, installation method, shape and material. The relative contribution of the pile dimensions, shape and material to the radiated sound levels and spectra are also analysed.

Chapter 3 presents the two main types of pile driver, impact and vibratory, their operation and mechanical characteristics, hammer sub-types and sound generation principle. The contribution of the hammer mechanical properties, driving energy and impact rate to the received sound levels and spectra are also described.

Chapter 4 presents the main operational factors in pile driving that contribute to the received sound. These factors include the contact between hammer and pile, soft start, pile direction and pile penetration depth.

Chapter 5 describes how various environmental factors (water depth, seabed composition, sea state) and receiver location contribute to the received sound.

Chapter 6 presents the most common attenuation devices and techniques used in pile driving and their effectiveness. The physical attenuation methods include air bubble curtains, air filled resonators, cofferdams, pile caps and pile driving silencers; the operational solutions comprise the selection of pile and hammer type, longer duration of the hammer stroke, jets of water on the pile, pre-drilled piles, reduction of the hammer impact energy and cancellation of secondary sound sources.

The review ends with the *references* and *appendices*. Appendix I includes tabulated published acoustic data from pile driving operations, carried out with different types of pile and hammer. Details about the content and interpretation of the tables are included in Section 1.3, "Notes on Tables". Appendix II includes two figures: sound absorption in sea water and the composite ambient sound spectrum in the oceans.

2 The Pile

The demand for energy has driven the development of offshore engineering structures for the recovery of natural and renewable sources (oil, gas, wind, waves and tidal currents). The foundations of offshore structures comprise pile groups (e.g. in oil and gas drilling and production platforms), monopiles (e.g. wind turbines) and gravity foundations (Chatzigiannelis et al, 2009).

Piles are used in unfavourable ground conditions to transfer the loads from a structure through the weak soil down to a strong sediment layer that can support the weight (Chatzigiannelis et al, 2009). Piles can be driven vertically or at an angle ("batter" or "raker"). Batter piles are used in harbour structures and in some offshore terminals to resist lateral loads. Lateral load resistance can also be improved by increasing the stiffness of the pile just below the mudline, by increasing the wall thickness, filling with concrete or grouting in this region of the pile (Gerwick, 2007). Groups of piles of smaller diameter than those used in offshore foundations are common in coastal and harbour construction.

Jacket structures are common in ports (e.g. berth facilities, marine terminals) and offshore engineering (e.g. oil platforms, wind turbines). These structures can be connected to the piles in two ways (see Figure 2.1): *skirt piles*, encased in sleeves and joined to the lower end of the jacker; or *pin piles*, centred inside the jacket leg and extended to the full height of the jacket (Chatzigiannelis et al, 2009; Gerwick, 2007).

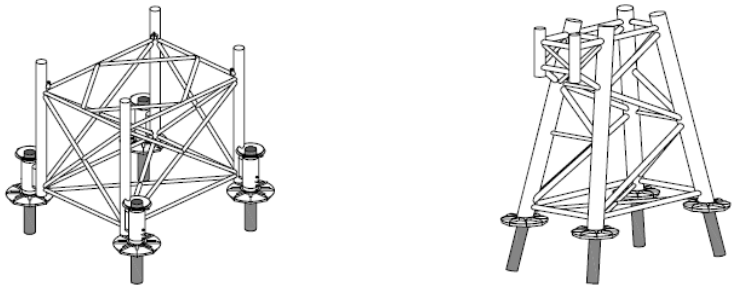

Figure 2.1 Jacket structure with skirt piles (left) and pin piles (right). From Chatzigiannelis et al., 2009

The main pile-related factors contributing to the radiated sound during pile driving include the type or *shape* of the pile, its *material*, and *dimensions*. Installation methods (e.g. batter piles) and pile reinforcement (e.g. grouting) alter the basic structure and mechanics of the pile, which may also have an effect on its acoustic radiation. Before introducing the details about piles and their applications, a brief analysis of the effects of the mentioned pile-related factors is presented below.

In relation to the dimensions of a pile, larger pile *diameters* are associated with higher sound pressure levels. In Figure 2.2, the graph on the left shows a consistent increase of sound pressure level with larger pile diameters. However, the relative contribution of the diameter of a pile to the emitted sound level, which certainly exists, cannot be estimated from the graph, since the diameter is not the only parameter involved. In fact, the increase in sound level with pile size is most likely caused by the higher blow energy required to drive larger piles. There is no rule of thumb to select the strike energy necessary for a given pile diameter (Nehls et al., 2007), but the graph on the right confirms an approximate linear relationship between both parameters. Larger pile diameters result in an increase of the friction force in the sediment and a larger radiating surface, at the expense of lower vibration amplitude, conditions that do not

necessarily lead to an increase in sound level (Nehls et al, 2007). In any case, the structural and mechanical properties of piles of different sizes are expected to have an effect on the radiated sound, but this effect cannot be easily separated from other factors such as soil type or drive head contact.

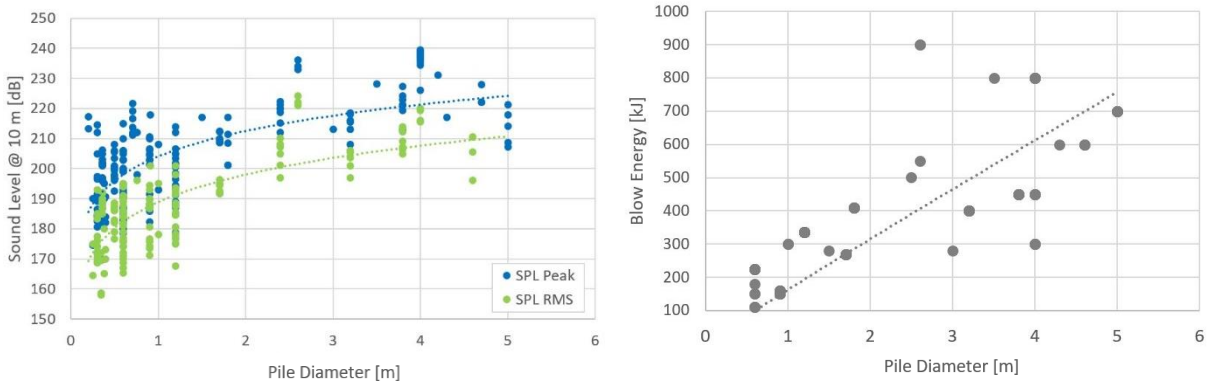

Figure 2.2 Relation between sound level and pile diameter for different types of piles driven by an impact hammer, including concrete and CISS piles, steel pipes and monopiles (left). An approximate linear relation between impact energy and pile diameter is found (right). The graphs are obtained from published data on pile driving sounds (see Appendix I).

Piles come in various shapes and geometries: pipes (round hollow pile with open or close end), solid piles (round, square, octagonal), H-beams and sheet piles. The left graph of Figure 2.3 represents the peak and RMS sound pressure levels with pile diameter for three different types of steel pile driven with impact hammer: pipe, H-beam and sheet pile. The data suggests that steel pipes produce higher sound levels than H-piles or sheets of a similar cross section. However, a definitive conclusion cannot be reached given the limited number of data points for H-beams and sheet piles, and the potential acoustic contribution of additional environmental and operational factors (e.g. sediment composition, strike energy, pile-hammer contact, sound propagation environment or receiver depth). In terms of frequency response, H-beams produce acoustic pulses with a higher frequency content (> 1 kHz) than steel pipes (Illinworth & Rodkin, 2007). A comparison between frequency responses of steel pipes and steel sheet piles are shown in the right-side graph of Figure 2.3. Steel-sheet piles produce a relative broadband sound in the range of 25-4000 Hz (Illinworth & Rodkin, 2007), with a higher relative high-frequency content than steel pipes. The spectrum of a steel pipe is characterised by a high energy region a few octave bands wide below 2 kHz. The rapid roll-off at the low end of the spectrum for both types of pile and hammers (impact and vibratory) is likely caused by the shallow depth of the water column, which constrains the sound propagation at low frequencies (see Chapter 5, "The Environment" for details about the acoustic cut-off frequency caused by the water depth).

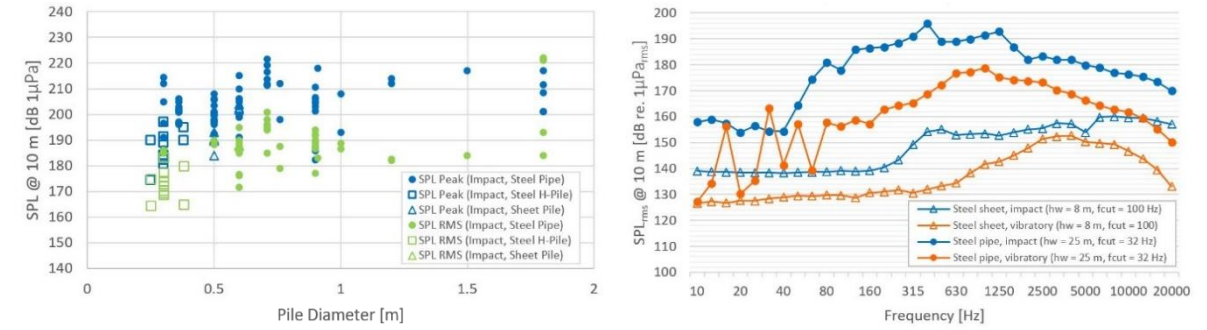

Figure 2.3 On the left, relation between sound level (peak, RMS) and pile diameter for steel piles of different cross section. The piles are installed with an impact hammer and include pipes, H-beams and sheet piles. On the right, band spectrum of a steel sheet pile (Scientific Fishery Systems, 2008) and a steel pipe (Blackwell, 2005) installed with impact and vibratory hammer.

Piles can be made of steel, concrete or wood. Figure 2.4 represents the sound pressure levels as a function of pile diameter for steel, concrete and timber piles, installed with an impact hammer. Steel pipes tend to produce the highest sound levels. The lower sound levels emitted by concrete piles can be partially explained by the widespread use of plywood caps, placed on top of the pile to protect the concrete from the high tensile forces generated after impact (see Chapter 6, "Sound Mitigation and Attenuation Methods"). Timber seems to produce the lowest sound levels, but there is not enough data in the graph to support this observation.

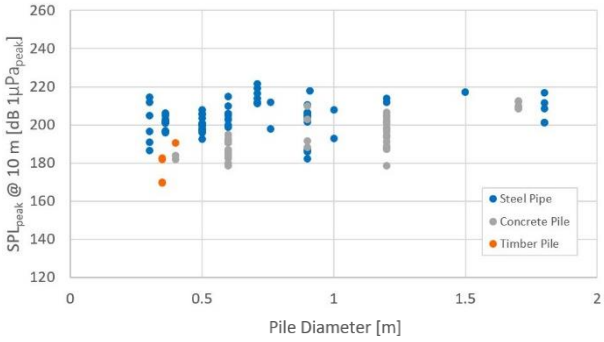

Figure 2.4 Relation between peak sound pressure level and pile diameter for steel, concrete and wooden piles. Graph obtained from published sound measurements from pile driving activities (see Appendix I).

2.1 Pile Type based on Load Transfer and Installation

Piles can be classified according to different aspects, such as load transfer, installation method, shape and material.

There are two fundamental types of piles based on their load transfer behaviour: end-bearing and friction (see Figure 2.5). In *end-bearing* piles the load is transferred through the bottom tip of the pile onto a solid stratum (compacted sediment or rock) located at a reasonable depth; the pile behaves as a column. In *friction* piles the load is transferred to the soil through the entire length of the pile by skin friction. Generally, end-bearing and skin friction resistances do not act simultaneously and one predominates, being the reason why piles are designed for one particular mode of load transfer. A closed or plugged bottom tip provides end-bearing weight transfer; pipes of larger diameters may not plug, but develop additional skin friction in the internal surface.

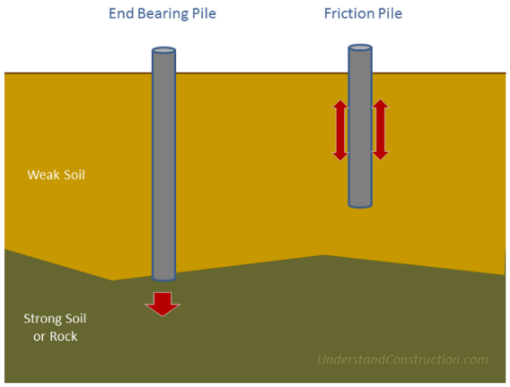

Figure 2.5 Graphical description of the operation of end-bearing and friction piles (from www.understandconstruction.com).

Piles can be of two types according to the installation method: displacement or replacement. Bored or *replacement* piles require a drilled hole where the pile is formed with concrete (see Figure 2.6). Replacement piles include micropiles or pin piles, Cast-In-Drilled-Holes (CIDH) and Cast-In-Steel-Shells (CISS). Micropiles

are thin pipes, 10-50 cm in diameter, consisting on a steel case filled with cement grout and a central reinforced-steel bar. CIDH and CISS are large diameter bored piles made of a steel case filled with reinforced concrete. Driven or *displacement* piles are built before being driven with a hammer; this is the category of piles addressed in this report. Driven steel piles are used in thick sediment deposits whereas drilled, cast-in-situ piles are constructed in rock (Chatzigiannelis et al, 2009). Piles driven in consolidated sediments and rock have square or blunt ends, since pointed tips will bend and break the pile (Gerwick, 2007).

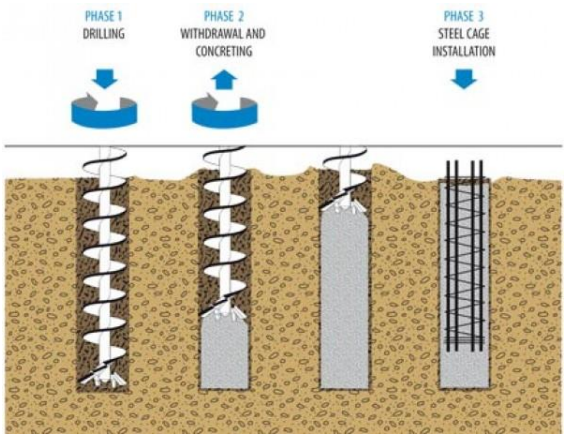

Figure 2.6 Graphical representation of the pile boring process for CIDH, CISS or micropiles (from pumpshop.in)

2.2 Pile Type based on Shape and Material

The most common types of pile according to shape and material are the steel pipe, steel H-beam and steel sheet pile, concrete pile and wooden pile.

Steel pipes are hollow piles used in most offshore foundations, with diameters of 0.6-2 m, wall thicknesses of 20-50 mm and lengths of the order of 40-60 m. In harbour works, diameters of 0.4-0.6 m are typical (Gerwick, 2007). Pipe piles are either open or close-end. Close-end pipes incorporate a steel plate to cover the bottom tip of the pile, which can be filled with concrete and is suitable for penetration of hard, consolidated sediments and rock. The monopile is the largest category of pipe piles, with diameters of around 4 m and lengths of 50 m or more, mostly used in windfarm construction.

The steel *H-beam* piles are most effective for penetrating hard strata, and are commonly used in dense soils or rock as end-bearing piles. Although capable of penetrating conglomerate and dense, coarse sands, they do not respond well to cobbles, boulders or irregular hard rock (Gerwick, 2007). H-beam piles are typical in harbours, frequently used as end-bearing piles for bridge piers, and can be used along with sheet piles to add lateral stiffness and bending resistance.

Sheet piles are steel plates with interlock connections to allow construction of long, continuous walls. The plates are 9-12 mm thick and up to 30 m long. Sheet piles are rarely part of permanent structures and are mostly employed for quay walls and cofferdams. These can be used in very deep cellular cofferdams, to enable dewatering and subsequent construction in the dry. Vibratory hammers are efficient in driving sheet piles, which are often installed as preassembled pairs; in hard soil conditions, an impact hammer may be required. Although steel is the most common material for sheet piles, new materials such as plastic, concrete and fiberglass has been proven to be equally effective, and often less expensive.

The most commonly used displacement *concrete piles* are *pre-cast*, i.e. piles that are cast and cured in one location and then transported to the pile driving site. These are moulded in circular, square, rectangular and octagonal form, with diameters of 0.3-0.7 m and lengths of 1-30 m. *Pre-stressed* piles are

heavily reinforced and highly stressed pre-cast concrete piles, characterised by a high lateral bending capacity and the ability to penetrate hard strata. Pre-stressed concrete piles are commonly used for harbour structures, such as wharves, quays and trestle bridges; harbour piles are typically hollow-core, with wall thicknesses of 10-20 cm, diameters of 0.5-0.6 m for square and octagonal shapes, and diameters of 0.9-2.1 m for cylindrical shapes, (Gerwick, 2007). In offshore terminals, larger pre-cast concrete piles have been extensively used, with diameters of nearly 2 m and lengths of up to 50 m. Unlike steel piles, which are sensitive to high compression stresses from hard impact driving, concrete piles are subject to damage by the tensile rebound stresses in soft driving (i.e. initial blows); concrete piles, on the other hand, are capable of resisting high compression forces (Gerwick, 2007).

Wooden piles are made from straight trunks, with the length limited to that of a single tree (~ 20 m). Wooden piles are generally used for temporary works, but are not uncommon as permanent foundations in places where timber is abundant. These piles are not suitable for firm grounds, where they can be easily damaged. To protect the pile tip for driving in harder substrates, a toe cover can be provided.

A pile's material will not only affect the acoustic radiation characteristics of the pile, but also the maximum length, diameter, bearing capacity and potential application. Steel piles are easy to splice, reach up to 50 m in length, have a high capacity and are best suited for end-bearing on rock, but are vulnerable to corrosion. Concrete is used to manufacture replacement (cast-in-place) or displacement (pre-cast – ordinary reinforcement or pre-stressed) piles, generally resistant to corrosion; pre-stressed concrete piles support higher lengths and capacities than reinforced pre-cast piles (18-25 m vs 10-12 m long; 3500 vs 350 kN bearing capacity). Timber piles are best suited as friction piles for granular sediments, have a limited length of 9-20 m, since they are difficult to splice and thus made of single tree trunks, are vulnerable to hard driving, and are resistant to decay when permanently submerged. Composite piles are made of two or more sections of different materials or pile types; for example, concrete or steel can be used above a section of timber to avoid decay in the wood above the waterline.

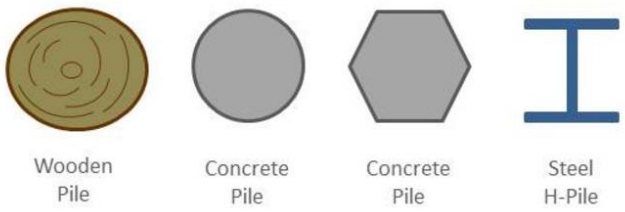

Figure 2.7 Common pile cross sections and materials (from www.understandconstruction.com)

3 The Hammer

The pile driver or *hammer* is the mechanical device used to drive piles into the ground. The type and dimensions of the pile driving equipment affect the sound generated during the pile driving activity (ICF Jones & Stokes, 2009). In particular, the mechanical principle, type of contact with the pile, driving energy and impact rate of the hammer are some of the hammer-related factors contributing to the acoustic emission during pile driving operations.

There are three main types of pile hammers based on their mechanical principle: impact, vibratory and push-in. Impact hammers use a large weight, which is raised to a certain height and released to strike the pile by the effect of gravity. Vibratory hammers use rotating eccentric weights to transmit a low frequency, vertical vibration to the pile. The push hammer is a newer technology that uses hydraulic rams to push piles into the ground using static force (ICF Jones & Stokes, 2009). Impact and vibratory hammers are the most common pile driving options, followed by push hammers. Vibratory and push hammers are quieter solutions, but they have limited pile driving capabilities and can only be used in a limited number of scenarios; moreover, pile proofing with an impact hammer may still be required.

According to the ram-lifting mechanism, impact hammers are further classified into drop, air/steam, diesel and hydraulic. Vibratory hammers are grouped into low, medium and high frequency devices. A detailed description of impact and vibratory pile drivers is included in Sections 3.1 and 3.2. A simple comparison of sound levels from the tables in Appendix I show no apparent contribution of the type of ram-lifting mechanism in impact hammers to the acoustic output. However, a similar comparison between impact and vibratory systems show that vibratory drivers generate broadband signals 10 to 30 dB lower than that from impact hammers (see Figure 3.1).

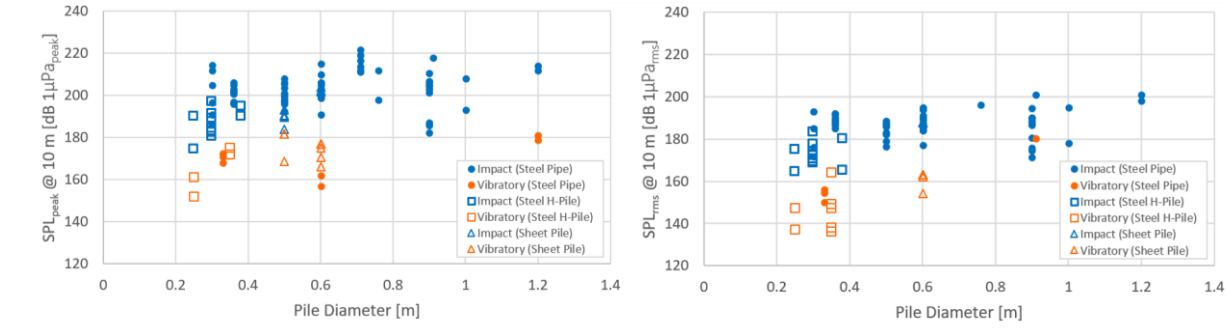

Figure 3.1 Sound pressure level peak (left) and RMS (right) with pile diameter for steel pipes, H-beams and sheet piles driven by an impact or vibratory hammer. Graphs obtained from published measurements on pile driving sounds (see Appendix I).

A higher blow or strike energy in an impact hammer tends to produce higher sound levels. Robinson et al. (2007) found a roughly linear relationship between hammer energy (J) and energy flux density of the acoustic pulse (J/m^2). The increase in sound level caused by an increase in blow energy can be approximated by $10\log(E_2/E_1)$, with E_1 and E_2 the initial and final blow energies. A steeper increase in sound level is expected in the main frequency range of impact pile driving (100-1000 Hz), where $13\log(E_2/E_1)$ is a more realistic approximation (Nehls et al., 2007). In Figure 3.2, the left-hand graph represents the sound levels (peak and RMS) of single impact hammer strikes on different types of piles and

locations, normalised to a distance of 10 m; despite the spread of sound levels, caused by the particular radiation and propagation characteristics of each measurement, there is a clear increase in sound level with the hammer's blow energy. The approximate strike-SPL relationship will change with location as a result of the local seabed composition (Haan et al., 2007). The dependence of the acoustic pulse amplitude on pile type and size, seabed composition and bathymetry is more complex (Robinson et al., 2007).

The increase in strike energy not only results in a higher broadband sound level, but also alters the spectral content of the radiated sound (Jong & Ainslie, 2012). The right-side graph of Figure 3.2 represents the third-octave band spectrum of a steel monopile for two strike energies; the higher impact energy results in an increase of the radiated sound above 1 kHz.

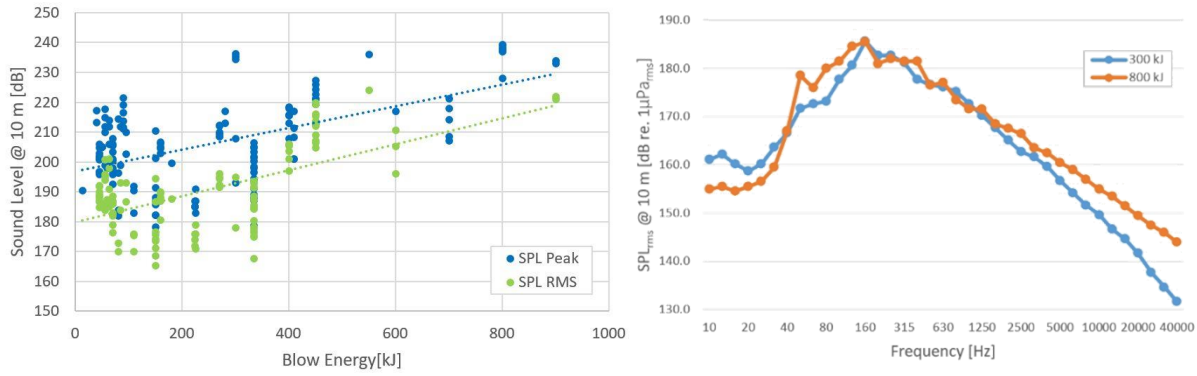

Figure 3.2 Sound pressure level (peak, RMS) as a function of blow energy from impact pile driving, for a combination of steel pipes and monopiles (left). The effect of blow energy on radiated sound spectrum of a 4 m diameter monopile is shown on the right (after Jong & Ainslie, 2012).

The strike repetition rate and the stroke height in an impact hammer are related to each other by the saximeter formula, in a way that a higher repetition rate will limit the maximum stroke height or impact energy that can be used (Haan et al., 2007). The repetition rate could vary between 30 to 60 blows per minute. In general, a higher repetition rate does not necessarily result in a faster pile driving operation, since the impact energy is compromised (i.e. larger number of hammer impacts of lower energy in a similar period of time). The selection of the repetition rate may not have a definitive effect on the cumulative sound exposure experienced by a marine animal, but the chances of that animal being exposed to high intensity acoustic events are greatly reduced.

The type of pile and soil are two major considerations when selecting a pile hammer. The pile is selected according to its function, material, weight, dimensions, capacity and required penetration. The soil can be *cohesive*, i.e. compact clay-based soils, or *non-cohesive*, such as loose gravel and sand. Vibratory drivers work better in non-cohesive soils, whereas strong impact blows are required for cohesive, stiff clays (Barber, 1978).

3.1 The Impact Hammer

Impact pile driving is the most commonly used method for driving piles, especially for piles with larger diameters. Impact hammers use a ram, raised to the desired height by various possible mechanisms (ignition, hydraulic, steam) and dropped against the pile (ICF Jones & Stokes, 2009). The size and type of impact hammer is selected according to the energy required to drive the pile to the aim depth in a given substrate. The impact energy equals the weight of the ram times the height of free fall, but is higher in double-acting hammers, which include mechanisms to increase the acceleration of the ram (Barber, 1978). Although larger piles require higher impact energy, there is no simple rule to calculate the strike energy as a function of pile diameter (Nehls et al., 2007). It is common practice to use a larger hammer and operate it at 2/3 of its maximum energy, to reduce the mechanical fatigue on the pile (Barber, 1978).

During the installation phase, the pile is first placed or *pitched* and allowed to penetrate the ground under its own weight (e.g. steel and concrete piles). The hammer is lowered, pushing the pile further into the ground. Then the pile driving operation starts. The driving head in the hammer is designed to transmit the impact to the pile head, and contains the pile head cushion. The cushion material (typically a 20-40 cm thick plywood block) is used in concrete piles to extend pulse duration and prevent cracking; in steel piles no cushion block is needed (Gerwick, 2007).

3.1.1 Types of Impact Hammer

According to the lifting mechanism and action principle, impact pile drivers are classified as: *drop*, *air/steam* (single, double, differential), *diesel* (single, double) and *hydraulic*; the last two are the most common today. All of them depend on the mass of the ram, accelerated by gravity and additional mechanisms. The energy of the stroke is transmitted into the pile in a fraction of a second. A recent driving technology called Blue Piling utilises a water-filled cylinder to extend the duration of the stroke; this method is described in detail in Chapter 6, "Sound Mitigation and Attenuation Methods".

The *drop hammer* is the oldest type of impact hammer, and also the simplest. The ram is operated between guides and lifted by a winch to a desired height, where it is released to impact the pile head with the kinetic energy acquired in free fall. The driving energy is the product of the weight of the ram and drop height. Typical ram weights are between 0.5 and 3 t. The drop hammer is still used today, but its operation is rather slow compared to other types of pile driver.

The *single-acting air* or *steam hammer* uses compressed air or steam to lift the ram, which falls by its own weight when the attached piston exhausts the gas after reaching a pre-defined height. The propelling force is exclusively due to gravity, so the manufacture's rated energy is simply based on ram weight and stroke height. Typical energy ratings go from 10 to 1600 kJ, with repetition rates of 35-60 bpm. Single-acting hammers are better suited for driving piles in cohesive soils, since lower repetition rates allow the soil and pile to settle before the next blow, improving maximum single-strike penetration. In *double-acting air/steam hammers* the compressed gas is used to both lift and accelerate the ram downwards. The downward acceleration contributes to increase the impact energy and the repetition rate to nearly double of that from a single-acting model. Double-acting hammers are more advantageous in coarse, non-cohesive soils and soft clays. The *differential air/steam hammer* is similar to a double-acting version, but with a different exhaust sequence (Barber, 1978).

In a *single-acting diesel hammer* the ram is lifted by an initialization mechanism to a pre-defined height, where the ram is released, falling under its own weight. An amount of fuel is injected in the anvil's chamber and the intake/exhaust ports are closed. When the ram strikes the anvil it transmits the impact to the pile, at the time the fuel in the combustion chamber is ignited; the explosion pushes the pile further into the ground and raises the ram. As the ram moves upward the intake/exhaust ports are open to discharge the gas from combustion and refill the chamber with fresh air. The cycle is repeated as the ram reaches the final height. Typical energy ratings are between 12 and 400 kJ, with repetition rates of 35-60 bpm. Compared to air/steam hammers, diesel hammers have the advantage of their smaller weight (1/3 of an air/steam hammer) and operation without auxiliary equipment, such as compressors or boilers (Barber, 1978). Single-acting diesel hammers are best suited to medium-hard sediments; in soft substrates the required compression for ignition may not be reached. In a *double-acting diesel hammer* a bounce chamber consisting of compressed air enclosed between compression rings is installed above the ram. The enclosed air constrains the upward displacement of the ram and its rapid expansion adds to the force of gravity to propel the ram downward and increase the repetition rate. The ram weight is twice that in a single-acting diesel hammer, while the stroke height is approximately halved. Stroke energies range from 11 to 110 kJ, with repetition rates of 80-100 bpm. The double-acting models are most effective in coarse sediments and soft clays (Barber, 1978).

3.1.2 Mechanisms of Sound Radiation

Unlike other types of industrial sound sources such as air guns or sonar systems, which emit sound in the water column, piles extend to three different regions: air, water and seafloor. Piles emit sound directly into the air and the water, and excite elastic waves in the seafloor which can have an important contribution to the sound field formed in the water column. The strike of an impact hammer creates a compressive wave that travels through the pile producing sound in three main ways: 1) direct acoustic radiation from the submerged pile, 2) vibration and sudden displacement of the embedded portion of the pile, and 3) surface waves propagating along the water-sediment interface (Duncan et al., 2010).

The primary source of sound generation in impact pile driving is the *Mach wave* formed when the radial expansion wave, produced after the hammer impact, propagates along the pile at higher speed than the speed of sound in water (Reinhall & Dahl, 2011). The sound pattern created by the Mach wave appears as a *cone* centred in the pile axis and pointing in the direction of propagation of the longitudinal wave, with the apex on the peak of radial deformation and an angle of aperture defined by $\varphi_w = \mathrm{asin}(c_w/c_p)$, where c_w and c_p are the speeds of sound in the water and the pile. Typical values of φ_w are of the order of 15-20° (see Figure 3.3). The resulting *plane wave* propagates in the water perpendicular to the direction of the sides of the cone.

The initial Mach wave is followed by weaker pressure variations due to oscillations in the pile wall, with low contribution to the total sound field, which is dominated by the peak pressure associated with the Mach cone. The Mach wave is partially reflected on the bottom-end of the pile, due to an impedance mismatch between pile and sediment, and then propagated upwards; another reflection occurs on the top of the pile. The original downward pulse carries most of the energy and only the first bottom and top reflections in the pile contribute to some extent to the total acoustic emission (Reinhall & Dahl, 2011).

Additionally, when the radial deformation reaches the seabed, both vertically polarised shear waves and compressional waves are created, with the first ones carrying most of the energy. Scholte waves appear in the seabed-water interface, which contribute with pressure variations near the seabed (0.5-1 m), increasing the acoustic energy especially at frequencies under 50 Hz (Tsouvalas & Metrikine, 2014). Stoneley waves can also propagate in the interface between sediment layers. A portion of the energy transmitted into the seabed can also travel within the substrate and return to the water column at some distance from the source (Hawkins, 2009).

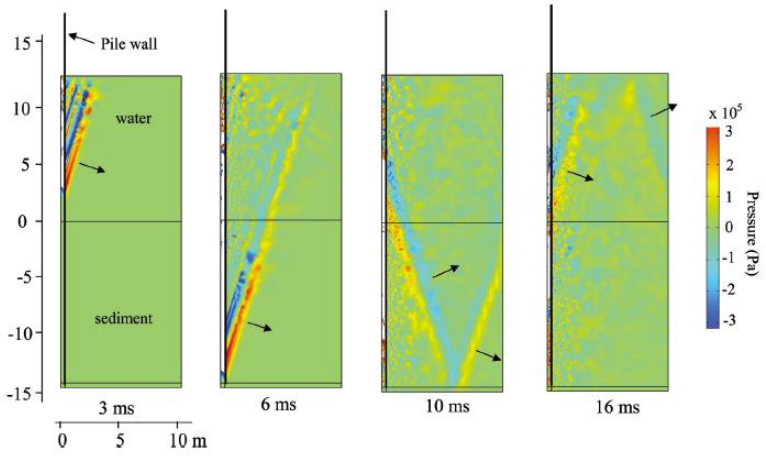

Figure 3.3 Coloured surface representation of the modelled sound pressure field created by a pile 3, 6, 10 and 16 ms after hammer impact. The arrows indicate the direction of propagation of the wavefront from the Mach wave (from Reinhall & Dahl, 2011).

The waveform of the acoustic pulse can be approximated to a sudden increase in amplitude at the moment of impact followed by a roughly exponential decay (Reinhall & Dahl, 2011); a smoother, bell-shape response

may be expected for damped hammer-pile connections (e.g. cushion on pile head, or pile made of soft material). The pulse of the downward Mach wave reaches the bottom tip of the pile in less than 10 ms after impact. For a given depth, the range of action of the downward Mach wave is limited to $h_w/\tan\varphi_w$, where h_w is the water depth (Reinhall & Dahl, 2011). In terms of spectral response, the sediment mainly contributes to frequencies below 160 Hz; at higher frequencies conical waves experience little influence by soil conditions. For harder substrates the peak in the spectrum shifts towards higher frequencies (Tsouvalas & Metrikine, 2014).

3.2 The Vibratory Hammer

Vibratory hammers use the rotation of eccentric weights to transmit vertical vibration to the pile, which loosens the sediment around it and allows the pile to penetrate into the ground. Vibratory drivers are most effective in granular, non-cohesive sediments; only large models can be effective in cohesive soils and clays, where the strong oscillatory motion reduces the grip of the soil and allows the pile tip to penetrate (Barber, 1978). The effectiveness of vibratory hammers is greatly improved in sediments with high water content, such as high porosity marine sediments.

Although vibratory hammers are suitable for non-cohesive soils, final seating and pile proof testing with impact hammer may be required for steel piles; concrete piles are generally driven with impact hammers (Gerwick, 2007). Piles with large tip areas, such as close-end pipes, and solid concrete and timber piles are not effectively driven with vibratory hammers. On the other hand, sheet piles, H-beam piles, and open-end pipes are better suited for vibratory drivers, since the displacement of the grains required for the pile to sink is much lower (Barber, 1978). Large vibratory drivers can be used to drive medium to large piles, but the required penetration depth may not be achieved (Matuschek & Betke, 2009).

The vibratory hammer provides some advantages over the more conventionally used impact hammer. It is a proven sound reduction technique with a reduction of about 15 – 20 dB over an impact hammer (Matuschek & Betke, 2009; Elmer et al., 2007). Most of the sound from vibratory pile drivers is radiated within the frequency range of the vibration frequency of the pile driver, which is generally between 20 and 40 Hz; this is generally a range at which marine mammals are not as sensitive (Elmer et al., 2007). The vibratory hammers are also able to extract piles by breaking the grip of the soil to allow a crane to pull the pile out of the ground. There is no need for a temporary guide frame for driving free-standing piles. Vibratory drivers are also lighter and faster at operating in non-cohesive soils with non-displacement piles such as sheet piles, H-beam piles and open-end pipes, which can be driven up to eight times faster than impact hammers (Jonker, 1987; Barber, 1978).

3.2.1 Parts of a Vibratory Hammer

The two main components in a vibratory hammer (see Figure 3.4) are *the exciter*, which generates the vibrating force, and the *power pack*, which provides the energy for the rotation of the eccentric weights (Warrington, 1992).

The exciter has three main components: the vibrator case, the suspension system and the clamp (Barber, 1978; Warrington, 1992). The *vibrator case* contains the rotating eccentric weights, which generate the centrifugal force. The *suspension system* is connected to the vibrator case by springs; it provides additional weight to push the pile into the ground and isolates the vibrator case from the crane boom to protect it from vibrations. The driving/extracting head or *clamp* connects the vibrator case to the pile; most clamps use frictional connection through hydraulic jaws, but few bolt the pile to the vibrator case.

The *power pack* is electric or hydraulic. Both power sources are external, and supply power to the eccentric weights by cables (Barber, 1978). Electric systems are less popular due to maintenance and reliability aspects (Warrington, 1992).

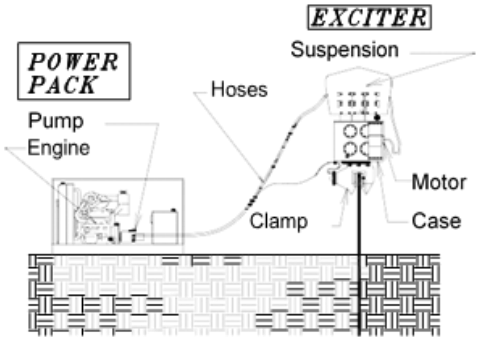

Figure 3.4 Parts of a vibratory pile driving system (from Warrington, 1992).

3.2.2 Operation of a Vibratory Hammer

The eccentric weights in a vibratory hammer have the same weight and rotate in opposite directions to transmit a repetitive, continuous vertical vibration to the pile through the hydraulic clamp. As the pile vibrates, the resistance of the soil in contact is reduced, so the pile can penetrate by its own weight or be easily pulled out by a crane (Barber, 1978; Warrington, 1992).

The performance of a vibratory hammer depends on the amplitude, eccentric moment, frequency, dynamic or centrifugal force and vibrating weight. The *amplitude* is the amount of vertical displacement of the driving head and is directly related to pile penetration; the *eccentric moment* increases with the amplitude. The *frequency* is the number of complete rotation cycles of the eccentric weights in a second (up and down movement). The *vibrating weight* includes the vibrator case, driving head and pile.

In vibratory pile driving the type of pile and the response of the soil to vibration, both frequency dependent, are the critical factors. Vibratory hammers are less effective in cohesive soils, but penetration can be improved by increasing the amplitude of vibration. Vibratory drivers are used in virtually any type of pile, but are most typically used on non-displacement piles such as open-end pipes, sheet piles and H-beams. In sheet walls the piles are normally set in place and driven two at a time, but can also be driven individually. Concrete pile installation with vibratory hammers is less common, and requires low-frequency, high amplitude drivers. Vibratory hammers are relatively common for the extraction of wooden piles (Warrington, 1992).

3.2.3 Types of Vibratory Hammer

Vibratory hammers can be classified according to their frequency of operation on low, medium and high frequency (Warrington, 1992). *Low frequency* drivers operate in the range of 5-10 Hz with large eccentric moments (i.e. high amplitude), and are mainly used with heavy piles with high toe resistance, such as concrete piles and close-end steel pipes. *Medium frequency* drivers operate in the range of 10-30 Hz, are best suited for sheet piles and small pipes, and are the most common since they have the adequate dynamic force, frequency and amplitude necessary to interact with most soils. *High frequency* drivers vibrate at frequencies between 30-40 Hz and are designed to minimise interaction with neighbouring structures, but are not effective in many types of soil. In a class by itself within the high frequency hammers is the *resonant driver*, which operates in the range of 90-120 Hz to match the resonant frequency of the pile and in this way facilitate penetration and extraction.

3.2.4 Mechanisms of Sound Radiation

In vibratory pile driving the acoustic energy is concentrated in the bottom of the water column and consists of low frequency components, in general much lower than those found in impact pile driving (Tsouvalas &

Metrikine, 2014). Most of the acoustic emission is caused by vertically polarised shear waves and Scholte waves (see Figure 3.5); the Mach wave radiation pattern, already described in Section 3.1, cannot be distinguished in the particular example presented by Tsouvalas and Metrikine, which would suggest a lower contribution of Mach waves to the sound field in the water column. Many pile foundations are found in shallow coastal waters, where low frequency components cannot easily propagate; this circumstance contributes to further attenuate the sound produced by vibratory pile driving (see Chapter 5, "The Environment").

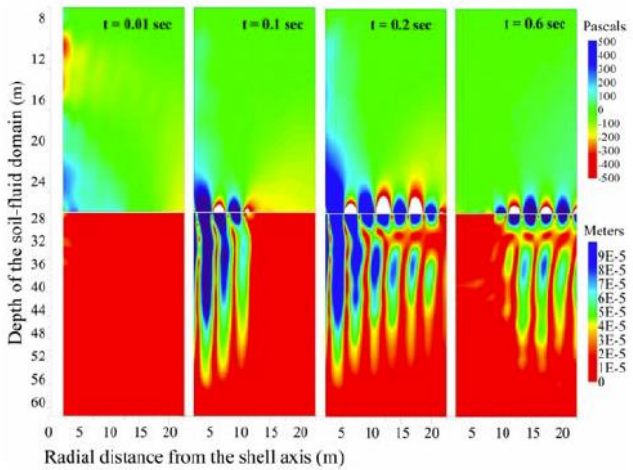

Figure 3.5 Coloured surface representation of the modelled sound pressure field created by a pile 10, 100, 200 and 600 ms after the start of vibratory driving (from Tsouvalas & Metrikine, 2014).

4 The Pile Driving Operation

4.1 Pile Installation

In a pile driving operation, the first step consists of placing the pile and hammer, allowing the pile to settle and checking for vertical alignment, then the pile driving starts. The operation commences with low-energy strikes to monitor and adjust the alignment of the pile, but also as a warning measure for marine animals in the area (see Section 4.3, "Soft Start"). Once the pile has been driven, further checks are carried out to ensure the pile attained the required depth.

The blow rate in impact pile driving is approximately 30-60 blows per minute and may last for several hours, depending on substrate conditions, pile type and stroke energy (Gordon et al., 2007). If a pile cannot be driven to the required depth, an insert pile is placed inside the primary pile and driven ahead, achieving further penetration due to the lack of skin friction. Where soil conditions do not permit pile driving, the pile can be grouted into a previously drilled hole (Gerwick, 2007).

An example of a four-legged steel jacket installation for wind turbines is described by Bailey et al. (2010). Four steel pipes 1.8 m in diameter and 44 m long were driven almost entirely into the substrate to 'pin' the jacket to the seafloor by its four corners. Two hours were spent on driving each pile, which required around 6000 strokes. The installation of monopiles for wind turbines is described by Jong & Ainslie (2012). Each monopile was 4 m in diameter and 54 m long, driven 30 m into the seabed. In a similar monopile installation project described by Lepper at al. (2007), the strike periodicity was 2 s (30 bpm) and became more erratic as the pile approached refusal. Pulse durations were in the range of 150-200 ms, with most of the energy concentrated at low frequencies and no important contributions beyond 22 kHz.

Some of the factors related to piling operations which contribute to the radiated sound include the hammer-pile contact, soft start period, pile direction and pile penetration. Additional operational factors with an effect on the acoustic signature that are already mentioned in other chapters include: jetting in piles, hammer driving parameters (e.g. blow energy, blow rate) and pile driving methodology (e.g. insert pile).

4.2 Pile-Hammer Contact

An improper connection between a vibratory hammer and the pile may result in abnormally high sound levels (ORPC Maine, 2012). Additionally, a hammer that is capable of operating underwater will have a different effect on the acoustic signature of the pile depending whether it is submerged or driving over the water line.

4.3 Soft Start

The *soft start* is a noise mitigation measure that takes place at the beginning of the pile driving sequence, and consists on a series of low energy blows which gradually increase in level over a period of time. After the soft start, the full pile driving energy is reached and maintained. A soft start reduces the level of the initial hammer strikes, minimising the potential impact on any animals in the vicinity and giving them a

chance to leave the area before the piling operation reaches full power (Robinson et al., 2007). Soft starts have also been reported for vibratory pile driving (ORPC, 2012).

Information published on soft starts suggests that the duration of the sequence varies considerably among pile driving projects, with values ranging from a few minutes to one hour. The level reduction that can be achieved during the soft start, compared to the full active period, is around 5-20 dB. Bailey et al. (2010) describe a soft start sequence consisting of five low energy hammer strokes with 15% of the total energy (63 kJ) separated by 5, 3, 2 and 1 minutes, followed by a slow energy increase over a period of 20 minutes. Lepper et al. (2007) report another soft start sequence, characterised by an increase of blow energy from 80 kJ (10%) to 800 kJ (100%) over a period of 68 minutes. The sound levels appeared to increase gradually (see Figure 4.1), with sound level differences from the start to the full active period of 12, 13 and 8 dB for SPL_{pk-pk}, SPL_{rms} and SEL.

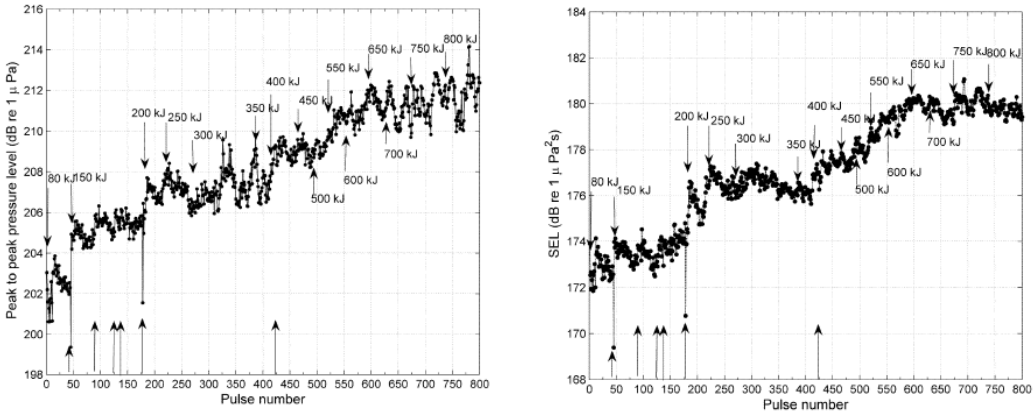

Figure 4.1 Evolution of peak to peak sound pressure level (left) and sound exposure level (right) during a soft start period applied on impact pile driving. The hydrophone is placed at a range of 57 m. The bottom arrows denote breaks in the piling sequence (Robinson et al., 2007).

The soft start sequence extends the duration of a typical piling operation by around 20% (e.g. 600 strokes during soft start described by Robinson et al., 2007). In general, a soft start minimises the risk of impact from high sound pressures (e.g. PTS), but may increase the chances of behavioural disruption and risk of high cumulative sound exposure (Gordon et al., 2007).

4.4 Pile Direction

Piles installed vertically (plum) or at an angle (battered) have a different acoustic response. Batter piles are typically used to resist lateral loads, and act in conjunction with a vertical or an opposing batter pile (Gerwick, 2007). Battered piles produced slightly higher sound levels (< 5 dB_{0-p}) than piles driven vertically in a study documented by Illinworth & Rodkin (2007).

4.5 Pile Penetration

The sound levels tend to increase with the first few blows (10-100) of an impact hammer driving at constant energy. These levels experience a slight decrease after reaching normal values. This effect has been shown in cedar piles and steel pipes (Vagle, 2003; Abbott & Reyff, 2004), but may also occur in other types of pile. The fast initial increase and later decrease in sound level during the piling operation are shown in Figure 4.2.

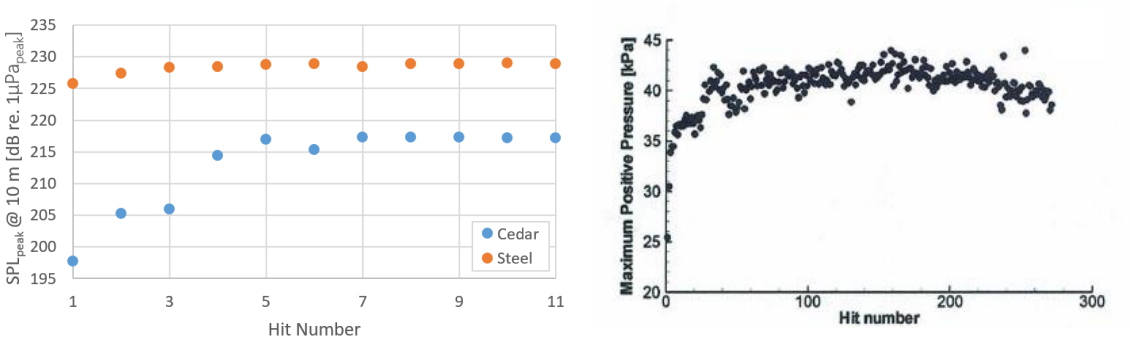

Figure 4.2 Effect of pile penetration depth, represented as hit number, on the peak sound pressure level for two types of pile: steel pipe (0.5 m ø, 210 kJ drop hammer, sand/clay) and cedar pile (0.2 m ø, 40 kJ drop hammer, mud/clay). A larger number of hits is shown in the right-side figure for the steel pipe; note the fast initial increase in sound pressure and slight, smooth decrease at the end of the piling operation (from Vagle, 2003).

Robinson et al. (2007) observed the same effect, particularly at the beginning of the soft start sequence. The soft start was characterised by a low blow energy, kept constant during the first ten minutes, with break periods in between. The level sometimes recovered after a break period, when the sequence restarts with the same blow energy. The reasons for the initial increase in sound level, subsequent decrease and level recovery after a break are still unclear (Vagle, 2003) but may be related to increase in substrate resistance and better transmission of vibrations through the sediment as the pile gradually penetrates the sea bottom (Robinson et al., 2007; Blackwell et al., 2004; Haan et al., 2007). Jong & Ainslie (2012) did not observe variation of piling sound with penetration depth during the Prinses Amaliawindpark project, and justified the lack of sound instabilities by the limited resistance exerted by the sediment on the driven pile. As Robinson et al. (2007) highlight, these variations in sound level associated with pile penetration are not always present, and may occur only during some of the piling sequences taking place during the installation of a pile.

Robinson et al. (2007) describe an additional effect related to pile penetration depth, consisting of a bounce or re-strike of the hammer as the pile approached refusal during the full energy phase, generating a series of pulses. The sound level at this stage experienced higher variability (see Figure 4.3).

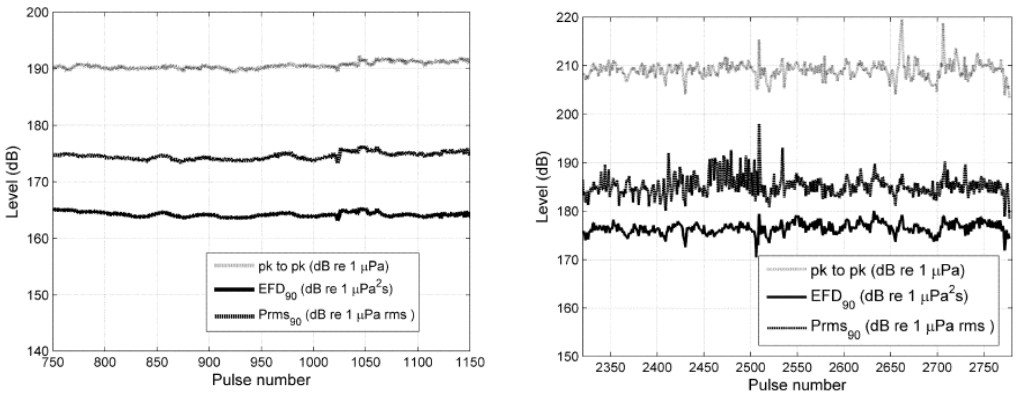

Figure 4.3 Received sound level during the main piling sequence (left) and at the end of it. Hydrophone placed at 57 m from the pile. Note the high sound level variability as the pile approaches refusal (from Robinson et al., 2007).

5 The Environment

The main factors related to the environment which contribute to the sound propagated underwater include the bathymetry and water depth, water properties, seabed composition and sea surface conditions. The sound field may also show high variations throughout the area; accordingly, the depth of the receiver and its distance from the source have an immediate effect on the received sound level. All these factors and their effects on the radiated sound are described in the following sections.

5.1 Bathymetry and Water Depth

The seabed topography is known to have an important effect on the propagation of sound, especially in shallow waters, enhancing multipath propagation and contributing to focusing (e.g. caustics) and shadowing effects. The directional dependency of the bathymetry also has an effect on the spatial pattern of the sound radiated by the pile (Bailey et al., 2010).

Water depth plays a critical role in the transmission of sound. Pile driving operations normally take place in shallow coastal waters. The transmission of low frequency sounds depends on the local water depth, which sets a cut-off frequency below which sound cannot effectively propagate (normal mode free region). The cut-off frequency is given by (Urick, 1983):

$$f_w = \frac{c_w}{4h_w}\sqrt{\frac{1}{1-(c_w/c_b)^2}} \qquad (5.1)$$

where f_w is the cut-off frequency, c_w the speed of sound in water, c_b the speed of sound (i.e. compressional velocity) in the sea bottom and h_w the depth of the water column. Eq. 5.1 can be approximated to $c_w/(4h_w)$ for hard substrates. Figure 5.1 shows and example of the low-frequency roll off at two different water depths for a 4 m ø monopile.

The attenuation caused by the limited water depth may be noticeable only in certain directions where the water depth is lower. This directional attenuation is shown by Abbot & Reyff (2004), who describe a faster pressure drop-off toward the East, where waters become shallower.

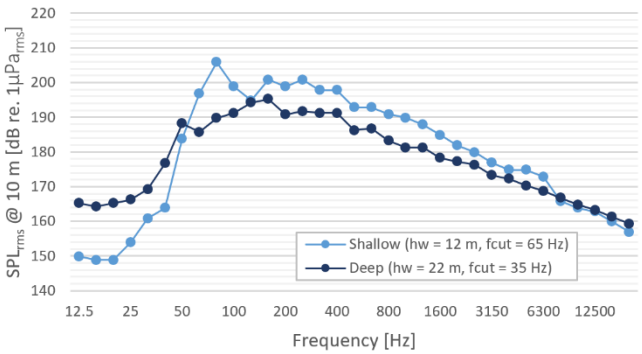

Figure 5.1 Effect of water depth on low frequency sound propagation. Measurements from 4 m diameter monopiles driven with impact hammer in two different projects (shallow water curve, from Betke, 2008; deeper water curve, from Jong & Ainslie, 2012).

At high frequencies the attenuation of sound increases due to higher absorption and seabed and surface scattering. The combination of the low-cut frequency and high frequency attenuation results in an optimal transmitted frequency band (Blackwell et al., 2004; Jensen et al., 2011). The overall sound level in shallow waters tends to be several decibels lower than in deeper waters; measurements from wind turbine construction presented by Betke (2008) show broadband sound level reductions of 8-13 dB at waters 2 m deep with respect to deeper waters of 10 m or more.

5.2 Seabed Composition

The seabed substrate plays a major role in the sound produced by pile driving activities, as the pile is in direct contact with the seabed. This contact conditions the type of pile and hammer to be used, the vibration of the pile, and provides an effective path for energy transmission. Additionally, the seafloor has an important effect on the frequency response of the sound in water.

The vibration generated by a driven pile is transferred into the substrate and can return to the water column at some distance from the source. Scholte waves can also be formed, which may have an important contribution to the received level, especially close to the seabed.

Sound pressure levels during pile driving can vary as much as 18 dB just as a result of the substrate (Blackwell et al., 2004). Coleman (2011) reports an increase of around 20 dB on a steel pipe driven in hard, consolidated sediment, compared to measurements made on an area of less compacted material. Evans (2008) found from published pile driving data that source levels produced by piles installed in hard substrates can exceed 240 dB_{rms}@1 m, a statement confirmed by several authors (see Appendix I).

5.3 Water Surface

The scattering from the sea surface can have an important effect on the underwater sound field. The sea surface under calm sea state conditions behaves as an almost perfect reflector, and nearly all the energy is reflected in the specular direction. In the presence of wind, the surface is altered and its roughness results in the scattering of sound in multiple directions. The energy in the specular direction is accordingly reduced, and the scattered energy contributes to the reverberant field.

In arctic waters, the generally positive gradient of the speed of sound with depth contributes to the generation of surface ducts. This effect, combined with the scattering and absorption from the ice canopy, results in high sound level attenuation with range (Jensen et al., 2011; Blackwell et al., 2004).

The wind and the action of waves generate microbubbles ranging in size from 1 to 100 µm. The air has a very different impedance than the water, and a layer of microbubbles will result in absorption and scattering effects. These bubbles resonate at frequencies between 50 to 300 kHz, well above the range of frequencies covered by pile driving sounds, and their effect on the overall sound level is expected to be negligible.

5.4 Receiver Distance

The sound level tends to decrease and the pulse duration to increase as the distance between source and receiver becomes higher (Bailey et al., 2010). High frequencies experience the highest attenuation with distance. In measurements reported by Abbott & Reyff (2004) the pulse duration is shown to vary considerably depending on receiver distance and the presence of an attenuation system (e.g. bubble curtain or cofferdam). Measurements from Bailey et al. (2010) show that at a distance of 1 km the initial peak is very pronounced (10 ms) and the total pulse lasts 200 ms; at 40 km the peak duration extends to 200 ms, with the total pulse lasting 600 ms.

Most authors report sound levels as a function of range, in the form of graphs, tabulated data or empirical regression equations. The latter, included in the tables of Appendix I, provides immediate information on the transmission loss with range in a particular environment.

5.5 Receiver Depth

The depth of the receiver during pile driving greatly affects the pressure amplitude, in particular its peak value. Abbot & Reyff (2004) state that peak sound levels close to the bottom can be up to 20 dB higher than near the sea surface. This drop in level is caused by the acoustic interference pattern produced by the combination from the direct signal and the specular, phase inverted reflection from the sea surface. Jong & Ainslie (2012) found from measurements of piling activities for wind farm construction that the most significant variation in sound level occurred in the first 8 m below the sea surface.

6 Sound Mitigation and Attenuation Methods

The methods used to mitigate the impact of pile driving noise on marine mammals can be classified into two groups: 1) those aimed at keeping the animals away from the piling area, such as physical barriers (e.g. nets), acoustic deterrents, marine mammal monitoring and temporary shutdown, and selected time and location of piling activities; and 2) those focused on reducing the sound radiated by the source. This chapter deals with the second group, which comprises several types of attenuation devices installed on or around the source (e.g. bubble curtain, pile cap, cofferdam, etc) and operational solutions (e.g. selection of a low-noise pile driver, controlled blow energy and impact duration, pre-drilled piles, etc...).

The sound attenuation methods are classified into two groups: *active* and *passive*. Active methods comprise modifications in the parameters of the pile stroke that can lead to the reduction of radiated sound, such as prolonging the duration of the impulse from an impact hammer, placing a cap or damper between hammer and pile, or using vibrators for small piles and non-cohesive soils. Passive methods comprise sound barriers installed on or around the pile to reduce the sound transmitted into the water, and include bubble curtains, pile sleeves, and cofferdams. Both methods, active (i.e. modified excitation parameters) and passive (i.e. sound barriers and dampers), can be combined to achieve a higher degree of noise reduction (Elmer et al., 2007; ICF Jones & Stokes, 2009). The details about some common attenuation methods and their potential sound level reduction are presented in the following sections. For further details about the attenuation methods described in this chapter, there is an exhaustive synthesis report from a workshop held in Maryland in February 2013 on quieting technologies for seismic surveys and pile driving (CSA, 2013). For further reading, a comprehensive report about noise abatement systems and their efficacy has been recently published by the Scottish Natural Heritage (Verfuss et al., 2019).

6.1 Air Bubble Curtains

An *air bubble curtain* creates a layer of air bubbles around the perimeter of a pile that inhibits the transmission of sound into the water column. Air bubble curtains can be *confined* or *unconfined*.

An *unconfined air bubble curtain* consists of a perforated ring or hosepipe lying on the seafloor and encircling the pile. Compressed air is pumped through the plastic pipe and a stream of bubbles ascends to the sea surface creating screen with a high impedance contrast. Unconfined systems are inexpensive but not as effective in areas with high tidal currents as bubbles can move horizontally, sweeping away from the pile (see Figure 6.1). In deeper waters (30-40 m), keeping the air bubble curtain concentrated around the pile becomes difficult. Additional rings can be placed at different heights of the pile to compensate for the bubble drift and generate a uniform screen along its length.

A *confined air bubble curtain* typically uses a combination of air resonators and fabric lining. In confined systems, the bubbles are contained within a rigid pipe or flexible material, and are most often used in areas with high tidal currents. These systems have been proven highly effective in currents of up to 3 kn (~1.5 ms^{-1}); the utility beyond 3 kn is limited by the maximum stress tolerated by the casing (PND

Engineering, 2005). The material of the confining casing has a minimal contribution to the overall sound reduction (ICF Jones & Stokes, 2009).

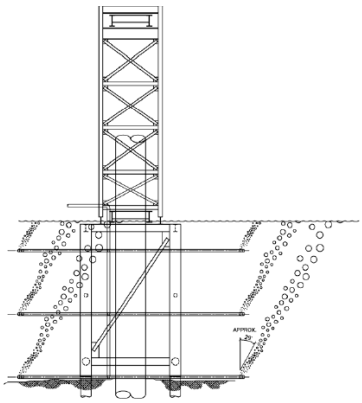

Figure 6.1 Deterioration of a three-ring unconfined air bubble curtain under a 1 knot current (from PND Engineering, 2005).

Examples of proprietary confined air bubble curtains include the Gunderboom® and the Hydro Sound Damper (HSD) (see Figure 6.2). The Gunderboom® Sound Attenuation System (SAS) consists of a double-walled fabric barrier used in combination with a bubble curtain confined within the two layers of fabric (Funk & Rodrigues, 2005). The fabric itself acts as an effective attenuator. The system is expensive, but more effective than unconfined air bubble curtains in attenuating low-frequency sounds (PND Engineering, 2005). The Hydro Sound Damper (HSD) consists of a fishing net placed around the pile with small gas-filled bladders and foam elements attached to it. The attenuation spectrum of the HSD net can be tuned to achieve the desired noise reduction on piles driven by impact or vibratory hammers. The HSD system is compact and economical (Bruns et al., 2014). Proprietary systems can be effective, but are generally more expensive than non-proprietary solutions and may not offer significant benefit (ICF Jones & Stokes, 2009).

Figure 6.2 Photography of the confined air bubble curtain Gunderboom® out of water (left) and details of the deployment of a Hydro Sound Damper (right, from Bruns et al., 2014).

Air bubble curtains rely on both the impedance difference between air and water and resonance characteristics of the air bubbles to reduce the acoustic energy transmitted into the water column (Vagle, 2003). A single air bubble in water behaves as a monopole, with the attenuation factor strongly dependent on frequency and bubble diameter. The resonant frequency of an isolated bubble f_b is given by (Matuschek & Betke, 2009):

$$f_b = \frac{3.25}{R_b}\sqrt{1 + 0.1h_w} \qquad (6.1)$$

where R_b is the bubble radius and h_w the bubble depth, both in metres. The attenuation spectrum of an air bubble curtain depends on the bubble concentration, and to some extent, on the thickness of the screen. The attenuation of the bubble curtain increases with the number of bubbles and thickness of the

screen. The bubble curtain provides a moderate attenuation above the resonance frequency (~ 5 kHz), at which the maximum absorption is reached (see Figure 6.3). The damping at the resonant frequency and overall attenuation of a bubble curtain is difficult to assess with analytical models, which make a number of simplifications (e.g. spherical and widely spaced bubbles) that may result in inaccurate predictions (Matuschek & Betke, 2009).

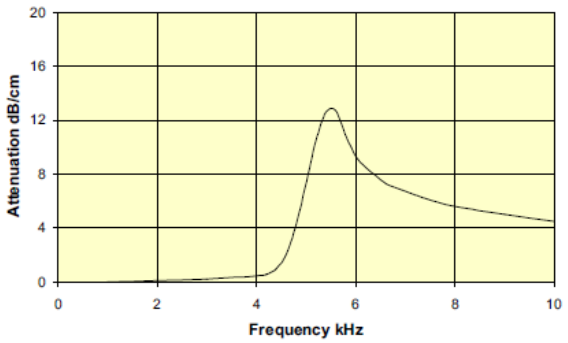

Figure 6.3 Attenuation spectrum of a bubble curtain with bubbles of diameters between 0.6 and 0.7 mm (from Elmer et al., 2007).

For the bubble curtain to be effective at reducing the sound from the driven pile, the bubbles must be evenly distributed around the perimeter of the pile and over its full length, and gaps or holes must be minimal (PND Engineering, 2005; Nehls et al., 2007). An air flow rate of around 0.5 m^3/s is generally enough for a bubble curtain 30-40 m long. Inclined or batter piles may require larger flow rates than vertical piles for total coverage (Funk & Rodrigues, 2005). For larger piles and water depths, Funk & Rodrigues (2005) suggest the use of additional hosepipes or bubble rings to compensate for the bubble drift caused as bubbles rise to the surface; Coleman (2011) states that a larger number of bubble rings does not necessarily improve the overall attenuation of the system. In addition, large compressors and high air flow rates do not necessarily result in improved attenuation (Vagle, 2003).

The average rise velocity of the air bubbles released by the hosepipe is 0.3 m/s. Tidal currents of 1 m/s (e.g. North Sea) would make bubbles drift 70 m before reaching the surface in water depths of 20 m. Confined air bubble curtains and stacked bubble rings are suitable solutions in high-current areas (see Figure 6.4); using larger bubble rings is impractical under these conditions, due to the required diameters and capacity of the air compressors (Nehls et al., 2007). Tidal currents can reduce the attenuation ability of a bubble curtain by approximately 10 dB (Abbot & Reyff, 2004).

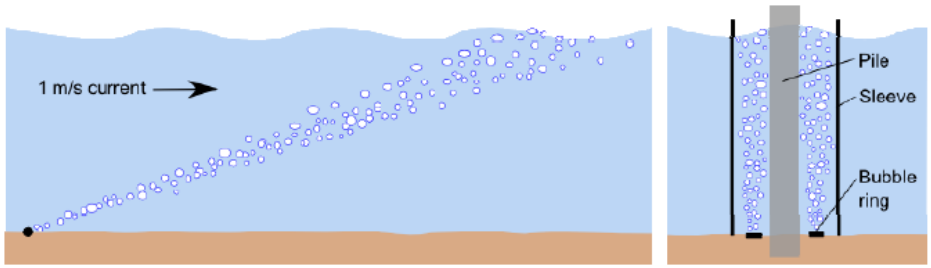

Fig. 3-12. Left: Bubble movement due to current; drift angle approximately to scale for 1 m/s. Right: Confined bubble curtain

Figure 6.4 Representation of the benefits of a conventional bubble curtain confined in a pile sleeve (from Nehls et al., 2007)

The effectiveness of air bubble curtains on attenuating sound varies greatly between models and installation conditions (ICF Jones & Stokes, 2009). The approximate total attenuation is given by $10\log(A/A_{hole})$, where A is the area of the screen and A_{hole} the bubble free area (e.g. a hole area of 5% would result in 13 dB attenuation). The attenuation characteristics of any screen can be greatly enhanced by generating a high percentage of small bubbles, but manufacturing bubble rings with small holes is

challenging (Vagle, 2003). However, in order to improve attenuation at frequencies below 1 kHz, the screen should contain a certain amount of large bubbles (> 10 mm; Nehls et al., 2007).

Some of the practical problems associated with unconfined air bubble curtains include the control of bubble size distribution, generation of a sufficient amount of large bubbles to achieve low-frequency attenuation, and avoidance of bubble leakage caused by currents (Matuschek & Betke, 2009).

The sound level attenuation achieved by unconfined air bubble curtains varies considerably, with values in the range of 0-20 dB (see Table 6.1). The reduction in peak sound levels is generally higher than in RMS or SEL. The lowest attenuation values occur in high current situations and do not generally exceed 5 dB_{rms}. The data from ICF Jones & Stokes (2009) indicate that the highest attenuations are reached for larger piles: for steel or concrete piles with a cross-section dimension of 0.6 m the system provides 5 dB reduction; for mid-sized piles (0.6-1.2 m cross-section) the system attenuates 10 dB; for larger piles (> 1.2 m cross-section) about 20 dB sound reduction is achieved.

Table 6.1 Effectiveness of unconfined air bubble curtains

Attenuation Method	Description	TL_{0-p}	TL_{rms}	TL_{sel}	τ_{0-p_ini} [ms]	τ_{0-p_att} [ms]	Pile type	Pile ø [m]	Blow energy [kJ]	Water depth [m]	Reference
Unconfined Air Bubble Curtain	2 m ø single ring	10	10				Steel pipe	0.9	170	4.5	Illinworth & Rodkin, 2007
		14	15				Steel pipe	1	300	12.5	Illinworth & Rodkin, 2007
	Single bottom ring	12	9	7	1.5	2.7	Steel pipe	0.3	50	8	Laughlin, 2006
	Single bottom ring, mid-flow	7	10	9	4	2.3	Steel pipe	0.6	80	12.8	Laughlin, 2005
	Single bottom ring, full-flow	2	4	1	0.6	1.2	Steel pipe	0.6	55	10	Laughlin, 2005
	Single bottom ring, full-flow	1	0	0	1.1	1	Steel pipe	0.6	55	10	Laughlin, 2005
	Single bottom ring	2	3	3		23.1	Steel pipe	0.76	55	10.3	Laughlin, 2005
	3-ring	10	9	9		13	Steel pipe	0.6	64	11	Coleman, 2011
	3-ring	13	11	10		15	Steel pipe	1.2	269	11	Coleman, 2011
	2-ring	22	21	22	17.2	19.3	Steel pipe	0.9	150	8.2	Laughlin, 2007
		18	13	13			CISS	0.9	95	9	Illinworth & Rodkin, 2007
		16	9				CIDH	1.7	270	4	Illinworth & Rodkin, 2007
		11	8	6			Concrete pile	0.6	224	8	Illinworth & Rodkin, 2007
		12	7				CISS	2.4	1780	10	Illinworth & Rodkin, 2007
	Single bottom ring, full-flow	16	12	10	2.2	28	Steel pipe	0.6	85	10	Laughlin , 2005
		3	3				Concrete pile	0.4	80	7	Illinworth & Rodkin, 2007
		9		14			Timber pile	0.4	14	4	Lucke et al., 2011

The bubble curtain has an effect on the peak rise time. For unattenuated impulses the rise time τ_{pk_ini} is generally of the order of 1-3 ms; the presence of the bubble curtain may increase or reduce the peak rise time depending on the range of frequencies that is more heavily attenuated. Greater low frequency attenuation results in shorter rise times. The pulse duration, considered as the time window containing 90% of the pulse energy, ranges from 50 ms to over 80 ms (Abbott & Reyff, 2004).

The degree of attenuation also depends on direction (Abbot & Reyff, 2004) and frequency. Figure 6.5 shows two examples of received pulse spectrum with and without bubble curtains.

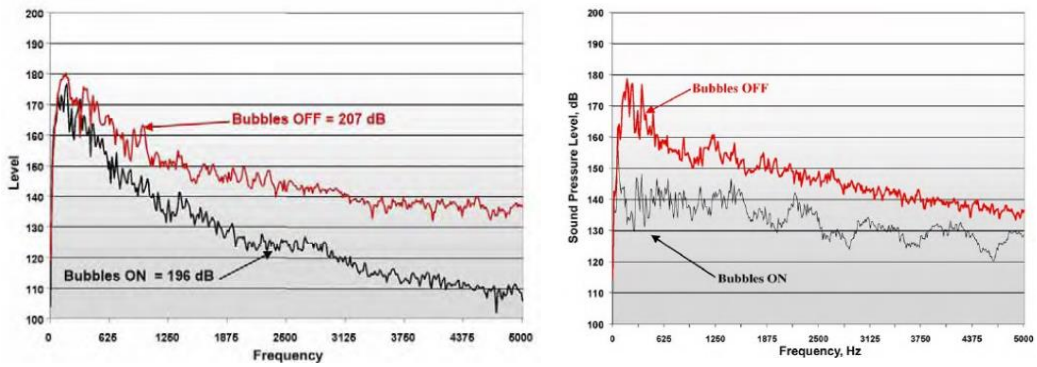

Figure 6.5 Effect in frequency of a two-ring (left) and a five-ring (right) unconfined air bubble curtain. The red and black curves represent the measured sound spectrum with the bubble curtain operating and shut off, respectively (ICF Jones & Stokes, 2009).

Confined air bubble curtains seem to achieve moderate but consistent levels of attenuation, between 5 and 15 dB for peak, RMS and SEL values. Measurements presented by Illinworth & Rodkin (2005) show an attenuation of 5 dB for the Gunderboom® (see Table 6.2). The HSD system is found to be particularly effective in the range of 100-2000 Hz, with sound level reductions of up to 19 dB; the average broadband attenuation is around 9 dB_E (Burns et al., 2014).

Table 6.2 Effectiveness of confined air bubble curtains

Attenuation Method	Description	TL_{0-p}	TL_{rms}	TL_{sel}	τ_{0-p_ini} [ms]	τ_{0-p_att} [ms]	Pile type	Pile ø [m]	Blow energy [kJ]	Water depth [m]	Reference
Confined Air Bubble Curtain		7-10	<5	<5			Steel pipe	0.5	70	4	Illinworth & Rodkin, 2007
		10	9	8		13	Steel pipe	0.6	64	11	Coleman, 2011
		14	13	11		15	Steel pipe	1.2	269	11	Coleman, 2011
	Gunderboom™	5	4	4			Steel pipe	2.6	1500	10	Illinworth & Rodkin, 2007

6.2 Air-Filled Resonators

The company AdBm has developed two techniques that use encapsulated air to attenuate the sound pressure produced by an acoustic source in a broad range of frequencies. These are the *encapsulated bubbles*, and the most recent creation, the *open-ended resonators* (Wochner et al., 2014). As bubble curtains, both systems are installed around the sound source. The encapsulated bubbles are similar to balloons filled with air, whereas the resonator consists of a square chamber filled with air with a combination of rigid and elastic walls and an opening at the bottom. Both systems achieve better sound reduction than bubble curtains (up to 50 dB), especially at low frequencies, and can be tuned to cover a specific frequency range. The open-ended resonators have some benefits compared to encapsulated bubbles, like a smaller size for equivalent resonance frequency, high quality factor (a better resonator), fewer resonators for the same sound pressure attenuation (thus the necessity of a lighter ballast to submerge the system), and a secondary peak of absorption below the main resonance frequency.

6.3 Cofferdams

A cofferdam is an enclosure most commonly constructed by interlocking sheet piles in a cell around the pile driving site. These are temporary structures used during in-water and near-water pile driving, and can be installed for acoustic or non-acoustic reasons. Cofferdams are limited to shallow and calm waters, since the sheet piles flex easily and are limited in length. These structures are expensive. The noise generated during their installation (normally with vibratory hammers) can be more harmful than the pile driving noise they intend to attenuate (PND Engineering, 2005).

The water inside the cofferdam may be either pumped out or left in place. A dewatered cofferdam is the most effective attenuation system (PND Engineering, 2005; ICF Jones & Stokes, 2009); the pile is completely decoupled from the water column and results in a substantial noise reduction in all directions (see Figure 6.6). The expected attenuation provided by a dewatered cofferdam is at least as great as that from a bubble curtain. However, the transmission path through the sediment is not eliminated, and high underwater sound levels can still be measured at certain distances (Abbot & Reyff, 2004; ICF Jones & Stokes, 2009). Cofferdams full of water provide limited attenuation; sometimes, bubble curtains are used within the cofferdam if dewatering is not practical (ICF Jones & Stokes, 2009).

ICF Jones & Stokes (2009) report an approximate reduction in peak sound pressure level of 10 dB from a dewatered cofferdam. The peak rise time for attenuated impulses is around 1-2 ms, with typical pulse durations of 50-90 ms. Most of transmitted acoustic energy is in the range of 50-500 Hz (Abbot & Reyff, 2004).

Figure 6.6 Examples of two dewatered cofferdams.

6.4 Pile Sleeves

An isolation casing, or *pile sleeve*, is a hollow casing (i.e. pipe pile) slightly larger in diameter than the pile to be driven and inserted on it. The sleeve forms an acoustic barrier that generally extends from the seafloor up to the sea surface. Pile sleeves comprise an internal chamber with an impedance much different than water, normally filled with air or closed-cell foam. The pile is normally driven through the dewatered casing (ICF Jones & Stokes, 2009; Matuschek & Betke, 2009).

Dewatered pile sleeves can be expected to provide a degree of attenuation at least as great as air bubble curtains, but not as high as that from cofferdams due to the thin isolating chamber (ICF Jones & Stokes, 2009). If holes are found in the sleeve the efficacy will be critically reduced (Nehls et al., 2007). Rubber sleeves 3-6 mm thick used to reduce airborne sound from pile driving were tested underwater in driven piles by Nehls et al. (2007), resulting in little to no reduction of radiated noise (see Figure 6.7, left).

Figure 6.7 Rubber sleeve 3-6 mm thick typically used for airborne sound attenuation (left) and foam-coated steel sleeve (right). From Nehls et al., 2007.

The placement and removal of the pile sleeve is difficult to integrate into the pile driving operation, and there are also difficulties fitting pile sleeves on jacket foundations to ensure no acoustic leakage (Matuschek & Betke, 2009).

Laughlin (2007) tested two Temporary Noise Attenuation Pile systems (TNAP), pile sleeves consisting of a steel pipe casing with a 5 cm chamber of air or closed-cell foam. The second type was found to be more effective, with an attenuation of 19 dB_{pk} (see Table 6.3).

Table 6.3 Effectiveness of pile sleeves.

Attenuation Method	Description	TL_{0-p}	TL_{rms}	TL_{sel}	τ_{0-p_ini} [ms]	τ_{0-p_att} [ms]	Pile type	Pile ø [m]	Blow energy [kJ]	Water depth [m]	Reference
Sleeve pile	Steel pile casing 5 cm internal air chamber	17				6.7	Steel pipe	0.9	150	7.3	Laughlin, 2007
	Steel pile casing 5 cm internal closed-cell foam layer	19	16			19.4	Steel pipe	0.9	150	7.9	Laughlin, 2007

Coleman (2011) investigated the effects of a watered steel pipe with internal air bubble curtain; the steel pipe itself, with the air compressor off, resulted in 2 dB_{pk} attenuation. Elmer et al. (2007) used a foam coated tube 2.2 m in diameter and 5 mm thick over a steel pile, which achieved 5-25 dB level reduction in frequency, with the highest attenuation in the lower end of the spectrum. Attenuation measurements made by Nehls et al. (2007) on a pile sleeve consisting of a 12 mm thick steel pipe, with and without a foam layer, showed that the casing had a minimal contribution to the overall sound level attenuation (see Figure 6.8).

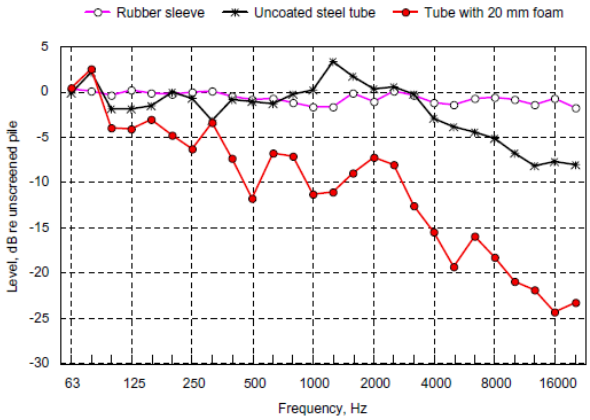

Figure 6.8 Sound level reduction spectra from a rubber sleeve (purple curve, see also Fig. 6.7, left) and a steel tube (see Fig. 6.7 right), uncoated (black curve) and with a 20 mm foam chamber (red curve). From Nehls et al., 2007.

6.5 Hammer Type

Choosing vibratory drivers, push-in drivers and *blue piling* as alternatives to traditional impact pile drivers is an effective way of minimising the sound radiated by a driven pile. These systems have limitations on the type, size and resistance of the pile to be driven. Vibratory hammers are normally used on small piles, but can also be applied to large piles (e.g. monopiles from offshore wind turbines), in which case the required penetration depth may not be reached.

Vibratory drivers produce lower peak sound pressure levels than impact hammers (Elmer et al., 2007). In ideal conditions, most of the acoustic energy emitted by piles driven with a vibratory hammer is in the range of its operational frequency (20-40 Hz), but due to non-linear coupling ("rattling") the vibration produces broadband noise of varying intensity (Matuschek & Betke, 2009). Figure 6.9 shows a comparison between typical frequency responses of an impact and vibratory hammer. Vibratory hammers result in a noise reduction of 15-20 dB, or even more, when compared to impact hammers.

Vibratory hammers are much quieter than impact hammers, however the cumulative sound exposure level can be higher due to their continuous operation and the potentially longer time required for pile installation (ICF Jones & Stokes, 2009). Additionally, an impact hammer is always necessary at the end of the pile installation to verify the stability of the piles (Matuschek & Betke, 2009) and may be required prior to vibratory driving to test the resistance of the pile, what is known as "proofing" (ICF Jones & Stokes, 2009).

A recently developed technology called Blue Piling, created by Fistuca, can be used to drive large piles into the seabed producing minimum underwater sound levels. The system consists of a hollow cylinder filled with water that is attached to the pile. The combustion of a gas mixture under the enclosed

water column moves the water upwards and exerts a downward force onto the pile; the water column falls back by effect of gravity, resulting in a second blow. The force is spread in time and that contributes to reduce the tensile forces and source level. It also reduces the cost associated with larger hammers.

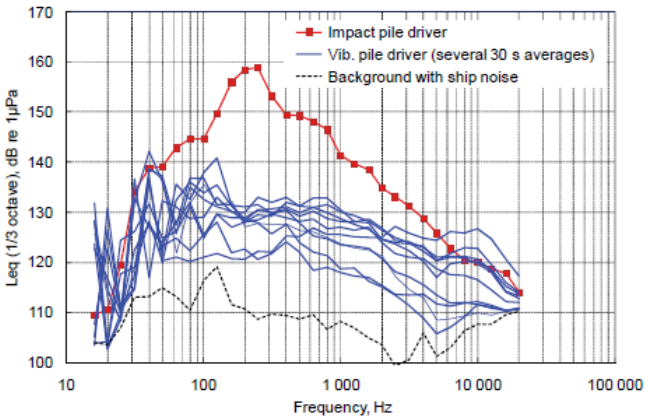

Figure 6.9 Third octave band spectrum measured at 1.2 km from the pile. The pile, 2.6 m in diameter, is driven with an impact and vibratory hammer. The driving frequency of the vibratory hammer is ~20 Hz (from Matuschek & Betke, 2009).

No documented acoustic measurements have been found on press-in systems or blue piling. However, press-in systems are expected to generate substantially lower sound levels than impact or vibratory hammers (ICF Jones & Stokes, 2009).

6.6 Pile Type

Piles are made of steel, wood or concrete, and come in various sizes and shapes, including pipes, H-beams, sheet piles, and piles with circular, square or octagonal cross-section. Selecting an alternative pile type can be useful to reduce the underwater sound levels. For example, driving concrete or steel H-beam piles instead of steel pipes will result in lower sound levels from individual pile strikes. Smaller piles will also produce lower sound levels, but more piles are often required to be driven, resulting in a larger number of piles strikes; the peak sound level is reduced, but the cumulative sound exposure can be higher (ICF Jones & Stokes, 2009).

6.7 Prolonging Impact Duration

Prolonging the duration of a hammer strike causes an overall sound level reduction of about 10 dB and the displacement of the spectral content to lower frequencies (Elmer et al., 2007; Nehls et al., 2007). The decelerated downward movement experienced by the pile when is hit by the hammer lasts around 2-5 ms, and the evolution of the impact force with time is rather bell-shaped (see Figure 6.10, left). The increase in impact time results in a reduction of peak force; this loss of force is not critical, since the longer duration of the pulse still contributes to drive the pile to a reasonable depth.

An increase in impact time can be achieved by reducing the acceleration at the moment of impact using a spring, pile cap, or drop hammer (instead of a double-acting pile driver). Increasing the impact force while maintaining the strike duration can be achieved with a heavier ram.

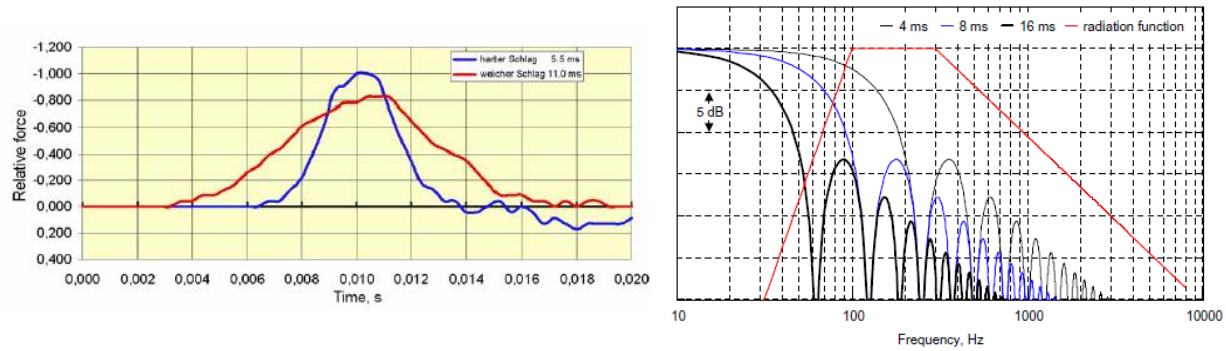

Figure 6.10 Time representation of hard stroke (blue curve) and soft stroke (red curve), the latter achieved with a steel cable ring placed between hammer and pile (left). The shift of the spectral content towards lower frequencies with longer pulse durations is also shown on the right-hand graph (from Nehls et al., 2007).

The construction of a specially shaped hammer or the use of a pile cap can extend the impact time by a factor of 2 (Nehls et al., 2007). A single-acting pile driver (e.g. drop hammer) produces significantly less noise in the frequency range of the spectral maximum, which results in a 10 dB broadband reduction (see Figure 6.11). The use of drop hammers for offshore installations can be problematic due to their low energy/weight ratio compared to double-acting hammers. Using large hammers to compensate for the reduction in peak force is not always practical due to the limited weight that cranes can support.

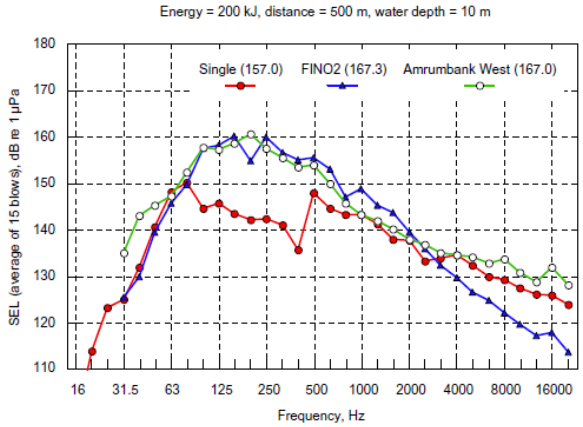

Figure 6.11 Example of a 200 kJ drop hammer on a 2.2 m pile compared to two double-acting hammers (from Nehls et al, 2007)

6.8 Pile Cap

A cushion block, or *pile cap*, is a piece of material placed on top of the pile to cushion the impact from the hammer. These caps are generally 5-20 cm thick, and can combine layers of more than one material. Typical pile caps are made of plywood and Nylon; other documented materials include Micarta and polyethylene. Plywood is commonly used with concrete piles to protect them and prevent shattering, but also provides the highest sound level attenuation of all tested materials in all sorts of piles. The durability of pile caps is very limited.

The block of material reduces the energy imparted by the hammer onto the pile. Larger hammers are used to compensate for the reduced driving capabilities caused by the pile cap (PND Engineering, 2005).

Laughlin (2006) conducted an experiment with pile caps of different material during a pile driving event to determine the induced attenuation. The pile cap materials tested were plywood, Micarta and Nylon, each of which were tested with and without an air bubble curtain. Wood had the largest sound reduction (see Table 6.4), however it is not feasible to use wood for the entire pile driving event as it

compresses easily and poses a fire risk. Laughlin (2006) recommends the use of Micarta or Nylon, which provided moderate attenuation.

Pile caps are particularly good at attenuating the high frequency content of the acoustic pulse and increasing its initial rise time, reducing the impulsive character of the sound.

Table 6.4 Effectiveness of pile caps.

Attenuation Method	Description	TL_{0-p}	TL_{rms}	TL_{sel}	τ_{0-p_ini} [ms]	τ_{0-p_att} [ms]	Pile type	Pile ⌀ [m]	Blow energy [kJ]	Water depth [m]	Reference
Pile cap	Plywood	17	14		1.5	34.8	Steel pipe	0.3	50	8	Laughlin, 2006
	Plywood	12	13	11	4.6	22.1	Steel pipe + H-wings	0.3	50	6	Laughlin, 2006
	Nylon	8	8	8	4.6	7.8	Steel pipe + H-wings	0.3	50	6	Laughlin, 2006
	Micarta	8	7	7	4.6	13.1	Steel pipe + H-wings	0.3	50	6	Laughlin, 2006

6.9 Jetting in Piles

The sediment around the pile is loosened by a strong jet of water, reducing skin friction and helping to drive the pile further with each impact. Jetting is used to assist pile penetration, especially in non-cohesive sediments such as dense sands, which will reconsolidate with subsequent driving (Gerwick, 2007).

This technique requires an impact hammer and is often used when the sediment is very dense and creates a refusal type scenario. At refusal most of the impact energy is transmitted into the water column in the form of an acoustic pulse (PND Engineering, 2005). The sound attenuation is minimal, but the active period tends to be shortened leading to lower cumulative sound exposure. Jetting does not take place over the entire pile driving period; after jetting is finished a specified number of blows (100-400) is still required to reconsolidate the soil around the pile (Gerwick, 2007).

No literature has been found to evaluate the extent of attenuation achieved by this method.

6.10 Pile Driver Silencer

In a *pile driver silencer* a soundproof casing is fitted around the impact zone between the hammer and the pile. The silencer generally comprises a steel frame filled with foam, surrounded by an aluminium casing which contains two separate layers to attenuate both high and low frequencies (Funk & Rodrigues, 2005).

This method has been successfully used for land based pile driving activities but there is little literature available on the use of this method in water. Funk & Rodrigues (2005) predict that the sound level reduction for an offshore pile driving activity using a pile driver silencer would be insignificant as the silencer would primarily attenuate the in-air sounds.

6.11 Pre-Drilled Pile

In *pre-drilled piles* the pile is initially seated into place with either a vibratory or an impact hammer. The hammer is then removed and a drill is placed above the hole. A pilot hole is drilled through the pile into the sediment and the drill is removed. The pile driving can then resume as normal. This method is most effective when the seabed sediment is dense (PND Engineering, 2005).

Pre-drilling the hole for a pile can be an effective way of reducing the number of pile strikes required to place a pile (ICF Jones & Stokes, 2009). No literature has been found about the extent of attenuation achieved by this method and its effects on the cumulative sound exposure.

6.12 Decoupling Sound Sources

The contribution of secondary sound sources associated with the pile driving activity (e.g. generators located on the deck of a pile driving barge) can be reduced by repositioning or decoupling the source from the radiating structure (Funk & Rodrigues, 2005).

This technique is unlikely to result in a significant reduction on the overall sound level, as the pile strike is by far the loudest source. However, no literature has been found to evaluate the effectiveness of this attenuation method.

6.13 Hammer Impact Energy

A lower blow energy will reduce the sound level produced by the pile. However, by reducing the impact energy, the penetration achieved per blow will also be reduced and the piling activity may take longer, in turn increasing the cumulative SEL (Gordon et al., 2007).

References

Abbott, R., and Reyff, J.A. (2004). *San Francisco – Oakland Bay Bridge, East Span Seismic Safety Project: Fisheries and hydroacoustic monitoring program compliance report*. California Department of Transportation (Caltrans), p. 148.

Bailey, H., Senior, B., Simmons, D., Rusin, J., Picken, G., and Thompson, P.M. (2010). "Assessing underwater noise levels during pile-driving at an offshore windfarm and its potential effects on marine mammals". *Marine Pollution Bulletin*, 60, 888-897. doi: 10.1016/j.marpolbul.2010.01.003

Barber, G.H. (1978). "PILETALK Seminar presentation" in *Associated Pile & Fitting Corp. PILETALK Seminar*, Miami, Florida, March 1978.

Betke, K. (2008). *Measurement of wind turbine construction noise at Horns Rev II*. Institut für technische und angewandte Physik (ITAP), Rep. 1256-08-a-KB, p.30.

Blackwell, S.B. (2005). *Underwater measurements of pile driving sounds during the Port MacKenzie dock modifications, 13-16 August 2004*. Greeneridge Sciences, Inc., LGL Alaska Research Associates, Inc., and HDR Alaska, Inc. Greeneridge Rep. 328-1, p. 33.

Blackwell, S.B., Lawson, J.W., and Williams, M.T. (2004). "Tolerance by ringed seals (*Phoca hispida*) to impact pile-driving and construction sounds at an oil production island". *J. Acoust. Soc. Am.*, 115(5), 2346-2357. doi: 10.1121/1.1701899

Brandt, M.J., Diederichs, A., Betke, K., and Nehls, G. (2011). "Responses of harbour porpoises to pile driving at the Horns Rev II offshore wind farm in the Danish North Sea". *Mar. Ecol. Prog. Ser.*, 421, 205-216. doi: 10.3354/meps08888

Bruns, B., Kuhn, C., Stein, P., Gettermann, J., and Elmer, K.H. (2014). "The new noise mitigation system 'Hydro Sound Dampers': history of development with several hydro sound and vibration measurements", in *Inter-Noise 2014*, 16-19 November, Melbourne, Australia.

Chatzigiannelis, I., Elsayed, K., and Loukakis, K. (2009). "Foundation engineering of offshore 'Jacket' structures". Conference paper, *International Foundation Congress and Equipment Expo 2009*, Orlando (Florida, US), March 15-19, p. 8. doi: 10.1061/41021(335)27

Coates, R. (2006). *Foundation course: basic underwater acoustics. The SONAR course*. Seiche Ltd.

Coleman, J., and Evans, J. (2011). *Columbia River Crossing test pile project hydroacoustic monitoring*. David Evans and Associates, Inc. Final report, p. 256

Crowser, H. (2009). *Acoustic monitoring and in-situ exposures of juvenile Coho salmon to pile driving noise at the Port of Anchorage Marine Terminal redevelopment Project, Knik arm, Anchorage, Alaska*. Hart Crowser, Inc., Pentec Environmental, and Illingworth and Rodkin, Inc. Rep. 12684-03, p. 72.

CSA (2013). *Quieting technologies for reducing noise during seismic surveying and pile driving. Information Synthesis*. Report prepared by CSA Ocean Sciences Inc. for the Bureau of Ocean Energy Management (BOEM). Workshop held in Maryland, 25-27 February 2013.

Dähne, M., Gilles, A., Lucke, K., Peschko, V., Adler, S., Krügel, K., Sundermeyer, J., and Siebert, U. (2013). "Effects of pile-driving on harbour porpoises (*Phocoena phocoena*) at the first offshore wind fam in Germany". *Environ. Res. Lett.* 8, p. 16. doi: 10.1088/1748-9326/8/2/025002

Degraer, S., Brabant, R., and Rumes, B. (Eds.) (2012). *Offshore wind farms in the Belgian part of the North Sea: Heading for an understanding of environmental impacts*. Royal Belgian Institute of Natural Sciences (RBINS), Management Unit of the North Sea Mathematical Models (MUMM), and Marine Ecosystem Management Unit. P. 155 + annexes.

Duncan, A. J., McCauley, R.D., Parnum, I., and Salgado-Kent, C. (2010). "Measurement and modelling of underwater noise from pile driving". *Proceedings of 20th International Congress on Acoustics, ICA 2010, 23-27 August, Sydney, Australia*, 5 p.

Elmer, K.H., Gerasch, W.J., Neumann, T., Gabriel, J., Betke, K., Schultz-von-Glahn, M. (2007). "Measurement and reduction of offshore wind turbine construction noise". *DEWI Magazine*, 30, p. 6.

Evans, P.G.H. (Ed.) (2007). *Proceedings of the workshop on offshore wind farms and marine mammals: impacts & methodologies for assessing impacts*. 21st Conference of the European Cetacean Society, April 2007, The Aquarium, San Sebastian, Spain.

Fisher F.H., and Simmons V.P. (1977). "Sound absorption in seawater", *J. Acoust. Soc. of Am*, 62, 558-564. doi: 10.1121/1.381574

Francois R.E., and Garrison G.R. (1982a). "Sound absorption based on ocean measurements: Part I:Pure water and magnesium sulfate contributions", *J. Acoust. Soc. of Am.*, 72(3), 896-907. doi: 10.1121/1.388170

Francois R.E., and Garrison G.R. (1982b). "Sound absorption based on ocean measurements: Part II:Boric acid contribution and equation for total absorption", *J. Acoust. Soc. of Am*, 72(6), 1879-1890. doi: 10.1121/1.388673

Funk, D.W., and Rodrigues, R. (2005). *Options for mitigating construction-related effects on beluga whales*. LGL Alaska Research Associates, Inc. LGL Final Report, no. P826, p. 30.

Gerwick, B.C. (2007). *Construction of marine and offshore structures.* 3rd Ed., New York: CRC Press, p. 792.

Gordon, J., Thompson, D., Gillespie, D., Lonergan, M., Calderan, S., Jaffey, B., and Todd, V. (2007). *Assessment of the potential for acoustic deterrents to mitigate the impact on marine mammals of underwater noise arising from the construction of offshore windfarms*. SMRU Ltd and COWRIE, Rep. COWRIE DETER-01-2007, p. 71.

Jong, C.A.F. de, and Ainslie, M.A. (2012). *Underwater sound due to piling activities for Prinses Amaliawindpark*. TNO Rep. R10081, p. 102 incl. appendices.

Haan, D. de, Burggraaf, D., Ybema, S., Hillem R., and Lambers, R. (2007). *Underwater sound emissions and effects of the pile driving of the OWEZ windfarm facility near Egmond aan Zee (Tconstruct)*. Wageningen IMARES, Rep. C106/07, p. 75.

Hawkins, A.D. (2009). "The impact of pile driving upon fish". Proc. Inst. of Acoust., 31(1), 72-79.

ICF Jones & Stokes (2009). *Technical guidance for assessment and mitigation of the hydroacoustic effects of pile driving on fish*. ICF Jones & Stokes, and Illingworth & Rodkin, Inc. Final report, p. 367.

Illingworth & Rodkin (2007). *Compendium of pile driving sound data*, p. 129.

Jensen, F.B., Kuperman, W.A., Porter, M.B. and Schmidt, H. (2011). *Computational ocean acoustics*. 2nd Ed., New York: Springer Science + Business Media

Laughling, J. (2005). *Friday Harbor Ferry Terminal Restoration Project: Underwater sound levels associated with restoration of the Friday Harbor Ferry Terminal*. Washington State Department of Transportation, p. 130.

Laughlin, J. (2006). *Washington State Parks Cape Disappointment Wave Barrier Project: Underwater sound levels associated with pile driving at the Cape Disappointment Boat Launch Facility, Wave Barrier Project*. Washington State Department of Transportation, p. 45.

Laughlin, J. (2007). *WSF Mukilteo Test Pile Project: Underwater sound levels associated with driving steel and concrete piles near the Mukilteo Ferry Terminal*. Washington State Department of Transportation, p. 67.

Lepper P.A., Robinson, S.P., Ablitt, J., and Leonard, G. (2007). *The measurement of the underwater radiated noise from a marine piling operation*. In *Pacific Rim Underwater Acoustics Conference 2007 (PRUAC 2007)*, 3-5 October 2007, Vancouver, Canada.

Lucke, K., Lepper, P.A., Blanchet, M.A., and Siebert, U. (2011). "The use of an air bubble curtain to reduce the received sound levels for harbour porpoises (Phocoena phocoena)". *J. Acoust. Soc. Am.*, 130(5), 3406-3412. doi: 10.1121/1.3626123

Lurton, X. (2010). *An introduction to underwater acoustics, principles and applications*. Berlin, Heilderberg: Springer-Verlag

MacGillivray, A. and Racca, R. (2005). Sound pressure and particle velocity measurements from marine pile driving at Eagle Harbor maintenance facility, Bainbridge Island WA. JASCO Research Ltd, Technical Report, p. 13.

Marine Mammal Commission (2007). *Marine Mammals and Noise: A Sound Approach to Research And Management*, p. 370

Matuschek, R., and Betke, K. (2009). "Measurements of construction noise during pile driving of offshore research platforms and wind farms". In *International Conference in Acoustics NAG/DAGA 2009*, 23-26 March 2009, Rotterdam, Netherlands.

Nedwell, J.R., Parvin, S.J., Edwards, B., Workman, R., Brooker, A.G., and Kynoch, J.E. (2007). *Measurement and interpretation of underwater noise during construction and operation of offshore windfarms in UK waters*. Subacoustech, Rep. 544R0738

Nehls, G., Betke, K., Ecklemann, S. and Ros, M. (2007). *Assessment and costs of potential engineering solutions for the mitigation of the impacts of underwater noise arising from the construction of offshore windfarms*. COWRIE Ltd., Rep. COWRIE ENG-01-2007, p. 47.

Norro, A., Haelters, J., Rumes, B., and Degraer, S. (2010). "Underwater noise produced by the piling activities during the construction of the Belwind offshore wind farm (Bligh Bank, Belgian marine waters)". In: Degraer, S., Brabant, R., and Rumes, B. (Eds.) *Offshore wind farms in the Belgian part of the North Sea: early environmental impact assessment and spatio-temporal variability*. Royal Belgian Institute of Natural Sciences (RBINS), Management Unit of the North Sea Mathematical Models (MUMM), and Marine Ecosystem Management Unit.

ORPC (2012). *Cobscook Bay Tidal Energy Project: Final report on the acoustic, marine mammal and bird monitoring studies during phase I pile driving activities*. ORPC Maine, LLC., p. 280.

PND Engineering (2005). *Pile Driving Noise Attenuation Measures*. PND Engineering, Inc., Final Technical Report, no. 21132, p. 15.

Popper, A.N., Carlson, T.J., Hawkins, A.D., Southall, B.L., and Gentry, R. (2006). "Interim criteria for injury of fish exposed to pile driving operations: a white paper". White paper, p. 15

Reinhall, P.G., and Dahl, P.H. (2011). "Underwater Mach wave radiation from impact pile driving: Theory and observation". *J. Acoust. Soc. Am.*, 130(3), 1209-1216. doi: 10.1121/1.3614540

Reyff, J.A. (2003). *Underwater sound pressures associated with the restrike of the pile installation demonstration project piles*. Illingworth & Rodkin, Inc., Final Report, p. 33.

Robinson, S.P., Lepper, P.A., and Ablitt, J. (2007). "The measurement of the underwater radiated noise from marine piling including characterisation of a 'soft start' period". *IEEE*, p. 6. doi: 10.1109/OCEANSE.2007.4302326

Ruggerone, G.T., Goodman, S., and Miner, R. (2008). *Behavioral response and survival of juvenile Coho salmon exposed to pile driving sounds*. Natural Resources Consultants, Inc., p. 46.

Scientific Fishery Systems (2009). *Port of Anchorage Marine Terminal Development Project: 2008 underwater noise survey during construction pile driving*. Rep. 08-06, p. 231.

Thompson, P.M., Lusseau, D., Barton, T., Simmons, D., Rusin, J., and Bailey, H. (2010). "Assessing the responses of coastal cetaceans to the construction of offshore wind turbines". *Marine Pollution Bulletin*, 60, 1200-1208. doi: 10.1016/j.marpolbul.2010.03.030

Tougaard, J., Carstensen, J., and Teilmann, J. (2009). "Pile driving zone of responsiveness extends beyond 20 km for harbour porpoises (Phocoena phocoena (L.))". *J. Acoust. Soc. Am.*, 126(1), 11-14. doi: 10.1121/1.3132523

Tsouvalas, A., and Metrikine, A.V. (2014). "Wave radiation from vibratory and impact pile driving in a layered acousto-elastic medium". In *Proceedings of the 9ths International Conference on Structural Dynamics (EURODYN 2014)*, 30 June to 2 July, Porto, Portugal. doi: 10.13140/2.1.2300.3847

Urick, R.J. (1983). *Principles of Underwater Sound*. 3rd Ed., McGraw-Hill, New York.

URS (2007). *Port of Anchorage Marine Terminal Development Project: Underwater noise survey test pile driving program, Anchorage, Alaska*, p. 109.

Vagle, S. (2003). *On the impact of underwater pile-driving noise on marine life*. Institute of Ocean Sciences, p. 44.

Verfuss, U.K., Sinclair, R.R. and Sparling, C.E. (2019). *A review of noise abatement systems for offshore wind farm construction noise, and the potential for their application in Scottish waters*. Scottish Natural Heritage Research Report No. 1070.

Wang, Z., Wu, Y., Duan, G., Cao, H., Liu, J., Wang, K., and Wang, D. (2014). "Assessing the underwater acoustics of the world's largest vibration hammer (OCTA-KONG) and its potential effects on the Indo-Pacific Humpbacked Dolphin (*Sousa chinensis*)". *PLOS ONE*, 9(10), p. 15. doi: 10.1371/journal.pone.0110590

Wyatt, R. (2008). *Joint Industry Programme on Sound and Marine Life/ Review of existing data on underwater sounds produced by the oil and gas industry, issue 1*. Seiche Measurements Ltd., Rep. S186, p. 110

A.I Tabulated Data

The current appendix includes various tables with data from measurements made during pile driving activities. There is one table per type of pile driver, which includes four types of impact hammer (drop, air/steam, diesel, hydraulic), impact hammers of unknown characteristics, and vibratory hammers. The content in the tables is organised by pile type to facilitate comparison and interpretation of results.

Impact Pile Driving: Diesel

Table A.1 Sounds produced by steel pipes driven with a diesel impact hammer.

Pile Type	Pile Dimensions	Hammer Type	Hammer Dimensions	h_w [m]	Seabed Type	Measurement		SL [dB re 1µPa@ 1 m]	Regression Equation	Signal Characteristics	Attenuation Method	Description	Reference
						SPL_{pk} [dB re 1µPa$_{pk}$]	SPL_{rms} [dB re 1µPa$_{rms}$]	SEL [dB re 1µPa^{2}s]					
Steel pipe	ø = 0.3 m^{*1}	Diesel impact	Small	2	N/A	191±1 @ 10 m	176±1 @ 10 m	N/A	N/A	τ = 60 ms, with most energy in the first 30 ms Main energy at 250-1000 Hz	No	Context: repair building foundation Area: San Francisco Bay, near El Cerrito (California) Operation: 1-2 min pre-driving, 5 min continuous driving (~5 dB higher) z_s = 2 m (at h_w = 3 m) *1 Centre pile, 7 m from land *2 East pile, near shore	Illinworth & Rodkin, 2007
	ø = 0.3 m^{*2}			1		186.5±1.5 @ 10 m	171.5±1.5 @ 10 m	N/A	N/A	N/A	No		
Steel pipe	ø = 0.36 m	Diesel impact (Delmag D19-42)	N/A	>15	N/A	190-196 @ 22 m 185-191 @ 28 m 187-191 @ 40 m 185-190 @ 50 m 169-172 @ 195 m	178-180 @ 20 m 179-181 @ 30 m 174-178 @ 40 m 173-176 @ 50 m 157-159 @ 195 m	170 @ 20 m 165 @ 40 m	227 dB_{pk} 209.8 dB_{rms}	TL_{pk} = 23.8 $log_{10}R$ TL_{rms} = 22.9 $log_{10}R$	No	Context: seismic retrofit of Richmond-San Rafael Bridge (California) Operation: <1 min continuous driving, 40-45 kJ hammer energy, piles driven adjacent to pier (sound obstruction) z_s = 10 m	Illinworth & Rodkin, 2007
Steel pipe	ø = 0.5 m	Diesel impact (Delmag D19-42)	N/A	3-4	N/A	206-208 @ 10 m 199-201 @ 20 m	186-187 @ 10 m 182-184 @ 20 m	175-176 @ 10 m 169-173 @ 20 m	N/A	N/A	No	Context: utility river crossing project at San Joaquin River (California) Operation: 70 kJ hammer energy z_s = 1 m above seabed Measurements on 2 piles	Illinworth & Rodkin, 2007
Steel pipe	ø = 0.5 m	Diesel impact (Delmag D19-42)	N/A	In land (0-2 m)	N/A	196-198 @ 10 m^{*1} 188 @ 20 m^{*2}	179-183 @ 10 m^{*1} 172 @ 20 m^{*2}	167-171 @ 10 m^{*1} 163 @ 20 m^{*2}	N/A	Main energy < 1.5 kHz	No	Context: utility river crossing project at San Joaquin River (California) Operation: 70 kJ hammer energy z_s = 1 m above seabed (at h_w = 3 m) Piles driven in land, next to water *1 Measurements on 4 piles *2 Measurements on 1 pile	Illinworth & Rodkin, 2007
Steel pipe	ø = 0.5 m	Diesel impact (Delmag D19-42)	N/A	3-4	N/A	197-201 @ 10 m 193-196 @ 20 m	182-186 @ 10 m 178-182 @ 20 m	171-175 @ 10 m 169-171 @ 20 m	N/A	N/A	Confined air bubble curtain TL = 7-10 dB_{pk} TL < 5 $dB_{rms,E}$ Effective at high freq.	Context: utility river crossing project at San Joaquin River (California) Operation: 70 kJ hammer energy z_s = 1 m above seabed (at h_w = 3 m) Measurements on 3 piles	Illinworth & Rodkin, 2007
Steel pipe	ø = 0.6 m	Diesel impact (Delmag D36-32)	N/A	>5	N/A	202-203 @ 10 m 189-191 @ 50 m	188-189 @ 10 m 178 @ 50 m	177-178 @ 10 m 166-167 @ 50 m	220 dB_{pk} 206 dB_{rms} 195 dB_E	TL ≈ 17 $log_{10}R$	N/A	No	Context: dock repair in San Francisco Bay (California) Operation: 25 min (pile 1) and 6 min (pile 2), continuous piling z_s = 3 m Measurements on 2 piles	Illinworth & Rodkin, 2007
Steel pipe	ø = 0.6 m, length = 30 m	Diesel impact	N/A	10-15	Hard	191-206 @ 10 m	177-194 @ 10 m	164-178 @ 10 m	N/A	N/A	T = 1.5 s	Unconfined air bubble curtain (fire hose with holes connected to air compressor) Poor and non-uniform (directional) performance due to strong tides	Illinworth & Rodkin, 2007
Steel pipe	ø = 0.6 m	Diesel impact (Delmag D46-32)	N/A	In land	Water saturated soil	197 @ 15 m 186 @ 35 m 175 @ 70 m	185 @ 15 m 174 @ 35 m 163 @ 70 m	173 @ 15 m 163 @ 35 m	235 dB_{pk} 223 dB_{rms} 205 dB_E	$TL_{pk/rms}$ ≈ 33 $log_{10}R$ TL_E ≈ 27 $log_{10}R$	N/A	No	Context: emergency bridge repair for the Russian River (California) z_s = N/A (at h_w = 3 m) Operation: 180 kJ hammer energy, 10-15 min continuous piling	Illinworth & Rodkin, 2007
Steel pipe	ø = 0.9 m	Diesel impact (Delmag D62-22)	N/A	4-5	N/A	205 @ 10 m 200 @ 20 m 199 @ 30 m 194 @ 40 m 195 @ 60 m	190 @ 10 m 185 @ 20 m 181 @ 30 m 178 @ 40 m 169 @ 60 m	170 @ 30 m	219 dB_{pk} 215 dB_{rms}	TL_{pk} ≈ 14 $log_{10}R$ TL_{rms} ≈ 25 $log_{10}R$	T = 1.5 s τ = 40 ms, pile ringing Most energy at 125-1000 Hz	No	Context: seismic retrofit of Richmond-San Rafael Bridge (California) Operation: 150-170kJ hammer energy, few minutes pre-drill (low SPL sporadic hits), 2-4 min continuous piling z_s = 2-3 m (at h_w = 3 m)	Illinworth & Rodkin, 2007
Steel pipe	ø = 1 m	Diesel impact (Delmag D80)	N/A	10-15	N/A	196 @ 10 m 191 @ 20 m 184 @ 40 m	180 @ 10 m 175 @ 20 m 169 @ 40 m	N/A	TL_{pk} ≈ 14 $log_{10}R$ TL_{rms} ≈ 25 $log_{10}R$	N/A	Unconfined air bubble curtain TL≈10 dB		
					N/A	193-208 @ 10 m	178-195 @ 10 m	175-180 @ 10 m	N/A	N/A	N/A	No	Context: piling at Bay Ship & Yatch Co. dock in Alameda (California) Operation: 300 kJ hammer energy Measurements on 20 piles
					N/A	194 @ 10 m^{*1} 208 @ 10 m^{*2}	180 @ 10 m^{*1} 195 @ 10 m^{*2}	170 @ 10 m^{*1} 180 @ 10 m^{*2}	N/A	N/A	N/A	*1 Unconfined air bubble curtain ON ($TL_{pk,rms}$ ≈ 15 dB) *2 Unconfined air bubble curtain OFF	Context: piling at Bay Ship & Yatch Co. dock in Alameda (California) Operation: 300 kJ hammer energy Measurements on 1 pile

Tab. A.1 Sounds produced by steel pipes driven with a diesel impact hammer (cont.)

Pile Type	Pile Dimensions	Hammer Type	Hammer Dimensions	h_w [m]	Seabed Type	Measurement			SL [dB re 1µPa@ 1 m]	Regression Equation	Signal Characteristics	Attenuation Method	Description	Reference
						SPL_{pk} [dB re 1µPa_{pk}]	SPL_{rms} [dB re 1µPa_{rms}]	SEL [dB re 1µPa^2s]						
Steel pipe	ø = 0.3 m thick = 1 cm	Diesel impact (Vulcan)	N/A	8	silt and mud, glacial till layer below	205 @ 10 m	185 @ 10 m	171 @ 10 m	N/A	N/A	τ_{pk} = 1.5 ms	No cap material Unconfined air bubble curtain OFF	Context: replacement of wood wave barrier at Cape Disappointment boat launch facilty Operation: 35-50 kJ hammer energy (70 kJ capacity) z_r = 1 m above seabed Measurements on 1 pile, maximum registered levels are quoted Single bottom ring air bubble curtain	Laughling, 2006
						193 @ 10 m	176 @ 10 m	164 @ 10 m	N/A	N/A	τ_{pk} = 2.7 ms	No cap material Unconfined air bubble curtain ON (TL ≈ 13 dB)		
						181 @ 10 m	168 @ 10 m	157 @ 10 m	N/A	N/A	τ_{pk} = 34.8 ms	Plywood cap material Unconfined air bubble curtain OFF		
						181 @ 10 m	169 @ 10 m	157 @ 10 m	N/A	N/A	τ_{pk} = 36.6 ms	Plywood cap material Unconfined air bubble curtain ON (TL ≈ 2 dB)		
						205 @ 10 m	188 @ 10 m	173 @ 10 m	N/A	N/A	τ_{pk} = 11.7 ms	Conbest cap material Unconfined air bubble curtain OFF		
						206 @ 10 m	187 @ 10 m	173 @ 10 m	N/A	N/A	τ_{pk} = 10.7 ms	Conbest cap material Unconfined air bubble curtain ON (TL ≈ 5 dB)		
Steel pipe	ø = 0.6 m, thick = 1.3 cm	Diesel impact (ICE *120S*)	N/A	12.8	sandy silt, layer of consolidated clay at 9 m	199 @ 10 m[*1] 192 @ 10 m[*2]	184 @ 10 m[*1] 174 @ 10 m[*2]	179 @ 10 m[*1] 170 @ 10 m[*2]	N/A	N/A	[*1] τ_{pk} = 4.0 ms [*2] τ_{pk} = 2.3 ms	[*1] Unconfined air bubble curtain OFF [*2] Unconfined air bubble curtain ON (mid-flow, TL ≈ 7 dB)	Context: repairment of Ferry Harbor Ferry Terminal, San Juan Island Operation: 40-55 kJ hammer energy (80 kJ capacity) z_r = 0.3 m above seafloor Single bottom ring air bubble curtain Measurements on pile 1, average registered levels are quoted	Laughling, 2005
Steel pipe	ø = 0.6 m, thick = 1.3 cm	Diesel impact (ICE *120S*)	N/A	10	sandy silt, rock layer at 10.5 m	210 @ 10 m[*1] 208 @ 10 m[*2]	194 @ 10 m[*1] 190 @ 10 m[*2]	185 @ 10 m[*1] 184 @ 10 m[*2]	N/A	N/A	[*1] τ_{pk} = 0.6 ms [*2] τ_{pk} = 1.2 ms	[*1] Unconfined air bubble curtain OFF [*2] Unconfined air bubble curtain ON (full-flow, TL ≈ 0 dB)	Context: repairment of Ferry Harbor Ferry Terminal, San Juan Island Operation: 40-55 kJ hammer energy (80 kJ capacity) z_r = 0.3 m above seafloor Single bottom ring air bubble curtain Measurements on pile 4, average registered levels are quoted	Laughling, 2005
Steel pipe	ø = 0.6 m, thick = 1.3 cm	Diesel impact (ICE *120S*)	N/A	10	sandy silt, rock layer at 10.5 m	215 @ 10 m[*1] 214 @ 10 m[*2]	195 @ 10 m[*1] 196 @ 10 m[*2]	187 @ 10 m[*1] 188 @ 10 m[*2]	N/A	N/A	[*1] τ_{pk} = 1.1 ms [*2] τ_{pk} = 1.0 ms	[*1] Unconfined air bubble curtain OFF [*2] Unconfined air bubble curtain ON (full-flow, TL ≈ 0 dB)	Context: repairment of Ferry Harbor Ferry Terminal, San Juan Island Operation: 40-55 kJ hammer energy (80 kJ capacity) z_r = 0.3 m above seafloor Single bottom ring air bubble curtain Measurements on pile 5, average registered levels are quoted	Laughling, 2005
Steel pipe	ø = 0.76 m, thick = 1.3 cm	Diesel impact (ICE *120S*)	N/A	12	sandy silt, layer of consolidated clay at 9 m	203 @ 10 m	189 @ 10 m	180 @ 10 m	N/A	N/A	τ_{pk} = 2.2 ms	Unconfined air bubble curtain ON (full-flow)	Context: repairment of Ferry Harbor Ferry Terminal, San Juan Island Operation: 40-55 kJ hammer energy (80 kJ capacity) z_r = 0.3 m above seafloor Single bottom ring air bubble curtain Measurements on pile 7, average registered levels are quoted	Laughling, 2005
Steel pipe	ø = 0.76 m, thick = 1.3 cm	Diesel impact (ICE *120S*)	N/A	10.3	sandy silt, layer of consolidated clay at 9 m	212 @ 10 m[*1] 210 @ 10 m[*2]	196 @ 10 m[*1] 193 @ 10 m[*2]	187 @ 10 m[*1] 184 @ 10 m[*2]	N/A	N/A	τ_{pk} = 23.1 ms	[*1] Unconfined air bubble curtain OFF [*2] Unconfined air bubble curtain ON (full-flow, TL ≈ 2 dB)	Context: repairment of Ferry Harbor Ferry Terminal, San Juan Island Operation: 40-55 kJ hammer energy (80 kJ capacity) z_r = 0.3 m above seafloor Single bottom ring air bubble curtain Measurements on pile 8, average registered levels are quoted	Laughling, 2005
Steel pipe	ø = 0.91 m, length = 46 m, thick = 2.54 cm	Diesel impact (Delmag *D62-22*)	weight = 12.3 t	16-36	Glacial till (mixture of fine and coarse sediments)	206 @ 62 m	189 @ 62 m	178 @ 62 m	239.5 dB_{pk} 222 dB_{rms} 208 dB_E	RL_{pk} = 239.5 - 17.8·$\log_{10}$R RL_{rms} = 222 - 17.5·$\log_{10}$R RL_E = 208 - 16·$\log_{10}$R 50[th] percentile, range of validity 60-2k m	$\tau_{(R=60\,m)}$ = 100 ms , $\tau_{(R=2000\,m)}$ = 200 ms , Most energy at 100-2k Hz Peaks or tones at 350-450 Hz	No	Context: crossing construction to provide direct transporation over the Knik Arm, between Anchorage and Port MacKenzie (Alaska) Operation: 2 piles, battered 12-15 m into seabed z_r = 10 m Average sound levels quoted (several pulses), measurements on 2 piles Strong tidal currents (< 3.4 m/s)	Blackwell, 2005

Tab. A.1 Sounds produced by steel pipes driven with a diesel impact hammer (cont.)

Pile Type	Pile Dimensions	Hammer Type	Hammer Dimensions	h_w [m]	Seabed Type	Measurement			SL [dB re 1µPa@ 1 m]	Regression Equation	Signal Characteristics	Attenuation Method	Description	Reference
						SPL_{pk} [dB re 1µPa_{pk}]	SPL_{rms} [dB re 1µPa_{rms}]	SEL [dB re 1µPa^2s]						
Steel pipe	ø = 0.6 m	Diesel impact (APE *D19-42*)	N/A	11	N/A	200 @ 10 m[*1] 190 @ 10 m[*2]	185 @ 10 m[*1] 176 @ 10 m[*2]	172 @ 10 m[*1] 163 @ 10 m[*2]	217 dB_{pk} 202 dB_{rms} 189 dB_E	TL ≈ 17·log_{10}R	τ = 33 ms , τ_{pk} = 13 ms ,	[*1]Unconfined air bubble curtain OFF [*2] Unconfined air bubble curtain ON (TL_{pk} = 10 dB, TL_{rmsE} = 9 dB, effective broadband attenuation for f>100 Hz)	Context: driving of test piles for the new Interstate 5 Bridge between Vancouver, Washington and Portland. Operation: 31-64 kJ hammer energy 3-ring unconfined air bubble curtain Average sound levels quoted ([*1]26 and [*2]241 pulses), measurements on 1 pile z_r = 5.5 m	Coleman & Evans, 2011
	ø = 1.2 m	Diesel impact (APE *D80-42*)	N/A	11	N/A	212 @ 10 m[*1] 199 @ 10 m[*2]	198 @ 10 m[*1] 187 @ 10 m[*2]	183 @ 10 m[*1] 173 @ 10 m[*2]	229 dB_{pk} 215 dB_{rms} 200 dB_E	TL ≈ 17·log_{10}R	τ = 27 ms , τ_{pk} = 15 ms ,	[*1]Unconfined air bubble curtain OFF [*2] Unconfined air bubble curtain ON (TL_{pk} = 13 dB, TL_{rms} = 11 dB, TL_E = 10 dB, effective broadband attenuation for f>100 Hz)	Context: driving of test piles for the new Interstate 5 Bridge between Vancouver, Washington and Portland. Operation: 172-269 kJ hammer energy 3-ring unconfined air bubble curtain Average sound levels quoted ([*1]33 and [*2]1006 pulses), measurements on 1 pile z_r = 5.5 m	
	ø = 0.6 m	Diesel impact (APE *D19-42*)	N/A	11	N/A	206 @ 10 m[*1] 195-197 @ 10 m[*2]	191 @ 10 m[*1] 181-183 @ 10 m[*2]	175 @ 10 m[*1] 165-169 @ 10 m[*2]	223 dB_{pk} 208 dB_{rms} 192 dB_E	TL ≈ 17·log_{10}R	τ = 33 ms , τ_{pk} = 13 ms	[*1]Confined air bubble curtain OFF [*2] Confined air bubble curtain ON (TL_{pk} ≈ 10 dB, TL_{rms} ≈ 8 dB, TL_E ≈ 7 dB, effective broadband attenuation for f>100 Hz)	Context: driving of test piles for the new Interstate 5 Bridge between Vancouver, Washington and Portland. Operation: 31-64 kJ hammer energy Confined air bubble curtain Average sound levels quoted ([*1]261 and [*2] 538 pulses), measurements on 2 piles z_r = 5.5 m	
	ø = 1.2 m	Diesel impact (APE *D80-42*)	N/A	11	N/A	214 @ 10 m[*1] 199-200 @ 10 m[*2]	201 @ 10 m[*1] 186-190 @ 10 m[*2]	185 @ 10 m[*1] 173-175 @ 10 m[*2]	231 dB_{pk} 218 dB_{rms} 202 dB_E	TL ≈ 17·log_{10}R	τ = 27 ms , τ_{pk} = 15 ms	[*1]Confined air bubble curtain OFF [*2] Confined air bubble curtain ON (TL_{pk} ≈ 15 dB, TL_{rms} ≈ 13 dB, TL_E ≈ 11 dB, effective broadband attenuation for f>100 Hz)	Context: driving of test piles for the new Interstate 5 Bridge between Vancouver, Washington and Portland. Operation: 172-269 kJ hammer energy Confined air bubble curtain Average sound levels quoted ([*1]148 and [*2]1291 pulses), measurements on 2 piles z_r = 5.5 m	
Pipe	N/A	Diesel impact (-)	weight = 6 t	~8	N/A	N/A	170 @ 250 m	N/A	N/A	N/A	N/A	No	Operation: 90 kJ hammer energy Average sound levels (20 pulses) No details about pile characteristics	Blackwell, 2005
Steel pipe	ø = 0.9 m thick = 2.5 cm	Diesel impact (Delmag *D62*)	N/A	7.3	sand and soil	182.2-185.9 @ 10 m (189.6 @ 10 m)[*]	171.2-175.7 @ 10 m (173.7 @ 10 m)[*]	168 @ 10 m[*]	N/A	N/A	τ_{pk} ≈ 6.7 ms	TNAP1: steel pile casing with 5 cm air chamber (internal hollow wall) $TL_{0-p,rms}$ ≈ 17 dB	Context: pile driving during Mukilteo Test Pile Project, at Mukilteo Fuel Pier Operation: 110-150 kJ (224 kJ capacity) z_r ≈ 4 m [*]Average sound levels, 34 pulses	Laughling, 2007
Steel pipe	ø = 0.9 m thick = 2.5 cm	Diesel impact (Delmag *D62*)	N/A	7.9	sand and soil (firm)	187-189.7 @ 10 m (188.5 @ 10 m)[*]	174.1-176.4 @ 10 m (175.4 @ 10 m)[*]	166 @ 10 m[*]	N/A	N/A	τ_{pk} = 19.4 ms	TNAP2: steel pile casing with 5 cm chamber filled with open cell foam, with perforated metal screen on the inside TL_{pk} ≈ 19 dB, TL_{rms} ≈ 16 dB	Context: pile driving during Mukilteo Test Pile Project, at Mukilteo Fuel Pier Operation: 110-150 kJ (224 kJ capacity) z_r ≈ 4 m [*]Average sound levels, 152 pulses	Laughling, 2007
Steel pipe	ø = 0.9 m thick = 2.5 cm	Diesel impact (Delmag *D62*)	N/A	8.2	sand and soil (soft)	201.4-210.6 @ 10 m[*1] (207.2 @ 10 m)[*3] 182.8-186.4 @ 10 m[*2] (184.8 @ 10 m)[*3]	186.7-194.5 @ 10 m[*1] (191.5 @ 10 m)[*3] 169.1-171.7 @ 10 m[*2] (170.5 @ 10 m)[*3]	184 @ 10 m[*1,3] 162 @ 10 m[*2,3]	N/A	N/A	[*1]τ_{pk} = 17..2 ms [*2]τ_{pk} = 19.3 ms	[*1]Double-ring unconfined air bubble curtain OFF [*2] Double-ring unconfined air bubble curtain ON $TL_{pk,rms}$ ≈ 22 dB	Context: pile driving during Mukilteo Test Pile Project, at Mukilteo Fuel Pier Operation: 110-150 kJ (224 kJ capacity) z_r ≈ 4 m [*3] Average sound levels, [*1]29 pulses and [*2] 86 pulses	Laughling, 2007
Steel pipe	ø = 0.76 m thick = 1.3 cm	Diesel impact (Berminghammer *B-3505*)	weight = 1.8 t	~30	clay and underlaying glacial till	198-202 @ 10 m (200.3 @ 10 m)[*]	N/A	168-170 @ 10 m (169.1 @ 10 m)[*]	N/A	N/A	N/A	No (3.8 cm plywood pile cap, between pile and hammer)	Context: pile driving for the installation of TIdGen™ device during Cobscook Bay Tidal Energy Project, Maine Operation: 62 kJ hammer energy (max. drop height 3.5 m), 36-60 blows/min, 30 m follower attached to pile due to water depth, driving during slack tide, impact hammer used after vibratory, when hard substrate was reached High tidal currents z_r = 3, 6 m Measurements on 3 piles [*]Average sound levels	ORPC Maine, 2012

Tab. A.1 Sounds produced by steel pipes and H-piles driven with a diesel impact hammer (cont.)

Pile Type	Pile Dimensions	Hammer Type	Hammer Dimensions	h_w [m]	Seabed Type	Measurement			SL [dB re 1µPa@1 m]	Regression Equation	Signal Characteristics	Attenuation Method	Description	Reference
						SPL_{pk} [dB re 1µPa_{pk}]	SPL_{rms} [dB re 1µPa_{rms}]	SEL [dB re 1µPa^2s]						
Steel pipe	ø = 0.5 m thick = 1.3 cm length ≈ 18 m	Diesel impact (Delmag *D30-23*)	weight = 3 t	4.3-5.2	soft mud and underlaying glacial till	208 @ 3 m 204 @ 5 m 197 @ 15 m	194 @ 3 m 191 @ 5 m 185 @ 15 m	177 @ 3 m 174 @ 5 m 170 @ 15 m	215 dB_{pk} 200 dB_{rms} 182 dB_E	$TL_{pk} \approx 15 \cdot \log_{10}R$ $TL_{rms} \approx 13 \cdot \log_{10}R$ $TL_E \approx 10 \cdot \log_{10}R$	N/A	No	Context: study of the effects of noise form impact pile driving construction of dock at Fishermen's Terminal, on Lake Washington Ship Canal Operation: vibratory hammer to set piles, diesel impact to drive piles, 59 kJ impact energy (drop height 2 m) z_r = 0.5 m	Ruggerone et al., 2008
Steel pipe	ø = 0.76 m thick = 2.5 m	Diesel impact (Delmag *D62*)	weight = 6.6 t	10	N/A	203.7 @ 16 m	192.5 @ 16 m	N/A	N/A	N/A	N/A	No	Operation: 36-50 blows/min	MacGillivrai & Racca, 2005
Steel pipe with H-type wings	1 x Open-ended hollow steel pipe ø = 0.3 m 2 x H-type steel interlocking piles 0.5 m wide, attached at each side of the pipe	Diesel impact (Vulcan)	N/A	4-8	silt and mud, glacial till layer below	202 @ 10 m	189 @ 10 m	176 @ 10 m	N/A	N/A	τ_{pk} = 4.6 ms	No cap material Unconfined air bubble curtain OFF	Context: replacement of wood wave barrier at Cape Disappointment boat launch facilty Operation: 35-50 kJ hammer energy (70 kJ capacity) z_r = 1 m above seabed Measurements on 4 piles, maximum registered levels are quoted U-shape air bubble curtain Strong tidal currents (no impact on efficiency of air bubble curtain)	Laughling, 2006
						195 @ 10 m	179 @ 10 m	166 @ 10 m	N/A	N/A	τ_{pk} = 12.6 ms	No cap material Unconfined air bubble curtain ON (TL ≈ 11 dB)		
						194 @ 10 m	182 @ 10 m	169 @ 10 m	N/A	N/A	τ_{pk} = 13.1 ms	Micarta cap material Unconfined air bubble curtain OFF		
						186 @ 10 m	175 @ 10 m	161 @ 10 m	N/A	N/A	τ_{pk} = 21.2 ms	Micarta cap material Unconfined air bubble curtain ON (TL ≈ 11 dB)		
						194 @ 10 m	181 @ 10 m	168 @ 10 m	N/A	N/A	τ_{pk} = 7.8 ms	Nylon cap material Unconfined air bubble curtain OFF		
						188 @ 10 m	176 @ 10 m	161 @ 10 m	N/A	N/A	τ_{pk} = 2.9 ms	Nylon cap material Unconfined air bubble curtain ON (TL ≈ 7 dB)		
						190 @ 10 m	176 @ 10 m	165 @ 10 m	N/A	N/A	τ_{pk} = 22.1 ms	Plywood cap material Unconfined air bubble curtain OFF		
						186 @ 10 m	179 @ 10 m	163 @ 10 m	N/A	N/A	τ_{pk} = 17.1 ms	Plywood cap material Unconfined air bubble curtain ON (TL ≈ 2 dB)		
Steel H pile	width = 0.3 m	Diesel impact	Small	In land	N/A	174 @ 25 m 169 @ 35 m 157 @ 95 m	159 @ 25 m 158 @ 35 m 145 @ 95 m	N/A	227 dB_{pk} 196 dB_{rms}	$TL_{pk/rms} \approx 26 \cdot \log_{10}R$	T = 1.5 s	No	Context: trestle piles for Noyo River Bridge replacement (California) Operation: 4-7' continuous driving	Illinworth & Rodkin, 2007
				2	N/A	179 @ 30 m 178 @ 55 m 165 @ 85 m	165 @ 30 m 164 @ 55 m 150 @ 85 m	N/A	216 dB_{pk} 205 dB_{rms}	$TL_{pk/rms} \approx 26 \cdot \log_{10}R$				
				5	N/A	168 @ 70 m 170 @ 90 m	156 @ 70 m 158 @ 90 m	N/A	N/A	N/A				
Steel H pile	width = 0.25 m	Diesel impact	Small	2	Mud	190 @ 10 m 170 @ 20 m	175 @ 10 m 160 @ 20 m	N/A	N/A	N/A	N/A	No	Context: construction of new sea wall in San Rafael Canal (California) Operation: 30 s continuous driving z_r = 1 m	Illinworth & Rodkin, 2007
Steel H pile	width = 0.38 m	Diesel impact	Small	2-3	N/A	190 @ 10 m[*1] 195 @ 10 m[*2]	165 @ 10 m[*1] 180 @ 10 m[*2]	155 @ 10 m[*1] 170 @ 10 m[*2]	N/A	N/A	Substantial energy at f > 1kHz (higher frequency content than steel pipes or steel shell piles)	No	Context: replacement of old sea wall at Ballena Isle Marina (California) Operation: 30 s continuous driving z_r = 1 m [*1] thin pile, battered [*2] thick piles, vertical	Illinworth & Rodkin, 2007
Steel H pile	width = 0.38 m	Diesel impact	N/A	0.5-2 m around cofferdam	N/A	172 @ 10 m	160 @ 10 m	147 @ 10 m	N/A	N/A	T = 1.4 s Most energy at f < 1.2 kHz	No	Context: piles driven in dewatered cofferdam adjacent to river channel, at Platte River Operation: excavated cofferdam (3 m below river bottom), 7-9 continuous pile driving z_r = 1 m	Illinworth & Rodkin, 2007
Steel H pile	ø = 0.35 m length = 27 m	Diesel impact (Delmag *D30-42*)	weight = 3 t	14-18	cobbles, pebbles, silt and clay	194 @ 19 m 182 @ 45 m 181 @ 150 m 178 @ 190 m 173 @ 230 m	176 @ 19 m 169 @ 45 m 169 @ 150 m 165 @ 190 m 160 @ 230 m	162 @ 19 m 157 @ 45 m 157 @ 150 m 154 @ 190 m 151 @ 230 m	213 dB_{pk} 190 dB_{rms} 174 dB_E	$TL_{pk} \approx 15 \cdot \log_{10}R$ $TL_{rms} \approx 11 \cdot \log_{10}R$ $TL_E \approx 9 \cdot \log_{10}R$	N/A	No	Context: pile driving at the Knik arm for improvement of Port of Anchorage, as part of the Marine Terminal Redevelopment Project Operation: vibratory hammer to set piles, diesel impact to drive piles, 100 kJ impact energy High tidal current z_r = 11-15 m	URS, 2007

Tab. A.1 Sounds produced by steel sheets and concrete piles driven with a diesel impact hammer (cont.)

Pile Type	Pile Dimensions	Hammer Type	Hammer Dimensions	h_w [m]	Seabed Type	Measurement			SL [dB re 1µPa@ 1 m]	Regression Equation	Signal Characteristics	Attenuation Method	Description	Reference
						SPL_{pk} [dB re 1µPa_{pk}]	SPL_{rms} [dB re 1µPa_{rms}]	SEL [dB re 1µPa^2s]						
AZ steel sheet	width = 0.6 m, length = 15 m	Diesel impact (ICE *60S*)	N/A	15	N/A	209 @ 5 m 203-205 @ 10 m 188 @ 40 m	195 @ 5 m 187-189 @ 10 m 173 @ 40 m	175-179 @ 10 m 175-178 @ 20 m	226 dB_{pk} 212 dB_{rms}	$TL_{pk;rms} \approx 24 \cdot \log_{10}R$	τ > 100 ms, with most energy in the first 40 ms T = 1.4 s Most energy at 25-4000 Hz	No	Context: underwater sea wall for deep port to accomodate large vessels, at Berth 23, Port of Oakland (California) Operation: 12-15 min continuous driving Measurements on 5 sheet piles	Illinworth & Rodkin, 2007
Concrete pile	width = 0.6 m Octagonal pile	Diesel impact (Delmag *D62-22*)	Small	2.5-4	Dense sand layer	180-186 @ 10 m [*1] 172-186 @ 10 m [*2]	167-174 @ 10 m [*1] 158-173 @ 10 m [*2]	N/A	N/A	N/A	N/A	No	Context: piling at to expand existing marina in San Francisco (California) Operation: wood cushion on pile's helmet to prevent damage from hammer, water jetting to soften the sediment, few min to 40 min driving z_r = 1.5-3 m [*1] high hammer energy [*2] low hammer energy + water jetting	Illinworth & Rodkin, 2007
Concrete pile	width = 0.6 m Octagonal pile	Diesel impact (Delmag *D62-22*)	Small	10-15	N/A	183-191 @ 10 m 174 @ 100 m	171-179 @ 10 m 163 @ 100 m	162-167 @ 10 m 152 @ 100 m	196-204 dB_{pk} 184-192 dB_{rms} 175-180 dB_E	TL ≈ 13·$\log_{10}$R	N/A	No	Context: reconstruction of Berth 22 at Port of Oakland (California) Operation: wood cushion on pile's helmet to prevent damage from hammer, 224 kJ hammer energy, 15-30 min continuous driving z_r = 3 m	Illinworth & Rodkin, 2007
		Diesel impact	Small	In land	N/A	192 @ 10 m 187 @ 20 m 184 @ 35 m 173 @ 85 m	181 @ 10 m 176 @ 20 m 171 @ 35 m 161 @ 85 m	174 @ 10 m 168 @ 20 m	212 dB_{pk} 201 dB_{rms}	TL ≈ 20·$\log_{10}$R	N/A	No	Context: reconstruction of Berth 22 at Port of Oakland (California)	
Concrete pile	width = 0.6 m Octagonal pile	Diesel impact (Delmag *D62-22*)	Small	7-8	N/A	184-185 @ 10 m	173-174 @ 10 m	161-163 @ 10 m	N/A	N/A	N/A	No	Context: strengthening of Berth 32 at Port of Oakland (California) Operation: 224 kJ hammer energy z_r = 3 m Measurements on 5 piles	Illinworth & Rodkin, 2007
Concrete pile	width = 0.6 m Octagonal pile	Diesel impact (Delmag *D62-22*)	Small	8	N/A	185-187 @ 10 m [*1] 173-180 @ 10 m [*2]	172-176 @ 10 m [*1] 163-168 @ 10 m [*2]	158-165 @ 10 m [*1] 153-158 @ 10 m [*2]	N/A	N/A	N/A	[*1] Unconfined air bubble curtain OFF [*2] Unconfined air bubble curtain ON (TL_{pk} = 5-10 dB, TL_{rms} ≈ 5 dB, broadband efficiency, greatest reduction at f = 250 Hz)	Context: wharf construction for Berth 32 at Port of Oakland (California) Operation: 224 kJ hammer energy z_r = 3 m [*1] Measurements on 2/5 piles [*2] Measurements on 5/5 piles	Illinworth & Rodkin, 2007
Concrete pile	width = 0.6 m, length = 38 m Octagonal pile	Diesel impact (Delmag *D62-22*)	Small	3-14	N/A	183-192 @ 10 m 186 @ 20 m	170-176 @ 10 m 171 @ 20 m	N/A	N/A	N/A	T = 1.4 s	No	Context: wharf reconstruction for Berth 23 at Port of Oakland (California) Operation: 110 kJ hammer energy (50% of maximum capacity, 220 kJ), 15-20 min continuous driving z_r = 3 m	Illinworth & Rodkin, 2007
						162-185 @ 10 m 157-179 @ 20 m	145-172 @ 10 m 145-168 @ 20 m	N/A	N/A	N/A	T = 1.4 s	Confined air bubble curtain (PVC pipe with air supply) TL ≈ 10-15 dB, with PVC pipe just under the surface TL ≈ 20-30 dB with top 1.5 m of PVC pipe above surface		
Concrete pile	ø = 0.6 m	Diesel impact (Delmag *D62*)	N/A	7.6	sand and soil (firm)	178.4-182.4 @ 10 m (180.6 @ 10 m)*	165.4-168.7 @ 10 m (167.2 @ 10 m)*	159 @ 10 m*	N/A	N/A	τ_{pk} = 5.4 ms	No (30 cm in plywood pile cap, between pile and hammer)	Context: pile driving during Mukilteo Test Pile Project, at Mukilteo Fuel Pier Pile: solid octagonal concrete Operation: 110-150 kJ (224 kJ capacity) z_r ≈ 4 m *Average sound levels, 184 pulses	Laughling, 2007
Concrete pile	ø = 0.9 m thick = 15 cm	Diesel impact (Delmag *D62*)	N/A	7.6	sand and soil (firm)	188.2-191.4 @ 10 m (190 @ 10 m)*	173.5-176.6 @ 10 m (175.2 @ 10 m)*	167 @ 10 m*	N/A	N/A	τ_{pk} = 12.8 ms	No (30 cm in plywood pile cap, between pile and hammer)	Context: pile driving during Mukilteo Test Pile Project, at Mukilteo Fuel Pier Pile: hollow cylindrical concrete Operation: 110-150 kJ (224 kJ capacity) z_r ≈ 4 m *Average sound levels, 204 pulses	Laughling, 2007

Tab. A.1 Sounds produced by concrete piles (CISS, CIDH) driven with a diesel impact hammer (cont.)

Pile Type	Pile Dimensions	Hammer Type	Hammer Dimensions	h_w [m]	Seabed Type	Measurement			SL [dB re 1µPa@ 1 m]	Regression Equation	Signal Characteristics	Attenuation Method	Description	Reference
						SPL_{pk} [dB re 1µPa_{pk}]	SPL_{rms} [dB re 1µPa_{rms}]	SEL [dB re 1µPa^2s]						
CISS steel pipe	ø = 0.9 m	Diesel impact (Delmag *D36-32*)	N/A	8-10	N/A	199 @ 10 m 188 @ 50 m	188 @ 10 m 177 @ 50 m	176 @ 10 m	212 dB_{pk} 199 dB_{rms}	$TL_{pk,rms} \approx 16 \cdot \log_{10}R$	τ ≈ 40 ms Most energy at 125-1000 Hz	Double-wall attenuator with air bubble curtain $TL_{pk} \approx 10$ dB, $TL_{rms} \approx 5$ dB Effective for f > 500 Hz	Context: re-strike of fully inserted piles for tests of sound attenuation systems, in Eureka Channel (California) Operation: 95 kJ hammer energy z_r = 5 m	Illinworth & Rodkin, 2007
						196 @ 10 m 178 @ 100 m	185 @ 10 m 165 @ 100 m	174 @ 10 m 153 @ 100 m	214 dB_{pk} 205 dB_{rms} 195 dB_E	$TL_{pk} \approx 18 \cdot \log_{10}R$ $TL_{rms} \approx 20 \cdot \log_{10}R$ $TL_E \approx 21 \cdot \log_{10}R$		Single-wall 1.5 ø pile casing with inside air bubble curtain $TL_{pk} \approx 18$ dB, $TL_{rms} \approx 7$ dB Effective for f > 500 Hz		
						192 @ 10 m 183 @ 50 m 179 @ 100 m	180 @ 10 m 172 @ 50 m 168 @ 100 m	170 @ 10 m 155 @ 100 m	205 dB_{pk} 192 dB_{rms} 185 dB_E	$TL_{pk} \approx 13 \cdot \log_{10}R$ $TL_{rms} \approx 12 \cdot \log_{10}R$ $TL_E \approx 15 \cdot \log_{10}R$		Unconfined air bubble curtain $TL_{pk} \approx 19$ dB, $TL_{rms} \approx 14$ dB Effective for f > 500 Hz		
						210 @ 10 m 198 @ 50 m	193 @ 10 m 182 @ 50 m	183 @ 10 m	227 dB_{pk} 209 dB_{rms}	$TL_{pk} \approx 17 \cdot \log_{10}R$ $TL_{rms} \approx 16 \cdot \log_{10}R$		No attenuation system		
CISS steel pipe	ø = 1.2 m	Diesel impact (Delmag *D100-13*)	N/A	In land	N/A	183-192 @ 20 m[*1] 180 @ 30 m[*1] 179 @ 40 m[*1] 166 @ 70 m[*1] 189-198 @ 10 m[*2] 190-199 @ 20 m[*2] 188-190 @ 50 m[*2]	172-180 @ 20 m[*1] 168 @ 30 m[*1] 166 @ 40 m[*1] 155 @ 70 m[*1] 178-185 @ 10 m[*2] 181-187 @ 20 m[*2] 174-177 @ 50 m[*2]	165 @ 20 m[*1] 157 @ 30 m[*1] 167-174 @ 10 m[*2] 167-172 @ 20 m[*2] 162-164 @ 50 m[*2]	N/A	N/A	N/A	No	Context: piles to support new bridge over the Russian River (California) Operation: 336 kJ hammer energy, 5-7 min driving for bottom section of the pile, 45-60 min drving for top section Measurements on 10 piles [*1] Bottom section driving [*2] Top section driving	Illinworth & Rodkin, 2007
				2		197 @ 20 m[*1] 188-205 @ 10 m[*2] 189-202 @ 20 m[*2] 192-195 @ 45 m[*2] 179-186 @ 65 m[*2]	184 @ 20 m[*1] 177-193 @ 10 m[*2] 176-189 @ 20 m[*2] 182-183 @ 45 m[*2] 166-174 @ 65 m[*2]	172 @ 20 m[*1] 165-183 @ 10 m[*2] 164-180 @ 20 m[*2] 162-174 @ 45 m[*2]	N/A	N/A				
CIDH steel pipe	ø = 1.7 m	Diesel impact (Delmag *D62/D100*)	N/A	4	N/A	219 @ 4 m 210 @ 10 m 205 @ 20 m 198 @ 40 m 187 @ 80 m	202 @ 4 m 195 @ 10 m 189 @ 20 m 180 @ 40 m 170 @ 80 m	173 @ 30 m 158 @ 60 m	233 dB_{pk} 216 dB_{rms}	$TL_{pk} \approx 24 \cdot \log_{10}R$ $TL_E \approx 24 \cdot \log_{10}R$	τ ≈ 40 ms, with most energy in the first 20 ms Pile ringing 10 ms after pulse Most energy at 125-1500 Hz	No	Context: piles driven through temporary trestle at Richmond-San Rafael Bridge Operation: 270 kJ hammer energy [*1] No currents present (slack tide) [*2] Currents present	Illinworth & Rodkin, 2007
						192 @ 10 m[*1] 203 @ 10 m[*2] 191 @ 20 m[*1] 183 @ 40 m[*1]	177 @ 10 m[*1] 185 @ 10 m[*2] 173 @ 20 m[*1] 165 @ 40 m[*1]	N/A	207 dB_{pk}[*1] 197 dB_{rms}[*1]	$TL_{pk} \approx 15 \cdot \log_{10}R$ $TL_{rms} \approx 20 \cdot \log_{10}R$		Unconfined air bubble curtain [*1] $TL_{pk,rms} \approx 14$-18 [*2] $TL_{pk,rms} \approx 7$-10		

Table A.2 Sounds produced by an steel pipe driven with an air impact hammer.

Pile Type	Pile Dimensions	Hammer Type	Hammer Dimensions	h_w [m]	Seabed Type	Measurement			SL [dB re 1µPa@ 1 m]	Regression Equation	Signal Characteristics	Attenuation Method	Description	Reference
						SPL_{pk} [dB re 1µPa_{pk}]	SPL_{rms} [dB re 1µPa_{rms}]	SEL [dB re 1µPa^2s]						
Steel pipe	ø = 0.6 m, thick = 1.3 cm	Air impact (Vulcan *200C*)	N/A	13.4	sandy silt, layer of consolidated clay at 9 m	205 @ 10 m[*1] 201 @ 10 m[*2]	186 @ 10 m[*1] 184 @ 10 m[*2]	179 @ 10 m[*1] 178 @ 10 m[*2]	N/A	N/A	[*1] τ_{pk} = 3.2 ms [*2] τ_{pk} = 2.4 ms	[*1] Unconfined air bubble curtain OFF [*2] Unconfined air bubble curtain ON (full-flow, TL ≈ 0 dB)	Context: repairment of Ferry Harbor Ferry Terminal, San Juan Island Operation: 35-50 kJ hammer energy (68 kJ capacity) z_r = 0.3 m above seafloor Single bottom ring air bubble curtain Measurements on pile 2, average registered levels are quoted	Laughling, 2005

Table A.3 Sounds produced by steel pipes driven with a hydraulic impact hammer.

Pile Type	Pile Dimensions	Hammer Type	Hammer Dimensions	h_w [m]	Seabed Type	Measurement			SL [dB re 1µPa@ 1 m]	Regression Equation	Signal Characteristics	Attenuation Method	Description	Reference
						SPL_{pk} [dB re 1µPa_{pk}]	SPL_{rms} [dB re 1µPa_{rms}]	SEL [dB re 1µPa^2s]						
Steel pipe	$ø_{in}$ = 2.4 m, $ø_{out}$ = 2.57 m, length = 108 m	Hydraulic impact (Menck *MHU500T*)	N/A	10	N/A	201 @ 200 m	189 @ 200 m	178 @ 200 m	N/A	$TL_{pk/rms,E} \approx 27 \cdot \log_{10}R$	N/A	No	Context: replacement of San Francisco-Oakland Bay Bridge. z_r = 3 m Operation: 550 kJ hammer energy Measurements on 1 pile (battered)	Illinworth & Rodkin, 2007
		Hydraulic impact (Menck *MHU1700T*)				207 @ 100 m 191 @ 360 m	195 @ 100 m 179 @ 360 m	183 @ 100 m 168 @ 360 m	261 dB_{pk} 249 dB_{rms} 237 dB_E	$TL_{pk/rms,E} \approx 27 \cdot \log_{10}R$	N/A	No	Context: replacement of San Francisco-Oakland Bay Bridge. z_r = 6 m Operation: 900 kJ hammer energy (capacity 1780 kJ) Measurements on 1 pile (plum)	
		Hydraulic impact (Menck *MHU1700T*)				188-189 @ 100 m[*1] 193 @ 100 m[*2]	175 @ 100 m[*1] 179 @ 100 m[*2]	163 @ 100 m[*1] 167 @ 100 m[*2]	243[*1], 247[*2] dB_{pk} 229[*1], 233[*2] dB_{rms} 217[*1], 221[*2] dB_E	$TL_{pk/rms,E} \approx 27 \cdot \log_{10}R$	N/A	[*1] Gunderboom ON ($TL_{pk/rms,E} \approx 5$ dB) [*2] Gunderboom OFF	Context: replacement of San Francisco-Oakland Bay Bridge. z_r = 1 m Operation: 1500 kJ hammer energy (capacity 1780 kJ) Measurements on 1 pile (battered)	
Steel pipe	ø = 0.6 m, thick = 1.3 cm	Hydraulic impact (ICE *220*)	N/A	14.3	sandy silt, layer of consolidated clay at 9 m	199 @ 10 m[*1] 203 @ 10 m[*2]	184 @ 10 m[*1] 186 @ 10 m[*2]	176 @ 10 m[*1] 179 @ 10 m[*2]	N/A	N/A	[*1] τ_{pk} = 3.0 ms [*2] τ_{pk} = 1.0 ms	[*1] Unconfined air bubble curtain OFF [*2] Unconfined air bubble curtain ON (full-flow, TL ≈ 0 dB)	Context: repairment of Ferry Harbor Ferry Terminal, San Juan Island Operation: 60-85 kJ hammer energy (120 kJ capacity) z_r = 0.3 m above seafloor Single bottom ring air bubble curtain Measurements on pile 3, average registered levels are quoted	Laughling, 2005
Steel pipe	ø = 0.6 m, thick = 1.3 cm	Hydraulic impact (ICE *220*)	N/A	10	sandy silt, rock layer at 10.5 m	212 @ 10 m[*1] 196 @ 10 m[*2]	193 @ 10 m[*1] 181 @ 10 m[*2]	184 @ 10 m[*1] 174 @ 10 m[*2]	N/A	N/A	[*1] τ_{pk} = 2.2 ms [*2] τ_{pk} = 28.0 ms	[*1] Unconfined air bubble curtain OFF [*2] Unconfined air bubble curtain ON (full-flow, TL ≈ 16 dB)	Context: repairment of Ferry Harbor Ferry Terminal, San Juan Island Operation: 60-85 kJ hammer energy (120 kJ capacity) z_r = 0.3 m above seafloor Single bottom ring air bubble curtain Measurements on pile 6, average registered levels are quoted	Laughling, 2005
Pipe	N/A	Hydraulic impact (Menck *MHU3000*)	N/A	18	N/A	175 @ 1500 m	165 @ 250 m	155 @ 1500 m	N/A	N/A	N/A	No	Context: piling on the Scotian Shelf Average sound levels (631 pulses) No details about pile characteristics	Blackwell, 2005
Steel pipe	ø = 1.5 m	Hydraulic impact (-)	N/A	N/A	N/A	189 @ 750 m	N/A	164 @ 750 m	N/A	N/A	N/A	No	Context: jacket foundation (4x pinpiles) for windfarm construction during FINO1 project, North Sea Operation: 280 kJ hammer energy	Elmer et al., 2007
Steel pipe	ø = 0.71 m thick = 2.1 cm	Hydraulic impact (IHC *S-90*)	weigth = 4.9 t	8.5-12.5	silt (4 m), fine sand (14 m), coase sand	196-204 @ 70 m 189-194 @ 340 m 182-184 @ 450 m	N/A	166-171 @ 70 m 157-160 @ 340 m 153-155 @ 450 m	236 dB_{pk} 200 dB_E	$TL_{pk} = 19 \cdot \log_{10}R$ $TL_E = 17 \cdot \log_{10}R$	N/A	No	Context: pile driving at Gellibrand Wharf, northern end of Port Phillip Bay, Victoria Operation: 2-90 kJ hammer energy z_r = 4 m	Duncan et al, 2010
Steel pipe	ø = 2.5 m	Hydraulic impact (Menck *MHU 500*)	N/A	4-6	N/A	180 @ 25 m 177 @ 50 m 196 @ 95 m[*]	164 @ 25 m 167 @ 50 m 184 @ 95 m[*]	N/A	N/A	N/A	N/A	Dewatered cofferdam	Context: Pile Demonstration Project (PIDP) during seismic retrofit of San Francisco-Oakland Bay Bridge (SFOBB) Operation: 500 kJ hammer energy The SPL_{rms} is calculated over the loudest 35 ms of the sound impulse [*]High levels at 95 m can be explained by the transmission of sound through the seabed and back into the water column	Abbott & Reyff, 2004
Steel pipe	ø = 2.5 m	Hydraulic impact (Menck *MHU 1700*)	N/A	4-5	N/A	182-187 @ 50 m 182-186 @ 90 m 196-200 @ 120 m 169 @ 500 m	170-173 @ 50 m 173-176 @ 90 m 185-188 @ 120 m 161 @ 500 m	N/A	N/A	N/A	N/A	Dewatered cofferdam	Context: Pile Demonstration Project (PIDP) during seismic retrofit of San Francisco-Oakland Bay Bridge (SFOBB) Operation: 1700 kJ hammer energy The SPL_{rms} is calculated over the loudest 35 ms of the sound impulse	Abbott & Reyff, 2004
Steel pipe	ø = 2.4-2.6 m	Hydraulic impact (Menck *MHU 500T*)	N/A	30	fine sand	N/A	N/A	164-170 @ 750 m	N/A	N/A	N/A	No	Context: jacket foundation (4x piles) for 'alpha ventus' wind farm in North Sea Operation: 500 kJ hammer energy	Dähne et al, 2013

Tab. A.3 Sounds produced by steel pin piles and monopiles driven with a hydraulic impact hammer (cont.)

Pile Type	Pile Dimensions	Hammer Type	Hammer Dimensions	h_w [m]	Seabed Type	Measurement			SL [dB re 1µPa@ 1 m]	Regression Equation	Signal Characteristics	Attenuation Method	Description	Reference
						SPL_{pk} [dB re 1µPa_{pk}]	SPL_{rms} [dB re 1µPa_{rms}]	SEL [dB re 1µPa^2s]						
Steel pin pile	ø = 1.8 m length = 21-48 m weight = 46-96 t	Hydraulic impact (IHC *S-800*)	N/A	< 30 m	N/A	196 @ 250 m 186 @ 500 m 173 @ 750 m 175 @ 1700 m (172-189 @ 750 m)*	N/A	145-168 @ 750 m*	232 dB_{pk} 211 dB_{rms}	TL = 15·log_{10}R	Most energy at 60-2k Hz	No	Context: construction windfarms for C-Power Project, Thorntonbank, using jacket foundations (4 pinpiles each) Operation: hammer energy 412 kJ (800 kJ capacity), 162-405' driving per jacket foundation,~40 blows per minute Measurements on 2 monopiles z_r = 10 m *normalised to 750 m using a spreading loss of 15·log_{10}R	Degraer et al, 2012
Steel monopile	ø = 4 m, thick = 3.5 cm length = 50 m weight = 270 t	Hydraulic impact (Menck *MHU500T*)*6	N/A	12	Gravelly sand, sandstone at 14 m	N/A	N/A	N/A	*1 249 dB_{pk-pk}	*1 RL_{pk-pk} = 249 - 17·log_{10}R -1.1·10^{-3}R	N/A	No	Context: construction of 5 windfarms in UK waters using steel monopiles *1 North Hoyle windfarm *2 Scroby Sands windfarm *3 Kentish Flats windfarm *4 Barrow *5 Burbo Bank Operation: *6 450 kJ hammer energy (550 kJ capacity), 35 blows/min; *7 344 kJ hammer energy (600 kJ capacity)	Nedwell et al, 2007
	ø = 4.2 m	N/A	N/A	0.5-5	N/A	N/A	N/A	N/A	*2 257 dB_{pk-pk}	*2 RL_{pk-pk} = 257 - 20·log_{10}R -3·10^{-3}R	N/A	No		
	ø = 4.3 m	Hydraulic impact (IHC *S-600*)*7	weight = 30 t	5	silt and sand	N/A	N/A	N/A	*3 243 dB_{pk-pk}	*3 RL_{pk-pk} = 243 - 20·log_{10}R -2·10^{-3}R	N/A	No		
	ø = 4.7 m	N/A	N/A	10-20	N/A	N/A	N/A	N/A	*4 252 dB_{pk-pk}	*4 RL_{pk-pk} = 252 - 18·log_{10}R -3·10^{-4}R	N/A	No		
	ø = 4.7 m	N/A	N/A	6-29	N/A	N/A	N/A	N/A	*5 249 dB_{pk-pk}	*5 RL_{pk-pk} = 249 - 21·log_{10}R -4.7·10^{-3}R, validity from 100 m to 5 km	N/A	No		
Steel monopile	ø = 5 m length = ~60 m weight = ~400 t	Hydraulic impact (IHC *S-1200*)	N/A	< 30 m	N/A	193 @ 770 m 185 @ 1580 m 177 @ 3000 m 166 @ 6990 m 160 @ 14150 m (179-194 @ 750 m)*	N/A	160-168 @ 750 m*	236 dB_{pk} 211 dB_{rms}	TL = 15·log_{10}R	Most energy at 60-1k Hz	No	Context: construction of Belwind windfarms, Blight Bank, using single steel monopile foundations Operation: hammer energy 706 kJ (1200 kJ capacity), 64-163' driving, ~40 blows per minute Measurements on 2 monopiles z_r = 10 m *normalised to 750 m using a spreading loss of 15·log_{10}R	Degraer et al, 2012; Norro et al, 2010
Steel monopile	ø = 3 m	Hydraulic impact (-)	N/A	N/A	N/A	185 @ 750 m	N/A	164 @ 750 m	N/A	N/A	N/A	No	Context: installation of monopile foundation for windfarm construction during Sky2000 project, Baltic Sea Operation: 280 kJ hammer energy	Elmer et al., 2007
Steel monopile	ø = 3.5 m	Hydraulic impact (-)	N/A	N/A	N/A	200 @ 750 m	N/A	175 @ 750 m	N/A	N/A	N/A	No	Context: installation of monopile foundation for windfarm construction in Amrumbank, North Sea Operation: 800 kJ hammer energy	Elmer et al., 2007
Steel monopile	ø = 4 m length = 54 m weight = 2.5 t	Hydraulic impact (Menck *MHU 1900S*)	ø = 1.6 m length = 22 m weight = 95 t	20-25	N/A	184.6 @ 1.84 km*1 181.3 @ 3.2 km*1 175 @ 5.6 km*1	N/A	167.1 @ 1.84 km*1 161 @ 3.2 km*1 156.3 @ 5.6 km*1	250 dB_{pk} 239 dB_E	TL_{pk} = 20·log_{10}R TL_E = 22·log_{10}R	τ ≈ 120 ms Most energy at 100-500 Hz	No	Context: installation of Prinses Amaliawindpark wind farm, 23 km off Dutch coast near IJmuiden Operation: *1 250-300 kJ or *2 800 kJ hammer energy (1900 kJ capacity), 2 h driving, 32 blows/min z_r = 20-25 m Averaged levels quoted, standard deviation *1σ<1.2 dB and *2σ<1.8	De Jong & Ainslie, 2012
						194.5 @ 0.89 km*2 194.4 @ 1.08 km*2 193.6 @ 1.21 km*2 186.5 @ 2.27 km*2 182.9 @ 3.20 km*2 176.5 @ 5.65 km*2	N/A	171.6 @ 0.89 km*2 171.7 @ 1.08 km*2 172.4 @ 1.21 km*2 166.1 @ 2.27 km*2 162.3 @ 3.20 km*2 157.3 @ 5.65 km*2	262 dB_{pk} 230 dB_E	TL_{pk} = 23·log_{10}R TL_E = 20·log_{10}R	τ ≈ 80 ms Most energy at 100-500 Hz			

Tab. A.3 Sounds produced by steel monopiles and sheets driven with a hydraulic impact hammer (cont.)

Pile Type	Pile Dimensions	Hammer Type	Hammer Dimensions	h_w [m]	Seabed Type	Measurement			SL [dB re 1µPa@ 1 m]	Regression Equation	Signal Characteristics	Attenuation Method	Description	Reference
						SPL_{pk} [dB re 1µPa_{pk}]	SPL_{rms} [dB re 1µPa_{rms}]	SEL [dB re 1µPa^2s]						
Steel monopile	ø = 4.6 m thick = 5 cm length = 41-47 m	Hydraulic impact (IHC *S1200*)	weight = 60 t	18	N/A	N/A	178 @ 1.5 km 170 @ 2.3 km 159 @ 3 km	N/A	N/A	N/A	Most energy at 150-500 Hz	No	Context: construction of OWEZ wind farm, 18 km off Dutch coast Operation: 500-600 kJ hammer energy (1200 kJ capacity), 40-75 blows/min, ~25 m penetration, 2 h driving cycle/24 h z_r = 4 m Measurements on monopile 13, which produced the highest levels out of the 6 measured monopiles	de Haan et al, 2007
Steel monopile	ø = 4 m	Hydraulic impact (IHC *S600*)	weight = 30 t	6-12	Sand (firm)	N/A	191 @ 230 m 190 @ 460 m 184 @ 930 m 175 @ 1900 m	N/A	235 dB_{rms}	TL_{rms} = 18·log_{10}R	τ ≈ 200 ms Peak energy at 160 Hz	No	Context: construction of Horns Rev Offshore Wind Farm, 25 km W Danish coast on Horns Reef Operation: 360-450 kJ hammer energy (600 kJ capacity), 30 m pile penetration, 60 blows/min, 0.5-2 h per pile Measurement of monopile No. 17 z_r = 4 m (at h_w = 6.5 m)	Tougaard et al, 2009
Steel sheet	width = 0.5 m, length = 27 m	Hydraulic impact (BSP *SL30*)[*1]	width = 0.82 m, length = 6 m weigth = 2.5 t	< 5 m	Glacial till (mixture of fine and coarse sediments)	189 @ 12 m 178 @ 25 m	N/A	163 @ 12 m 155 @ 25 m	N/A	N/A	N/A	No	Context: construction of new bulkhead waterproof structure on the Knik Arm, Port of Anchorage (Alaska) Operation: [*1]84 kJ and [*2] 62 kJ hammer energy	Hart Crowser and Illinworth & Rodkin, 2009
		Hydraulic impact (J&M 115)[*2]	width = 0.66 m, length = 6 m weigth = 5.2 t			195 @ 5 m 193 @ 10 m 182 @ 33 m	N/A	165 @ 5 m 166 @ 10 m 154 @ 33 m	N/A	N/A	N/A			
Sheet pile	N/A	Hydraulic impact (J&M *115*)	weigth = 5.2 t length = 6.7 m width = 0.66 m	5.8-9.3	N/A	145-183 @ 34-521 m (171 dB @ 238 m)*	127-159 @ 34-521 m (150 dB @ 238 m)*	N/A	219 dB_{pk}* 198 dB_{rms}*	TL ≈ 20·log_{10}R	Most energy > 400 Hz	No	Context: improvement of facilities in Port of Anchorage, Knik Arm (Alaska) Face wall sheet pile High tide range z_r = 1 m above seafloor * Average sound levels	Scientific Fishery Systems, 2008
Sheet wye pile	N/A	Hydraulic impact (J&M *115*)	weigth = 5.2 t length = 6.7 m width = 0.66 m	8.2-8.5	N/A	152-173 @ 155-364 m (161 dB @ 299 m)*	132-151 @ 155-364 m (141 dB @ 299 m)*	N/A	210 dB_{pk}* 190 dB_{rms}*	TL ≈ 20·log_{10}R	Most energy at 3-20 kHz	No	Context: improvement of facilities in Port of Anchorage, Knik Arm (Alaska) Wye sheet pile * Average sound levels	Scientific Fishery Systems, 2008
Sheet pile	N/A	Hydraulic impact (J&M *115*)	weigth = 5.2 t length = 6.7 m width = 0.66 m	5.6-8.1	N/A	145-168 @ 32-322 m (158 dB @ 128 m)*	123-145 @ 32-322 m (138 dB @ 128 m)*	N/A	200 dB_{pk}* 180 dB_{rms}*	TL ≈ 20·log_{10}R	Most energy at 2-20 kHz	No	Context: improvement of facilities in Port of Anchorage, Knik Arm (Alaska) Tail wall sheet pile High tide range * Average sound levels	Scientific Fishery Systems, 2008

Tab. A.3 Sounds produced by concrete piles (CISS) driven with a hydraulic impact hammer (cont.)

Pile Type	Pile Dimensions	Hammer Type	Hammer Dimensions	h_w [m]	Seabed Type	Measurement			SL [dB re 1µPa@ 1 m]	Regression Equation	Signal Characteristics	Attenuation Method	Description	Reference
						SPL_{pk} [dB re 1µPa_{pk}]	**SPL_{rms}** [dB re 1µPa_{rms}]	**SEL** [dB re 1µPa^2s]						
CISS steel pipe	ø = 2.4 m	Hydraulic impact (Menck *MHU500T*)	N/A	10-15	N/A	227 @ 5 m 220 @ 10 m 214 @ 20 m 210 @ 50 m 204 @ 100 m 188 @ 500 m 180 @ 1000 m	215 @ 5 m 205 @ 10 m 203 @ 20 m 196 @ 50 m 192 @ 100 m 174 @ 500 m 165 @ 1000 m	201 @ 5 m 194 @ 10 m 190 @ 20 m 184 @ 50 m 180 @ 100 m 164 @ 500 m 155 @ 1000 m	238 dB_{pk} 226 dB_{rms} 212 dB_E	$TL = 16 \cdot \log_{10} R$	N/A	No	Context: permanent piles for new Benicia-Matinez Bridge foundations z_r = 5-7 m	Illinworth & Rodkin, 2007
CISS steel pipe	ø = 2.4 m	Hydraulic impact (Menck *MHT700T*)	N/A	~10	N/A	198-208 @ 100 m 182-198 @ 460 m	184-195 @ 100 m 171-185 @ 460 m	N/A	238-248 dB_{pk} 224-235 dB_{rms}	$TL = 20 \cdot \log_{10} R$	τ ≈ 80 ms, with most energy in the first 35 ms Pile ringing 10 ms after pulse Most energy at 125-1500 Hz	No	Context: restrike of piles for San Francisco-Okland Bay Bridge Operation: 1780 kJ hammer energy	Illinworth & Rodkin, 2007; Reyff, 2003
						179-201 @ 100 m 175-191 @ 460 m	169-189 @ 100 m 161-180 @ 460 m	N/A	219-241 dB_{pk} 215-231 dB_{rms}	$TL = 20 \cdot \log_{10} R$		Two-ring unconfined air bubble curtain, tightly fitted to the pile TL_{pk} = 6-17 dB TL_{rms} = 3-10 dB Effective for f > 1000 Hz		
CISS steel pipe	ø = 3.2 m	Hydraulic impact (Submersible IHC)	N/A	>15	N/A	208-218 @ 10 m 200 @ 55 m 192- 195 @ 100 m 187-190 @ 230 m	197-206 @ 10 m 190 @ 55 m 180-185 @ 100 m 175-177 @ 230 m	170 @ 100 m 165 @ 230 m	229-239 dB_{pk} 218-227 dB_{rms}	$TL_{pk,rms} = 21 \cdot \log_{10} R$	T = 1-2 s	No	Context: seismic upgrade work of Richmond-San Rafael Bridge Operation: 350-400 kJ hammer energy, 40 min continuous driving every 1-1.5 h z_r = 10 m	Illinworth & Rodkin, 2007
CISS steel pipe	ø = 3.8 m	Hydraulic impact (Submersible IHC)	N/A	>15	N/A	205-215 @ 20 m 202-205 @ 55 m 194 @ 95 m 192 @ 230 m 169 @ 1000 m	197-206 @ 20 m 188-193 @ 55 m 181 @ 95 m 178 @ 230 m 157 @ 1000 m	N/A	239-249 dB_{pk} 233-242 dB_{rms}	$TL_{pk} = 26 \cdot \log_{10} R$ $TL_{rms} = 28 \cdot \log_{10} R$	T = 1-2 s τ ≈ 80 ms, with most energy in the first 60 ms	No	Context: seismic upgrade work of Richmond-San Rafael Bridge Operation: 450 kJ hammer energy, 45 min continuous driving every 1-2 h z_r = 10 m Measurements on 2 piles	Illinworth & Rodkin, 2007

Table A.4 Sounds produced by steel pipes, concrete piles and wooden piles driven with a drop impact hammer.

Pile Type	Pile Dimensions	Hammer Type	Hammer Dimensions	h_w [m]	Seabed Type	Measurement			SL [dB re 1µPa@ 1 m]	Regression Equation	Signal Characteristics	Attenuation Method	Description	Reference
						SPL_{pk} [dB re 1µPa_{pk}]	SPL_{rms} [dB re 1µPa_{rms}]	SEL [dB re 1µPa^2s]						
Steel pipe	ø = 0.33 m	Drop Weight	N/A	4.5-5.5	N/A	183-186 @ 10 m[*1] 177 @ 20 m[*2]	166-169 @ 10 m[*1] 161 @ 20 m[*2]	N/A	216 dB_{pk} 195 dB_{rms}	$TL_{pk} = 30 \cdot \log_{10}R$ $TL_{rms} = 26 \cdot \log_{10}R$	N/A	Air bubble curtain	Context: retrofit of water pipeline at the Mad River Slough (California) Operation: 1 min driving (~10 strikes) Piles firstly introduced by vibration z_r = 3 m [*1] Measurements on 4 piles [*2] Measurements on 1 pile	Illinworth & Rodkin, 2007
Steel pipe	ø = 0.2 m thick = 5 mm	Drop hammer (-)	weight = 1 t	3	mud and clay	202.3-206 @ 60 m	N/A	N/A	N/A	N/A	τ = 20-100 ms Most energy at 1-5 kHz	No (5 cm polyethilene + 10 cm hardwood pile cap)	Context: study of the effects of pile driving noise on juvenile salmon at the Sicamous Narrows Operation: 40 kJ typ. hammer energy at 4 m drop height (40-110 kJ, 2-6.5 m) z_r = 1.5 m	Vagle, 2003
Steel pipe	ø = 0.3 m	Drop hammer (-)	weight = 1 t	10-15	gravel and sand	186-204 @ 50 m[*]	N/A	N/A	N/A	N/A	τ = 20-100 ms	No (wooden pile cap)	Context: replacement of an old wooden structure at Nine Mile Narrows, Kootenay Lake Operation: 80 kJ typ. hammer energy at 2 m drop height (40-80 kJ, 2-4 m) z_r = 7 m [*]large sound level variation attributed to differences in drop height	Vagle, 2003
Steel pipe	ø = 0.5 m	Drop hammer (-)	weight = 3.5 t	10-18	sand and clay	211.8-212.8 @ 150 m	N/A	N/A	N/A	N/A	τ = 50-200 ms	No (wooden pile cap)	Context: construction of new dolphin at Norske Canada's pull mill at Elk Falls, Campbell River Operation: battered pile, 210 kJ hammer energy at 3 m drop height z_r = 9 m Strong tidal currents	Vagle, 2003
Concrete pile	width = 0.4 m, length = 25 m Square pile	Drop hammer, steam powered (Conmaco *200*)	N/A	7	Mud	182-184 @ 10 m[*1] 178-182 @ 10 m[*2]	170-173 @ 10 m[*1] 168-170 @ 10 m[*2]	N/A	N/A	N/A	τ ≈ 100 ms (first 50 ms with lower frequency content) Most energy at f < 3 kHz	[*1] Unconfined air bubble curtain OFF [*2] Unconfined air bubble curtain ON (TL < 6 dB, effective for f > 500 Hz)	Context: piling at Concord Naval Weapons Station (California) Operation: wood cushion on pile's helmet to prevent damage from hammer, 80 kJ hammer energy z_r = 3 m	Illinworth & Rodkin, 2007
Timber pile	ø = 0.3-0.35 m	Drop hammer	weight = 1360 kg	2-4	N/A	170-182 @ 10 m 165-178 @ 20 m	158-172 @ 10 m 154-165 @ 20 m	N/A	N/A	N/A	τ > 170 ms Most energy at f < 400 Hz	No	Context: piling at Ballena Bay Marina, in Alameda (California) Operation: cushion (2x 1 cm rubber mating + plastic block + 18 cm wood) on pile's helmet to prevent damage from hammer, 1.5-4.5 drop height z_r = 1-3 m	Illinworth & Rodkin, 2007
Timber pile	ø = 0.4 m length = 15 m	Drop hammer (-)	N/A	4	N/A	175 @ 110 m[*1] 166 @ 110 m[*2]	N/A	149 @ 110 m[*1] 135 @ 110 m[*2]	N/A	N/A	N/A	Unconfined air bubble curtain OFF[*1] Unconfined air bubble curtain ON[*2] (TL ≈ 14 dB)	Context: replacement of harbour wall in Kerteminde harbour, Denmark Operation: 14 kJ hammer energy, 40-50 blows/min, ~11 min per pile Pile: tropical hard wood [*2] 20 m linear air bubble curtain, hydrophone at 1.2 m from it z_r = 2 m	Lucke et al., 2011
Cedar pile	ø = 0.2 m	Drop hammer (-)	weight = 1 t	3	mud and clay	201.6-205.6 @ 60 m	N/A	N/A	N/A	N/A	τ = 20-100 ms Most energy at 500-2k Hz	No (5 cm polyethilene + 10 cm hardwood pile cap)	Context: study of the effects of pile driving noise on juvenile salmon at the Sicamous Narrows Operation: 40 kJ typ. hammer energy at 4 m drop height (40-110 kJ, 2-6.5 m) z_r = 1.5 m	Vagle, 2003

Table A.5 Sounds produced by steel pipes with an impact hammer (unknown characteristics).

Pile Type	Pile Dimensions	Hammer Type	Hammer Dimensions	h_w [m]	Seabed Type	Measurement			SL [dB re 1µPa@ 1 m]	Regression Equation	Signal Characteristics	Attenuation Method	Description	Reference
						SPL_{pk} [dB re 1µPa_{pk}]	SPL_{rms} [dB re 1µPa_{rms}]	SEL [dB re 1µPa^2s]						
Steel pipe	ø = 0.71 m thick = 2.1 cm	N/A (KV Johnson Marine custom)	weigth = 5 t	8.5-12.5	coarse sand (4 m), calcarenite	197-203 @ 50 m 195-198 @ 120 m 180-185 @ 260 m	N/A	165-171 @ 50 m 163-167 @ 120 m 151-153 @ 260 m	243 dB_{pk} 205 dB_E	$TL_{pk} = 25 \cdot \log_{10}R$ $TL_E = 22 \cdot \log_{10}R$	N/A	No	Context: pile driving at South Channel, southern end of Port Phillip Bay, Victoria Operation: 59 kJ hammer energy (1.2 m drop height) z_r = 4 m	Duncan et al, 2010
Pipe	N/A	N/A	N/A	In land (60 m from water)	N/A	138 @ 1000 m	N/A	N/A	N/A	N/A	N/A	No	Context: piling on Sandpiper Island, NW Prudhoe Bay (Alaska) Pile type: conductor pipe Operation: pipe driven 21 m deep No details about pile characteristics	Blackwell, 2005
Steel monopile	ø = 3.9 m	N/A	N/A	10-13	N/A	195 @ 720 m[*1] 180 @ 2300[*2]	N/A	176 @ 720 m[*1] 164 @ 2300[*2]	244 dB_{pk} 225 dB_E	TL ≈ 17·$\log_{10}$R	N/A	No	Context: windfarm project Horns Rev II in North Sea, 30 km W coast of Blåvand (Denmark) Operation: 21 m penetration, 30' operation (50% of the time piling) Maximum values quoted, measurements on a single monopile z_r = [*1]1.5 m above seabed or [*2]7-8 m under sea surface	Betke, 2008; Brandt et al, 2011
Pipe	ø = 1.5 m	N/A	N/A	N/A	N/A	184 @ 750 m	N/A	158 @ 750 m	N/A	N/A	N/A	No	Context: port construction, coast Operation: 280 kJ hammer energy	Elmer et al., 2007
Pile	ø = 0.9 m	N/A	N/A	11	N/A	188 @ 340 m	N/A	162 @ 340 m	231 dB_{pk} 205 dB_E	TL ≈ 17·$\log_{10}$R	N/A	No	Context: port construction	Betke, 2008
	ø = 1 m	N/A	N/A			190 @ 340 m	N/A	164 @ 340 m	233 dB_{pk} 207 dB_E	TL ≈ 17·$\log_{10}$R	N/A	No		
Pile	ø = 1.6 m	N/A	N/A	30	N/A	188 @ 400 m	N/A	166 @ 400 m	232 dB_{pk} 210 dB_E	TL ≈ 17·$\log_{10}$R	N/A	No	Context: FINO 1	Betke, 2008
Pile	ø = 2.7 m	N/A	N/A	28	N/A	197 @ 1100 m	N/A	167 @ 1100 m	249 dB_{pk} 219 dB_E	TL ≈ 17·$\log_{10}$R	N/A	No	Context: Alpha Ventus	Betke, 2008
Pile	ø = 3 m	N/A	N/A	10	N/A	N/A	N/A	166 @ 720 m	215 dB_E	TL ≈ 17·$\log_{10}$R	N/A	No	Context: Utgrunden	Betke, 2008
Pile	ø = 3 m	N/A	N/A	21	N/A	196 @ 260 m	N/A	170 @ 260 m	237 dB_{pk} 211 dB_E	TL ≈ 17·$\log_{10}$R	N/A	No	Context: SKY 2000	Betke, 2008
Pile	ø = 3.3 m	N/A	N/A	24	N/A	190 @ 530 m	N/A	170 @ 530 m	236 dB_{pk} 216 dB_E	TL ≈ 17·$\log_{10}$R	N/A	No	Context: FINO 2	Betke, 2008
Pile	ø = 3.5 m	N/A	N/A	23	N/A	196 @ 850 m	N/A	174 @ 850 m	246 dB_{pk} 224 dB_E	TL ≈ 17·$\log_{10}$R	N/A	No	Context: Amrumbank West	Betke, 2008
Pile	ø = 4 m	N/A	N/A	7-11	N/A	196 @ 850 m	N/A	174 @ 850 m	246 dB_{pk} 224 dB_E	TL ≈ 17·$\log_{10}$R	N/A	No	Context: North Hoyle	Betke, 2008
Pile	ø = 4 m	N/A	N/A	20	N/A	200 @ 750 m	N/A	177 @ 750 m	249 dB_{pk} 226 dB_E	TL ≈ 17·$\log_{10}$R	N/A	No	Context: Q7	Betke, 2008
Pile	ø = 4.7 m	N/A	N/A	15-20	N/A	198 @ 500 m	N/A	N/A	244 dB_{pk}	TL ≈ 17·$\log_{10}$R	N/A	No	Context: Barrow	Betke, 2008
Pile	ø = 4.7 m	N/A	N/A	23	N/A	195 @ 900 m	N/A	171 @ 900 m	245 dB_{pk} 221 dB_E	TL ≈ 17·$\log_{10}$R	N/A	No	Context: FINO 3	Betke, 2008

Table A.6 Sounds produced by steel pipes and H-beams driven with a vibratory hammer.

Pile Type	Pile Dimensions	Hammer Type	Hammer Dimensions	h_w [m]	Seabed Type	Measurement			SL [dB re 1µPa@ 1 m]	Regression Equation	Signal Characteristics	Attenuation Method	Description	Reference
						SPL_{pk} [dB re 1µPa_{pk}]	SPL_{rms} [dB re 1µPa_{rms}]	SEL [dB re 1µPa^2s]						
Steel pipe	ø = 0.33 m	Vibratory	N/A	4.5-5.5	N/A	168-171 @ 10 m 168 @ 20 m	150-156 @ 10 m 150 @ 20 m	N/A	N/A	N/A	N/A	No	Context: retrofit of water pipeline at the Mad River Slough (California) Operation: 1 min driving (~ 10 strikes). Piles firstly introduced by vibration z_r = 3 m Measurements on 3 piles	Illinworth & Rodkin, 2007
Steel pipe	ø = 0.91 m, length = 46 m, thick = 2.54 cm	Hydraulic vibratory (APE *400B King Kong*)	N/A	6-42	Glacial till (mixture of fine and coarse sediments)	N/A	164 @ 56 m	N/A	199 dB_{rms}	RL_{rms} = 199.1 - 21.8·log_{10}R 50th percentile, range of validity 50-2k m	Most energy at 400-2.5k Hz Tones at 15 Hz and harmonics	No	Context: crossing construction to provide direct transporation over the Knik Arm, between Anchorage and Port MacKenzie (Alaska) Operation: 2 piles, battered 12-15 m into seabed, 20 min vibratory driving z_r = 10 m Average sound levels quoted (several pulses), measurements on 2 piles Strong tidal currents (< 3.4 m/s)	Blackwell, 2005
Steel pipe	ø = 0.6 m	Hydraulic vibratory (APE *400B King Kong*)	N/A	11	Soft	N/A	157-162 @ 10 m	N/A	173-178 dB_{rms}	TL = 15.5·log_{10}R	N/A	No	Context: driving of test piles for the new Interstate 5 Bridge between Vancouver, Washington and Portland. Operation: <1 min driving, 16-24 m pile penetration Average sound levels quoted, measurements on 2 piles z_r = 5.5 m	Coleman & Evans, 2011
Steel pipe	ø = 1.2 m	Hydraulic vibratory (APE *400B King Kong*)	N/A	11	Soft	N/A	161 @ 10 m[*1]	N/A	177 dB_{rms}	TL = 15.5·log_{10}R	Most energy at f = 0.1-0.3 kHz (these frequencies rapidly attenuate with distance compared to higher frequencies - shallow water)	No	Context: driving of test piles for the new Interstate 5 Bridge between Vancouver, Washington and Portland. Operation: [*1] <1 min driving and 27 m pile penetration; [*2] 4-9 min driving and 61 m pile penetration Average sound levels quoted, measurements on [*1] 1 and [*2] 2 piles z_r = 5.5 m	Coleman & Evans, 2011
					Hard	N/A	179-181 @ 10 m[*2]	N/A	195-197 dB_{rms}					
Pipe	N/A	Hydraulic vibratory (APE *200*)	length = 0.26 m width = 0.37 m	8.3-8.5	N/A	N/A	120-144 @ 16-67 m (132 dB @ 35 m)[*]	N/A	163 dB_{rms}[*]	TL ≈ 20·log_{10}R	Most energy at 200-20k Hz	No	Context: improvement of facilities in Port of Anchorage, Knik Arm (Alaska) Operation: max. vibration freq. 27 Hz Round pile (pipe) [*] Average sound levels	Science Fishery Systems, 2008
Steel pile	ø = 0.76 m thick = 1.3 cm	Hydraulic vibratory (H&M *H-1700*)	height = 2.7 m weight = 3.2 t width = 0.3 m	26-32	clay and underlaying glacial till	170-195 @ 10 m (188.4 @ 10 m)[*]	N/A	171-188 @ 10 m (184.6 @ 10 m)[*]	N/A	N/A	N/A	No	Context: pile driving for the installation of TidGen™ device during Cobscook Bay Tidal Energy Project, Maine Operation: 1200 vpm driving frequency (~60 hz), 30 m follower attached to pile, driving during slack tide High tidal currents z_r = 3, 6 m Measurements on 5 piles [*]Average sound levels	OCRP Maine, 2012
Steel H pile	ø = 0.25 m	Vibratory	Small	2	Mud	161 @ 10 m 152 @ 20 m	147 @ 10 m 137 @ 20 m	N/A	N/A	N/A	N/A	No	Context: construction of new sea wall in San Rafael Canal (California) z_r = 1 m	Illinworth & Rodkin, 2007
Steel H pile	ø = 0.35 m length = 27 m	Hydraulic vibratory (APE *200*)	length = 0.26 m width = 0.37 m	9-20	cobbles, pebbles, silt and clay	175 @ 16 m 172 @ 20 m	164 @ 20 m 149 @ 40 m 147 @ 80 m 138 @ 250 m 136 @ 325 m	N/A	191 dB_{rms}	TL_{rms} ≈ 21·log_{10}R	N/A	No	Context: pile driving at the Knik arm for improvement of Port of Anchorage, as part of the Marine Terminal Redevelopment Project Operation: vibratory hammer to set piles, diesel impact to drive piles High tidal current z_r = 2 m above seabed	URS, 2007

Tab. A.6 Sounds produced by steel sheets driven with a vibratory hammer (cont.)

Pile Type	Pile Dimensions	Hammer Type	Hammer Dimensions	h_w [m]	Seabed Type	Measurement			SL [dB re 1µPa@ 1 m]	Regression Equation	Signal Characteristics	Attenuation Method	Description	Reference
						SPL_{pk} [dB re 1µPa_{pk}]	SPL_{rms} [dB re 1µPa_{rms}]	SEL [dB re 1µPa^2s]						
AZ steel sheet	width = 0.6 m, length = 15 m	Hydraulic vibratory (APE *400B King Kong*)	N/A	15	N/A	177 @ 10 m 166 @ 20 m	163 @ 10 m	162 @ 10 m	N/A	N/A	Continuous broadband sound Most energy at 400-2500 Hz	No	Context: underwater sea wall for deep port to accomodate large vessels, at Berth 23, Port of Oakland (California) Operation: 23 Hz hammer frequency, vibratory driving used for *stabbing* Measurements on 5 sheet piles	Illinworth & Rodkin, 2007
AZ steel sheet	width = 0.6 m, length = 15 m	Hydraulic vibratory (APE *400B King Kong*)	N/A	15	N/A	166-175 @ 10 m	154-162 @ 10 m	162 @ 10 m	N/A	N/A	Important tonal content	No	Context: sheet pile installation at Berth 30, Port of Oakland (California) Operation: 23 Hz hammer frequency z_r = 3-5 m Measurements on 5 sheet piles	Illinworth & Rodkin, 2007
AZ steel sheet	width = 0.6 m	Hydraulic vibratory (APE *600B Super Kong*)	N/A	15	N/A	177 @ 10 m	163 @ 10 m	163 @ 10 m	N/A	N/A	N/A	No	Context: sheet pile installation at Berth 35, Port of Oakland (California)	Illinworth & Rodkin, 2007
Steel sheet	width = 0.5 m, length = 27 m	Hydraulic vibratory (APE *200-6*)	height = 3.6 m force = 2.27 kN	< 5 m	Glacial till (fine and coarse sediments)	181 @ 1.5 m 184 @ 7 m	N/A	166 @ 1.5 m 171 @ 7 m	N/A	N/A	N/A	No	Context: construction of new bulkhead waterproof structure on the Knik Arm, Port of Anchorage (Alaska)	Hart Crowser and Illinworth & Rodkin, 2009
Sheet pile	N/A	Hydraulic vibratory (APE *200*)	length = 0.26 m width = 0.37 m	5.8-9.3	N/A	N/A	120-157 @ 32-1208 m (141 dB @ 757 m)*	N/A	199 dB_{rms}*	TL ≈ 20·$\log_{10}$R	Most energy at 2-12 kHz	No	Context: improvement of facilities in Port of Anchorage, Knik Arm (Alaska) Operation: max. vibration freq. 27 Hz Face wall sheet pile High tide range * Average sound levels	Science Fishery Systems, 2008
Steel sheet	N/A	Hydraulic vibratory (APE *200*)	length = 0.26 m width = 0.37 m	7	cobbles, pebbles, silt and clay	181 @ 15 m 174 @ 40 m	163-169 @ 15 m 155-160 @ 40 m	N/A	N/A	N/A	N/A	No	Context: pile driving at the Knik arm for improvement of Port of Anchorage, as part of the Marine Terminal Redevelopment Project Operation: vibratory hammer to set piles, diesel impact to drive piles High tidal current z_r = 2 m above seabed Bent pile, forward-backward movement	URS, 2007
Steel shell pile (SSP_{22})	ø = 22 m thick = 1.6 cm length = 39-60 m weight = 450-600 t	Hydraulic vibratory (Octa Kong)	N/A	7-8	N/A	154 @ 60 m	143 @ 60 m	122 @ 60 m	N/A	N/A	N/A	No	Context: construction of Hongkong-Zhuhai-Macao Bridge in the Pearl River Estuary Hammer: the Octa-Kong consists of 8 APE 600 working simultaneously Operation: 15-16 Hz vibration frequency z_r = 2 m * Average sound level, 50 measurements on 1 pile	Wang et al., 2014
Sheet wye pile	N/A	Hydraulic vibratory (APE *200*)	length = 0.26 m width = 0.37 m	8.1-8.2	N/A	N/A	122-139 @ 88-152 m (134 dB @ 126 m)*	N/A	176 dB_{rms}*	TL ≈ 20·$\log_{10}$R	Most energy at 1-10 kHz	No	Context: improvement of facilities in Port of Anchorage, Knik Arm (Alaska) Operation: max. vibration freq. 27 Hz Wye sheet pile * Average sound levels	Science Fishery Systems, 2008
Sheet wye pile	N/A	Hydraulic vibratory (APE *200*)	length = 0.26 m width = 0.37 m	8.1-8.2	N/A	N/A	119-122 @ 47-108 m (120 dB @ 84 m)*	N/A	158 dB_{rms}*	TL ≈ 20·$\log_{10}$R	Most energy at 20-300 Hz	No	Context: improvement of facilities in Port of Anchorage, Knik Arm (Alaska) Operation: max. vibration freq. 27 Hz Tail wall sheet pile * Average sound levels	Science Fishery Systems, 2008

A.II Noise & Absorption in Sea Water

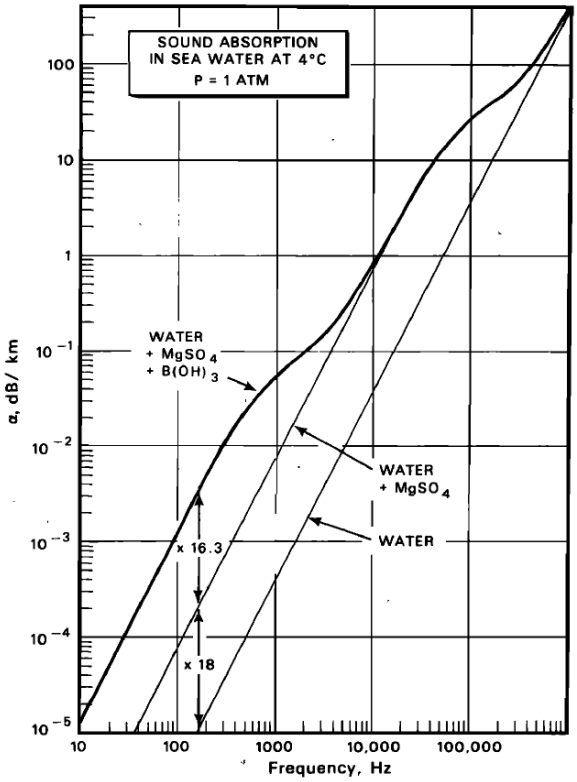

Figure A.1 Absorption coefficient in sea water at 4 °C, 1 atm, salinity 35 ppt and pH 8.0 (from Fisher & Simmons, 1977).

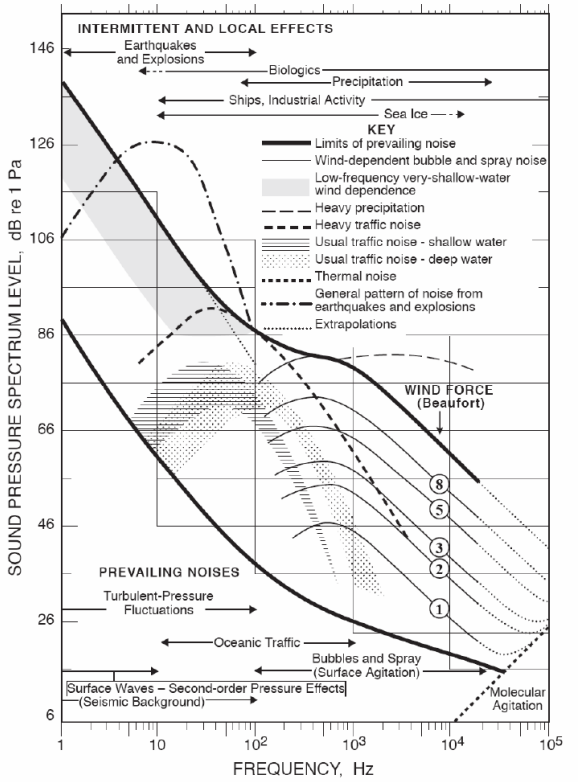

Figure A.2 Composite of ambient noise spectra. An estimate of the expected ambient noise can be obtained by selecting the pertinent combination of ambient noise components (from Wenz, 1962).

Contact us

General enquiries

info@soundandmarinelife.org

Media enquiries

press@soundandmarinelife.org
+44 (0) 20 7413 3416

E&P **SOUND & MARINE LIFE** PROGRAMME